Methamphetamine-induced cytogenesis in the mouse striatum: neurochemical and behavioral studies.

By

Ingrid Tulloch

A dissertation submitted to the Graduate Faculty in Psychology in partial fulfillment of the requirements for the degree of Doctor of Philosophy.
The City University of New York
2011

This manuscript has been read and accepted for the Graduate Faculty in Psychology in satisfaction of the Dissertation requirements for the degree of Doctor of Philosophy

Jesus Angulo. Ph.D

_____ _____

Date Chair of Examining Committee

Maureen O'Connor_____

_____ _____

Date Executive Officer

Jesus Angulo, Ph.D

Vanya Quinones-Jenab, Ph.D

Shirzad Jenab, Ph.D

Peter Serrano, Ph.D

Jean Lud Cadet, MD.

Supervisory Committee

THE CITY UNIVERSITY OF NEW YORK

Abstract

METHAMPHETAMINE-INDUCED CYTOGENESIS IN THE MOUSE STRIATUM: NEUROCHEMICAL AND BEHAVIORAL STUDIES

By

Ingrid Tulloch

Adviser: Professor Jesus Angulo

The commonly abused drug methamphetamine (METH) is toxic to monoamine axon terminals, and cause neuron death. However, the mechanisms and events following neurotoxic METH exposure are not fully understood. For example, numerous studies with rodent models of METH–induced damage show a disparity in the duration of neuron death. Additionally, the striatal volume of some human users is enlarged after METH, and is accompanied by normal cognitive and motor performance. However, participants with smaller striatal volume after METH have poor cognitive outcome. Gliogenesis and swelling from inflammation have been proposed as reasons for volume changes. However, explanations for variability in the time course of METH-induced cell death have not been addressed until now. Presented in this thesis are results from neurochemical and behavioral studies, which provide evidence that cytogenesis is in part, a mechanism for cognitive but not motor recovery after toxic METH damage. Cytogenesis is accompanied by increased striatal volume in adult mice. A significant proportion of the new cells die in a protracted manner over three months, accounting for the disparities in time course of METH-induced cell death. Furthermore, the results suggest volume changes may be due to both gliogenesis and neurogenesis because

proportions of the newly generated cells remaining at 12 weeks express histochemical markers for astrocytes, microglia, and neurons. Small sub-populations of the new neurons express histochemical markers for parvalbumin and choline acetyltransferase interneurons that were lost during acute METH damage. Neuron maturation is accompanied by improved habit learning on a reinforced T-maze task. However, motor deficits persist and even worsen as METH-treated mice age. Measures of activity in the open-field suggest these behavioral effects were not due to anxiety, as METH-treated mice also show deficits in motor related measures but hardly differ from control mice on anxiety measures. More studies are needed to advance understanding of the underlying mechanisms of damage and facilitate recovery from the effects of this increasingly abused substance. Therefore, studies designed to identify the remaining new cells and the role damage-induced cytogenesis may play in addiction and motor disorders are not only needed, but are logical extensions of the data presented.

Acknowledgements

I would like to thank the many people without whose help I would have been unable to complete this project. I am thankful for my parents, Beverly and Henry Tulloch for always being supportive of what I choose to do and the many hours of babysitting so I could complete this work. I thank my sister Denise Tulloch whose courage in the face of adversity gave me the strength and reasons for returning to school and pursuing a doctoral degree in biological psychology. I am extremely thankful to my husband Elan and daughter Jafira who were forever patient and understanding of "I can't, I have to work" or "don't wait up I'm working late." Their sacrifices allowed me to pursue my dreams and words cannot express enough thanks. The Hunter College staff in the MBRS and Gene Center offices, as well as Ellen Breheny in the Biopsycology office, made the paperwork much easier, so I could focus on the science. I have also been fortunate to have several mentors over the years that encouraged and helped me grow as a scientist and a person. Dr Cheryl Harding gave me a chance in her lab, and my first real lessons in thinking like a scientist. Dr Victoria Luine has been a tireless advocate and made sure I had support to do the work. The folks at Columbia University have taught me some of the techniques that I used in completing this project. Thus, many thanks are also due to Dr Richard Marks, Dr Erik Kandel, Dr Christoph Kellendonk and Dr Eleanor Simpson at Columbia University Center for Neurobiology and Behavior. I am thankful to Dr. and Mrs. Jadczyk and the QFS for providing a heaven for learning and growth so I can pursue the objective studies they emphasize the world needs. I am extremely grateful to my thesis committee members: Dr Jesus Angulo, Dr Jean Lud Cadet, Dr Vanya Quinones-Jenab, Dr Shirzad Jenab, and Dr Peter Serrano. They have challenged me and provided

guidance toward the completion of this work. Drs. Serrano and Harding generously allowed me the use of their laboratory equipment in completing the behavioral component of this work. Dr Angulo has been more than a thesis advisor. He is a wonderful example of what I would like to be as a scientist. I am forever in his debt for the many ways in which he has helped me to grow as a scientist and person. Last but not least, I am also thankful to my peers in Dr Angulo's lab and the interns that have worked with me over the course of the studies described in this thesis. Ina Mexitaj, Nane Gharzaryan, Dalila Ordonez, Lisa Baker, Lauriaselle Afanador, Haley Yarosh, Arturo Garza -Gongorra and Holly Payne. At various times each would lend an ear when I needed to vent about a failed assay and each was always willing to be an extra pair of hands when I needed someone blind to the treatment conditions for quantification. I suspect that very few people undertake a doctorate degree without a supportive network of individuals. I have been very fortunate and am extremely thankful to be surrounded by a very supportive friends, family and mentors.

Table of Contents

Title **Page#**

Continues…

Continues.…

List of Abbreviations

5-HT…….....Serotonin

5-HTT……Serotonin Transporter

6-OHDA……...6-Hydroxydopamine

7-OH-DPAT….7-hydroxy-dipropylaminotetralin

ACh……..Acetylcholine

βIII-tub…….Beta-III-Tubulin

BBB……..Blood brain barrier

BrdU……5-bromo-2-deoxyuridine

ChAT……Choline Acetyltransferase

D1R……..Dopamine Receptor 1

D2R……..Dopamine receptor 2

DA…….....Dopamine

DAB……3,3'-Diamininobenzedine

DAT….....DA Transporter

DCX…….....Doublecortin

ER……....Endoplasmic reticulum

GABA…….Gamma Aminobutryic Acid

GAD_{67}…….Glutamic Acid Decarboxylase

Glu……..Glutamate

GluR……...Glutamate receptor

mGluR……Metabotropic glutamate receptor

[‘H] MRS……Proton MR spectroscopy

IB4……Isolectin B4

MPTP……1-methyl-4-phenyl-1,2,3,6-tetrahydropyridine

MAO……Monoamine oxidase

MRI……..Magnetic Resonance Imaging

NE…….....Norepinephrine

NeuN…….Neuronal nuclear Protein

Nk/Nk1R…...Neurokinin/NK1 receptor for substance P

NMDA……...N-Methyl-D-Aspartate

NMDAR…....N-Methyl-D-Aspartate receptor

NO……...Nitric Oxide

nNOS…. …….Neuronal Nitric oxide synthase

NPY…….Neuropeptide Y

PV…….……Parvalbumin

ROS……..Reactive oxygen species

SP…….…….Substance P

SST…….……...Somatostatin

SVZ…….……..Subventricular zone

TH……..Tyrosine hydroxylase

TpH……Tryptophan hydroxylase

VMAT……...Vesicular monoamine transporter

VTA……..Ventral Tegmental Area

List of figures

Continues….

List of tables

Note: Tables 7-11 are found in the appendix.

Chapter 1

Introduction

The purpose of this study was to investigate the neurochemical and behavioral events that follow acute methamphetamine (METH)-induced cell death in the striatum after a neurotoxic dose of the drug. The three underlying questions driving the study were: Are new cells generated after striatal damage induced by a neurotoxic dose of METH to influence volume changes? If so, do new cells survive and mature to phenotypes shown in previous studies to die during the acute response to METH? How would behaviors that require striatal function change over the time course of events following neurotoxic exposure to METH? In order to answer these questions a series of studies were undertaken with the following working hypothesis. After METH exposure and acute striatal damage, the generation and maturation of new cells over the same time course as variations in motor and habit learning is a compensation for damage. To provide the background and rationale that led to the hypothesis and methods used to generate results, several topics are discussed in this chapter. First the general background will cover the history of METH use and its clinical effects. Second, a review of the animal models that provided evidence for METH-induced neural damage is discussed. Third, likely mechanisms based on animal models are reviewed along with the corroborating human data. Fourth, an overview of striatal neurochemistry which makes this structure both vulnerable to damage, and a likely candidate for METH-induced cytogenesis is presented. Fifth, the role of the striatum in specific behaviors and METH effects on behavior are reviewed along with evidence for cytogenesis in response to neural damage. Finally, this chapter concludes with the proposed model of striatal events

following METH exposure, and the three study aims used to test the working hypothesis. This extensive background and rationale was presented because it is necessary for designing experiments to advance knowledge of METH effects on neural systems that can later be enhanced to aid improved recovery outcomes for individuals exposed to toxic levels of the drug.

.

I. Background and significance

A. What is methamphetamine? Attributes, history and epidemiology.

Methamphetamine (METH) is a potent psychostimulant with highly addictive properties. It is actually an amphetamine with an added methyl group, which results in high lipid solubility. These characteristics allow METH to easily cross the cell membrane to exert its effects (Barr et al., 2006). As an amphetamine analog, METH belongs to the second most abused class of drugs worldwide (UNDOC, 2008). It appears as a white odorless crystalline powder with a chemical structure similar to that of the neurotransmitter dopamine (NIDA, 2006). The chemical similarity to dopamine (DA) is a significant component of its effects on this and other monoaminergic neurotransmitter systems. METH can be ingested, inhaled/smoked or injected (NIDA, 2006) and was developed from ephedrine around the late nineteenth and early twentieth century in both Japan and Germany (Grinspoon and Hedblom, 1975). Not initially popular, the drug was used during the early part of the twentieth century for treating various ailments. For example, METH and other amphetamine variants were once prescribed for treating obesity, depression, narcolepsy, alcohol, addiction and even schizophrenia and Parkinson's disease (Grollman, 1954).

The relatively long half-life of METH (approximately 12 hours) induces a significant duration of intoxication relative to other abused substances (Gonzales et al., 2000). When smoked METH can produce a high lasting anywhere from 8 to 24 hours (NIDA, 2006). Due to its stimulant properties, during the Second World War amphetamines became popular amongst military personnel that required sustained attention and stamina. For example, under the trade name Prevartin, METH tablets were given to German pilots and Panzer troops. The Japanese forces used it under the name Philopon. Allied forces also used METH under the trade name Methedrine along with other forms of amphetamine-like drugs (Grinspoon and Hedblom, 1975; Rasmussen, 2008).

METH became a popular recreational drug and attempts to curb its increasing use in the 1950s and in the 1960s restricted its clinical availability to prescription only. However, it was not until 1971 that the drug enforcement agency designated METH a schedule II drug (Angelin et al., 2000; Colman, 2005; Rasmussen, 2008). This meant that despite its medicinal value, as a "highly addictive substance" it required strict regulation for access and use (Angelin et al., 2000; Colman, 2005). With the increasing awareness of its clinical effects, by the 1980s the FDA rescinded its approval of METH for all but ADHD and short term-obesity treatment under the trade name Desoxyn. However, it is used off label for narcolepsy (Lundbeck Inc, 2009). Amphetamines in general are now only legally available via non-refillable prescription from a physician. However, the illegal manufacture and use of METH has been an ongoing public health and criminal justice issue worldwide.

METH can be synthesized from precursors in over-the-counter decongestants containing epinephrine and pseudo-epinephrine (US dept. of justice, 2007). As previously mentioned, the half- life of METH also allows for a longer duration high. Thus, it is a popular and relatively cheap drug, aptly named by former white house drug czar, Barry R McCaffery, "the poor man's cocaine" (Knight, 1997). Starting in the 1980s, laws were passed in the United States and other countries making it illegal to possess equipment for the manufacture of METH and other "designer drugs" (Colman, 2005). Currently under the US patriot Act, there are restrictions on the quantity of non-prescription drugs that can be purchased which contain METH precursors (US Dept. of Justice, 2007). According the UN Office on Drugs and Crime 2008 report, METH is the most illegally synthesized drug in the United States. The increase in illegal manufacture of METH is such that it is common for hospital emergency rooms to encounter patients with injuries related to the operation of illegal METH labs in the United States (Santos et al., 2005).

Today, METH goes by several street names including: "speed", "chalk", crystal, 'ice," "glass" or "crank". According a US Substance Abuse and Mental Health Services Administration (SAMHSA) study, in 2008 over 300,000 Americans 12 years or older used METH at least once during the prior year, and 95,000 of them were new users SAMHSA, 2009a). In 2009 the number of new METH users increased by 60% (SAMHSA, 2010). Furthermore, agencies that provide early warning trends in drug related emergency room visits and arrests, suggest that METH abuse may be much worse than survey reports indicate (National Drug Intelligence Center, 2009).

The drug abuse warning network (DAWN) report sponsored by SAMHSA shows that METH-related emergency room visits and criminal justice encounters actually had an increasing trend between 1995 and 2006, with a slight decrease in 2007 (SAMHSA-TED, 2009). Additionally, the 2009 National Drug Intelligence Center (NDIC) *National Methamphetamine Threat Assessment* suggested that the increased seizure of METH products imported from Mexico and Southern Asia might have led to increased domestic production in the US. METH abuse and trafficking is also a worldwide problem. In addition to the United States, Australia and Canada, several Southeast Asian and Pacific Ring nations have had to contend with issues related to METH abuse and trafficking (United Nations office on Drugs and Crime, 2007). Japan, for example, has had a number of METH abuse epidemics over several decades (Jenner and McKetin, 2004), while trafficking through the near and Middle East has increased, with one third of amphetamine–type drug seizures occurring in Saudi Arabia in 2008 (United Nations Office on Drugs and Crime highlights, 2009). Particular concerns with METH abuse are the economic burden on the public health and criminal justice system, as well as, lost productivity in users. In 2005, the estimated public burden of METH abuse was 23.4 billion (Nicosa et al., 2009).

B. Clinical features of use

The clinical effects of METH include a number of physiological and psychological symptoms that can result in significant health complications. The acute effects however, are similar to that of other stimulant substances such as caffeine and cocaine. The longer duration high, as well as its effects on multiple monoamine transmitters (dopamine, serotonin and norepinephrine) makes METH a more potent

psychostimulant. For example, acute METH exposure increases heart rate and blood pressure, pupil dilation (Peck et al., 2005) and hyperthermia (Brown et al., 2003; Sandoval et al., 2000). METH-overdose can result in heart attacks, convulsions, stroke and death (Dean 2004; NIDA, 2006).

METH also results in several physiological and psychological features that further promote its use. Depending on the dose and method of use, acute METH, for example, causes an increase in attention, energy, wakefulness, sensory acuity, physical activity, along with decreased anxiety, and appetite (Dean, 2004; Homer et al., 2008; Meredith et al., 2005). These effects of the drug make it attractive for individuals requiring sustained alertness, wish to lose weight or overcome shyness in seeking sexual relationships. Psychologically, METH produces feelings of euphoria and confidence while lowering inhibitions (Barr et al., 2006; Dean, 2004). In a study of gay males seeking treatment, for example, the physically and psychologically rewarding effects of METH were self-reported as contributing factors in use (Peck et al., 2005).

In contrast to the rewarding effects, aversive METH effects, particularly with long-term use, includes dry mouth, sweating, chest pains, and shortness of breath, anxiety, agitation and psychosis. The latter three are similar to the positive symptoms of schizophrenia, and METH has been used in animal models of this disorder (Machiyama, 1992). As the drug is cleared from the body, the initial agitation and hypermotor activity declines and the user becomes fatigued (Dean, 2004; Kalant, 1973; Meredith et al., 2008).

METH use has long-term risks and consequences that can affect several aspects of health. An increased risk for Parkinson’s disease and HIV is associated with use, for

example (Callaghan et al., 2010; Garwood et al., 2006). Compared to individuals without the disease, individuals diagnosed with Parkinson's disease show greater incidence of prior METH use (Callaghan et al., 2010). METH use also increases the risk for contracting HIV, due to the risky behaviors, such as unprotected sex while intoxicated, and hyper sexuality that accompany use (Garofolo et al., 2007; Mansergh et al., 2006; Thiede et al., 2003). Like other addictive substances, repeated METH use escalates as pleasurable effects diminish and aversive effects increase. Repeated use is a component of the long-term health effects of METH. For example, chronic METH use is often accompanied by skin picking and needle bruising, which results in disfiguring skin lesions and infections. However, users at this stage find it difficult to stop (Lee et al., 2005). Furthermore, according to the American Dental Association (2005), chronic METH use is also accompanied by tooth decay that may be driven by a variety of factors ranging from the acidity of the drug to poor nutrition and oral hygiene (Shaner, 2002). METH users are also at risk for stroke due to drug-induced hypertension (Lineberry and Bostwick, 2006), as well as, respiratory distress from its deleterious effects on lung and heart tissue (Dean, 2004). Finally, METH use results in changes in cognitive and motor performance though studies have found mixed results regarding enhanced or diminished cognition.

There have been suggestions that acute effects of amphetamine-type drugs include improved cognitive performance for new users (Gelowitz et al., 1994; Kirkpatrick et al., 2008; Pieterzack et al., 2010; Soetens et al., 1995). For individuals under extended wakefulness, the improved performance with METH was more pronounced (Hart et al., 2001; Wiegmann et al., 1996). Many of these studies of enhanced cognition used low

doses not typical with abuse. Furthermore, the recognition of frequent multi-drug use by substance abusers required studies that account for this phenomenon. Some studies show a different effect than improved cognition. For example, METH exposure results in cognitive deficits in memory recall and recognition tasks for current (Simon et al., 2000) and abstinent users (Newton et al., 2004; Rendell et al., 2009; Scott et al., 2007). Moreover, Rendell et al. (2009) revealed that former users had impairments on tasks that test for memory of future intentions compared to drug naïve individuals. Additional supportive evidence come from METH related emergency room visits. A significant proportion of visits are related to central nervous system disturbances and cognitive behavioral changes that increase the negative health outcome for patients (Lineberry and Bostwick, 2006).

II. Animal models demonstrate METH-induced neural damage

A. Early studies demonstrated damage

Attributes of METH, such as its lipid solubility and similarity to the chemical structure of monoamines confer easy access to neural tissue. In the brain it then exerts potent effects resulting in damage. A series of animal studies beginning the 1970s and continuing today have provided evidence that brain monoaminergic systems are particularly vulnerable to METH-induced damage. Escalante and Ellinwood (1970) found that cats chronically exposed to amphetamines had neuronal chromatolysis. However, many of the groundbreaking studies revealed toxicity of monoamine pathways in rodents and non-human primates after METH treatment (Hotchkiss and Gibb, 1980; Seiden et al.,

1976). More recent confirmation of similar effects has been revealed in humans (Chang et al., 2005; Volkow et al., 2001a).

The role of dopamine in the induction of METH damage was presented in an early study showing diminished striatal tyrosine hydroxylase (TH) activity; the rate limiting step for DA and subsequent NE synthesis (Fibiger and McGeer, 1971). The damage may be due, in part, to DA auto-oxidation, which increases the formation of toxic substances such as 6-OHDA and other reactive species following METH treatment (Kita et al., 1995; Seiden and Vosmer, 1984). Based on reports from numerous studies, serotonin (5-HT) systems are similarly vulnerable to damage (see review by Krasnova and Cadet, 2009). However, it is thought that DA overflow into the cytosol and extracellular space is the beginning of multiple biochemical cascades that end in neural damage, subsequent dependence and alterations in cognition and behavior (Sonsalla et al., 1986)

B. Studies with mice

Depletion and subsequent terminal toxicity (degeneration) is seen in axon endings of neurons containing DA metabolites, NE, or 5-HT. METH-induced neural damage can be revealed in several ways (see Krasnova and Cadet, 2009 review). Damage can be measured via transporter (VMAT, DAT and 5-HTT) binding or protein levels. Damage can also be measured via immunoreactivity or protein levels of TH or TpH, respectively, the rate limiting enzymes for DA/NE, and 5-HT synthesis. Microdialysis studies that measure the extracellular levels of monoamines or their metabolites, and histochemical

methods for apoptotic cell death and glial activation markers are among a variety of additional neurochemical methods for assessing METH damage. However, as transporters are a measure of terminal integrity, many studies examining DAT, revealed METH had a toxic effect on the DA system without killing DA releasing neurons.

In mice, most of the striatal DA depletion has been observed from twelve hours to three weeks after METH (Achat-Mendez et al., 2007; Bowyer et al., 2008; Deng et al., 1999; Green et al., 1992; O'Callaghan and Miller, 1994; Zhu et al., 2005). Toxicity studies also show decreased DA and DAT levels or binding in the striatum up to three weeks (Achat-Mendes et al., 2005; Green et al., 1992), as well as, in the cortex and amygdala up to two weeks after METH (Anderson and Itzhak, 2006; Fantegrossi et al., 2008; Landenheim et al., 2000). Decreased 5-HTT levels or binding in the striatum and hippocampus has also been observed forty-eight hours to two weeks after METH exposure (Fumagalli et al., 1999; Landenheim et al., 2000). Many of the studies from the late 1990s up to the present have also shown significant cell death in response to METH.

Using TUNEL immunohistochemistry as a marker for apoptotic cell death, for example, decreases in hippocampal and cortical neurons were observed at time points ranging from twenty-four hours to one week after METH (Deng et al., 1999; 2001; Thieret, et al., 2005; Zhu et al., 2005; 2006). Death of striatal projection neurons immunopositive for enkephalin (Thieret et al., 2005) as well as ChAT and parvalbumin (PV) interneurons (Zhu et al., 2006) were seen in METH treated animals. It is interesting that neuronal nitric oxide synthase/somatostatin/ neuropeptide Y (nNOS/SST/NPY) containing interneurons were spared the damage (Zhu et al., 2006). The mechanisms of this protection and its role in METH damage are currently being researched in our lab.

Glial cells are another cell type in the brain involved in a variety of important functions but affected by METH. Glia helps to maintain brain homeostasis, immunoprotection, survival and differentiation of neurons (Allen and Barres, 2009). For these functional reasons, it is not surprising that reactive gliosis accompany the damaging effects of METH. For example, whether administered in a single bolus dose (30-40mg/kg bodyweight), or by four binge doses (5-10 mg/kg bodyweight each) two hours apart, increased GFAP staining of astroglia were seen in the striatum at two, three and five days after injections (Achat-Mendes et al., 2007; Zhu et al., 2005). Activated microglia were also observed one, three and fourteen days after METH injection (Bowyer et al., 2008; Fantegrossi et al., 2008; Landenheim et al., 2000; Thomas et al., 2004c). Of notable interest is that repeated intermittent low dose treatment with METH reduces migroglial activation in mice. Furthermore, METH-induced microglia activation is suggested to mediate the tolerance effect of METH in mice (Thomas and Kuhn, 2005a).

C. Studies with rats

Some of the early studies demonstrating METH-induced damage to monoaminergic systems were also done in rats (see Krasnova and Cadet, 2009 review). Hotchkiss and Gibb (1980) for example, revealed that METH reduced TH activity in the striatum up to a month, and tryptophan hydroxylase (TpH) up to a week in the hippocampus. Wagner et al. (1980) found that METH decreased rat striatal DA levels up to two weeks, and DAT sites up to eight weeks after treatment. Furthermore, Ricuarte et al. (1980) found reduced mesolimbic and nigrostriatal DA as well as 5-HT in multiple

structures of the limbic and motor systems three weeks after treatment. The overwhelming evidence from these animal models revealed that early (within the first thirty-six hours) and long-term (more than three months) effects of METH include reduced TH, and 5-HT and NE in the striatum and hippocampus (Bakhit et al., 1981, Graham et al., 2008). These studies also provided evidence implicating monoaminergic mechanisms in METH-induced neural damage. For example, Lorez (1981) found swollen nerve fibers in the striatum at six and eleven days after METH, while Commins and Seiden (1986) revealed cortical neuronal degeneration at two days. Morphological studies of both DA and 5-HT terminals also revealed evidence of degeneration (Axt and Molliver, 1991; Fukui et al., 1989; Ricuarte et al., 1982). However, the reduction of striatal DA transporter (DAT) numbers (Eisch et al., 1992, Guillarte et al., 2003, Segal et al., 2003), monoamine vesicle transporter-2 (VMAT-2) binding (Guillarte et al., 2003; Segal et al., 2003 and 2005), and protein faction (Johnson-Davis et al., 2004) provided the strongest evidence for the role of dopamine transport in METH-induced damage.

As in mice, studies in rats using TUNEL immunostaining also revealed METH-induced cortical cell loss up to nineteen days after the first of a twelve-day regimen of 5mg/kg injections (Kadota and Kadota, 2004). A 40mg/kg bolus injection of METH also resulted in cell death; however, this was seen in the striatum between 1 and 3 days after the injection (Jayanthi et al., 2005). As late as 30 days after the last injection of an escalating binge dose of METH there are signs of apoptotic damage. Kuczenski et al. (2007) for example, found reactive gliosis as well as cortical and hippocampal neuron death of calbindin interneurons in long-term studies with rats. Furthermore, neuron death

was found in both the developing (Pu et al., 1996) and the adult rat brain in response to METH (Eisch and Marshall, 1998)

As mechanisms of METH-induced damage were being elucidated, several studies in rats also demonstrated ways in which the brain may be protected from METH. For example, despite the extensive damage with binge or bolus dosing schedule, neural systems can become tolerant in a manner such that monoaminergic depletion is attenuated when animals were later given a challenge dose (Danaceau et al., 2007; Riddle et al., 2002a). Moreover, protection has been seen from acute and long term DA and 5-HT depletion in the striatum and cortex after a single high dose (bolus) challenge of METH. The protection occurs if preceded by low dose treatments or increasing doses of METH over a period of time (Gygi et al., 2006; Schmidt et al., 1985b; Stephans and Yamamoto, 1996). Animals treated with these protective regimens also show lower levels of methamphetamine concentration in the brain during the acute response (Alburgess et al., 1990).

Additional protection from striatal DA terminal injury and cortical cell death was revealed when Eisch and Marshall (1998) treated rats with a DAT inhibitor, and then used fluoro-jade histochemistry to measure parameters of cell death. Furthermore, DA receptor blockade reduced toxic damage and cell death (Broening et al., 2005; O'Dell et al., 1993). However, as rodent models allowed more accessible ways of studying the mechanisms of damage, as well as, protection from damage after METH, studies in non-human primates provided the advantage of a closer approximation of the drug's effects in humans.

D. Studies with non-human primates

Non-human primates have long been used to study the effects of methamphetamine on neural systems. In 1976 Sieden and associates demonstrated that rhesus monkeys given METH in escalating binge doses over time had reduced NE and DA in several areas of the brain. It is notable that this dosing pattern is similar to the human pattern of METH use and it is accompanied by long term-effects in the striatum. For example, with the escalating binge method, Sieden et al. (1976) found up to 80% DA depletion in the monkey brain after six months. Several follow up studies demonstrated that similar dosing regimens also decreased 5-HT levels in the cortex, thalamus, striatum and hippocampus, as well as, DA levels or binding sites in the striatum ranging from one to six months after injections (Ando et al., 1985; Finnegan et al., 1982; Preston et al., 1985a; 1985b; Villemange et al., 1998; Woolverton et al., 1989).

Like the previously cited studies in rodents, although METH affects 5-HT systems, pronounced long-term effects in non-human primates are most evident on the striatal DA system. Confirmation of these effects can be found in more recent studies using positron emissions tomography (PET) imaging. For example, PET imaging of both monkeys and baboons show reduced DA production, DA levels and DAT binding in the striatum (Melega et al., 1997; 2000; 2008; Villemagne et al., 1998). Melega et al. (2008) further demonstrated significant decreases in the percent of DA and DAT binding in the striatum of vervet monkeys treated with a long term (thirty-three weeks) escalating doses similar to the human pattern of use.

While the previously described METH-induced effects on DA were observed in the striatum, DA cell bodies in the substantia nigra remained intact after METH. This provided evidence for striatal DA terminal toxicity specifically in response to METH injections (Melega et al., 1997). Furthermore, the effects on both 5-HT and DA in non-human primates persist after long-term abstinence (Woolverton et al., 1989). Despite the many studies with animal models that have provided a significant amount of information regarding METH action on neural systems, the mechanisms and even a complete time course of events after METH are still poorly understood. As the previous sections have shown, what is generally known and is still an active area of study, are the neurotransmitter systems affected by METH exposure.

III. Mechanisms of neural damage

A. DA overflow triggers a cascade of events

The precise molecular mechanisms of METH damage are still being worked out in multiple research studies. However, based on the works already cited, it is clear that METH's similarity to the chemical structure of dopamine implicates this neurotransmitter. Several mechanisms of damage have been proposed to include toxic substances and free radicals resulting from excess dopamine, glutamate and NO signaling. Furthermore, activated glial cells, which can release additional damaging substances, have also been suggested as a mode of damage (Kita et al., 2009 review; Lavoie et al., 2004). Blood brain barrier (BBB) dysfunction, altered thermoregulation (hyperthermia, in particular) and gene expression are among other proposed mechanisms of damage (Boyer and Ali, 2006; Kiyatkin et al., 2007; also see review by Krasnova and

Cadet, 2009). Pre and post-synaptic mechanisms triggered by altered DA trafficking and subsequent DA overflow in the cytosol and extracellular space, result in increased free radicals and multiple signaling cascades leading to damage.

METH inhibits monoamine oxidase (MAO), the enzyme that inactivates monoamine neurotransmitters (Carlsson, 1970; Glowinski, 1970). METH also causes reversed DAT mediated release of dopamine into the extracellular space and reduced VMAT-2 uptake of DA from the cytosol of axon terminals (Cubells et al., 1994; Sulzer et al., 2005). A direct result of METH effects on MAOs and neurotransmitter trafficking is excess extracellular and cytosolic DA. Excess DA leads to auto-oxidation and subsequent reactive oxygen species (ROS) formation (Guillot et al., 2008; Larsen et al., 2002; LaVoie and Hastings, 1999b). These events overwhelm antioxidant and free radical scavenging systems leading to damage and cell death (Chen et al., 2007; Jayanthi et al., 1998; Krasnova et al., 2001). Lavoe and Hastings (1999) for example, found that high doses of METH led to increased cysteinyl-DA metabolites in the striatum. Furthermore, MAO effects on DA increase hydroxol radicals and iron, (Cadet and Brannock, 1998; Giovanni et al., 1995; Melega et al., 2007). The free radicals and iron increase lipid peroxidation (Acikgoz et al., 1998) that damage terminal membranes, mitochondria and nuclear DNA, which leads to terminal degeneration and cell death (Potashkin and Meredith, 2006).

Evidence for free radical damage in response to METH was provided by studies in which increased antioxidants conferred protection. Krasnova et al. (2001) for example, found that mice overexpressing the antioxidant copper- zinc-super oxide dismutase (CuZnSOD) show less DA toxicity. In addition, pre-treating monkeys with powerful

antioxidants like n-acetyl-L-cysteine before METH prevents terminal damage (Hashimoto et al., 2004). These studies all suggest the need for significantly more than the normal levels of antioxidants to counter increased free radical production after METH. Based the role of transporters in DA overflow and subsequent damage, transport manipulation offers another mechanism of protection. Studies in which TH or DAT are inhibited or VMAT-2 function is enhanced have shown protection from METH-induced damage. For example, inhibition of TH with alpha methyltyrosine prevents DA depletion (Wagner et al., 1983). DAT inhibition with amphoneic acid protects against METH-induced reduction in TH, DA and DAT binding in the striatum (Marek et al., 1990; Schmidt and Gibb, 1985).

Studies also revealed that animals lacking DATs do not have the levels of DA depletion, astroglia upregulation or free radical damage that is common after METH treatment (Fumagalli et al., 1998). Furthermore, although reverse DA transport appears to alter vesicle uptake of cytosolic DA, treatment with DAT inhibitor methylphenidate attenuates METH-induced reduction in VMAT-2 binding (Sandoval et al., 2003). The result of attenuated VMAT-2 decrease is less damage. Post-METH treatment with lobeline-an exogenous ligand for VMAT-2- also attenuates VMAT-2 deficits and confers protection from METH–induced DA damage in the striatum (Eyerman and Yamamoto, 2005; Wilhelm et al., 2004). In contrast, knockout mice heterozygous for loss of VMAT-2 show increased METH-induced toxicity (Fumigalli et al., 1999), increased DA synthesis and ROS formation (Larsen et al., 2002). Additionally, while inhibition of VMAT-2 with reserpine causes an increase in toxicity, DA receptor mediated activities

seems to also play a role in vesicular alterations as well as other aspects of damage (Albers and Sonsalla, 1995; Wagner et al., 1983)

Results from a study by Ugarte et al. (2003) suggested that D1 receptor antagonist SCH23390 did not protect from METH-induced deficits in vesicular uptake. However, other studies have demonstrated that D1R blockade confers protection from other damaging effects of METH. For example, D1R blockade prevented DA depletion and increased glial activity, inhibited FasL and caspase-3 cell death pathways in striatal neurons, and reduced but did not eliminate cell death (Angulo et al., 2004; Jayanthi et al., 2005; Xu et al., 2005). In the same study by the Ugarte group, D2 receptor antagonist ecticlopride attenuated vesicular trafficking deficits along with hyperthermia induced by METH (Ugarte et al., 2003). Interestingly, D2R activation by agonists like cocaine or DAT inhibitor methylphenidate increased vesicular trafficking and redistributed VMAT-2 protein (Riddle et al., 2002b; Sandoval et al., 2003; Truong et al., 2004; Ugarte et al., 2003). These studies also suggests METH- induced damage involves interactions between specific DA receptor subtypes and other regulatory mechanisms, and may explain the slightly less damaging effects of cocaine.

Since DA plays a role in thermoregulation for example, (Balthazar et al., 2010; Chaperon et al., 2003; Ito et al., 2008; Zarrindast, 1992), METH effects on DA function involves body temperature changes. During the acute phase of METH, increases in core body temperature upregulates DAT activity (Xie et al., 2000); further potentiating excess DA and the subsequent biochemical cascades. For example, reactive species formation and oxidative stress are components of METH damage affected by temperature (Albers and Sonsalla, 1995; Bowyer et al., 1994; Miller and O'Callaghan, 1994). Evidence for

the role of hyperthermia was revealed in studies that show hyperthermia is accompanied by increased DA quinones and DA oxidation after METH (Lavoie and Hastings, 1999). Hyperthermia may inhibit TH (Kuhn et al., 1999), as well as, proteins involved in detoxification (Zafar et al., 2006). For example, Zafar et al. demonstrated that the oxidation of dopamine by tyrosinease products inhibits proteosomes. The proteasome inhibition was not reduced by the antioxidant superoxide dismutase but the addition of quinine reductase and NADH protected against this effect, and it correlated with temperature changes. Furthermore, hyperthermia induced changes in protein activity and upregulation of toxic reactive species cause damage specific to DA cells (Montine et al., 1997; Spencer et al., 2002). In contrast, reactive species formation is prevented in animals kept at low environmental temperature (Lavoie and Hastings, 1999).

In addition to the study that demonstrated D2 receptor blockade induces reduction of hyperthermia and toxicity, (Ugarte et al., 2003), DAT and 5-HTT-knockout mice show reduced hyperthermic response to METH (Numachi et al., 2007). However, the presence of the DAT or the 5-HTT genes is accompanied by hyperthermia in experimental animals (Numchi et al., 2007). This suggests 5-HT activity also has a role in the hyperthermic response and subsequent damage after METH. Furthermore, METH increases interlukin-1β, and this protein also induces hyperthermia (Numchai et al., 2007, Yamaguchi et al., 1991). For example, administration of interlukin-β receptor antagonist blocks METH-induced hyperthermic effects (Bowyer et al., 1994).

A notable observation is that hyperthermia appears to increase oxidative damage via blood brain barrier (BBB) dysfunction, which further exposes the brain to damaging substances (Sharma et al., 2007; Sharma and Kiyatin, 2009). For example, Sharma and

Kiyatin (2009) found abnormal cytoplasm and nuclear folding of epithelial cells of the choroid plexus, and this finding correlated with hyperthermia after METH. Abnormal cytoplasm and nuclear folding are significant for BBB permeability because epithelial cells of the choroid plexus are actively involved in plasma filtering and the formation of cerebrospinal fluid (Emerich et al., 2004). Bowyer and Ali (2006) corroborated findings that implicated hyperthermia in BBB dysfunction when they failed to observe BBB dysfunction in animals that did not have hyperthermia after METH. Consequently, BBB dysfunction that correlated with temperature increases was observed in follow up studies (Bowyer et al., 2008). However, studies in which hyperthermia is prevented only provides partial protection from METH damage (Albers and Sonsalla, 1995; Ali et al., 1996; Bowyer et al., 1994; Tata et al., 2007). These findings suggest that non-hyperthermic mechanisms acting through either dopamine or other transmitter mediated cellular cascades contribute to damage.

In addition to the previously reported DA transporter effects, evidence of a dopaminergic trigger for damage are studies in which, D1 and/or D2 receptor blockade protects against METH-induced neurochemical deficits and cell death (Angulo et al., 2004; O'Dell et al., 1993; Sonsalla et al., 1986; Xu et al, 2005). For example, O'Dell et al. (1993) gave rats D1R antagonist SCH23390 or D2 antagonist eticlopride 15 minutes before injections in a binge-dosing regimen (4 X 10 mg/kg). D1 and D2R blockade attenuated acute DA overflow, and subsequent DA depletion a week after treatment. Using a single bolus treatment, Xu et al. (2005) demonstrated that D1R antagonist SCH23390 or the D2R antagonist raclopride before METH completely prevented striatal apoptosis, TH depletion and glial fibrillary acidic protein (GFAP) up regulation. In the

same study Xu et al., also found that DA receptor blockade did not prevent hyperthermia again suggesting both hyperthermic and non-hyperthermic mechanisms of damage involving DA.

Suggestions that glutamate activity stimulated by DA may also induce hyperthermia were revealed by studies with glutamate receptor antagonist MK-801. MK-801 prevents hyperthermia and reduces DA terminal toxicity (Sonsalla et al., 1989). However, another piece of evidence for non-hyperthermic mechanisms of damage is the finding that treatment with glutamate receptor antagonists that do not prevent hyperthermia also protects from damage (Bowyer et al., 2001; Fuller et al., 1992). As with DA, these studies suggest glutamate-mediated damage in response to METH can be temperature dependent and independent. The latter will be explored further below.

B. The involvement of glutamate.

As mentioned above, METH also increases glutamate signaling, which plays a role in toxic damage. Increased glutamate signaling and the subsequent nitric oxide upregulation it causes, results in additional reactive species and subsequent damage (see Krasnova and Cadet, 2009 review). Evidence from blocking its mGlu5 receptors have shown that inhibition of glutamate signaling either reduces dopamine overflow or have no effect on DA overflow when accompanied by reduced toxicity. For example, Battaglia et al. (2002) pre-treated mice with mGlu1, mGlu 2 and 3 or mGlu 5 glutamate receptor antagonists before METH administration. ROS formation and striatal DA terminal toxicity were attenuated with mGlu5R antagonist treatment without affecting dopamine release. In contrast, blocking mGlu1 and Glu2 or 3 receptors did not alter

METH-induced toxicity. Furthermore, in both primates and rodents, Tokunaga et al. (2009) used the same mGlu 5R antagonist used in the Battaglia et al. study and demonstrated significant decreases in dopamine overflow.

In addition to glutamate release, METH also increases glutamate transporters, and intracellular calcium and calmodulin binding (Mark et al., 2007). This process also induces excitotoxicity (Takano et al., (2003). Thus, glutamate receptor activity can directly induce or exacerbate METH damage. Lending further evidence to the glutamate hypothesis of damage, are findings which show that glutamate receptor agonist N-methyl-D-aspartate (NMDA) administered with a non-toxic dose of METH results in toxicity (Sonsalla et al., 1998). In contrast, treatment with NMDA receptor antagonists without hyperthermia blocks METH-induced toxicity (Bowyer et al., 2001; Fuller et al., 1992). These results suggest glutamate NMDA receptor activity as a specific mechanism of damage. Metabotropic glutamate receptors (mGluR) may also play role, as one subtype -mGluR type 5 is coupled with NMDA receptors and further enhances NMDA activity (Kew and Kemp, 2005; Pisani et al., 1997). The activity of these coupled receptors led to cell death (Bruno et al, 2000). The reduction in reactive species formation after mGlu5 blockade is probably because mGlu5 activity also increases DA release (Imperato et al., 1990). Regardless of the reason, excess glutamate induces reactive superoxide radicals to form that cause toxicity (Gunasekar et al., 1995). However, as explained below, other transmitters and neuropeptides may also be involved.

C. The involvement of substance P (SP) and nitric oxide (NO)

In addition to complex interactions between DA and glutamate in the damaging effects of METH, SP and NO provide additional avenues for damage, particularly in the striatum. The distribution of the neuronal phenotypes post-synaptic to striatal DA releasing cells enhances NMDA receptor and SP receptor activity. These enhanced receptor actions also increase NO and reactive species formation (Gunasekar et al., 1995; Lafon-Cazal et al., 1993). D1 receptors for example, are found on striatal SP containing projection neurons (Gerfen et al., 1990). Furthermore, both D1Rs and the neurokinin 1 receptor (NK-1R) for SP are found on striatal somataostatin, neuropeptide Y and nitric oxide synthase (SST/NPY/NOS) containing interneurons. SST/NPY/NOS neuron phenotype regulates neuronal nitric oxide synthesis through the presence of nNOS (Gerfen et al., 1990; Kawaguchi et al., 1997; Le Moine et al., 1991; Li et al., 2001).

SP activity through its NK-1Rs has been shown to be involved in METH-induced toxicity, reactive astrocytosis and apoptosis in the striatum (Angulo et al., 2004; Yu et al., 2002; 2004). For example, our lab has shown that METH- induced damage is significantly reduced in animals pre-treated with SP receptor antagonists (Wang et al., 2008). Furthermore, DA terminal toxicity and apoptosis in the striatum were both attenuated in mice pre-treated with the NK-1R antagonist WIN-51708 before METH injections (Wang et al., 2008). In the same study, Wang et al. also found that the NK-1R is almost exclusively internalized (endocytosis) into the NPY/SST/nNOS interneuron after METH treatment. An interesting observation is that METH treatment increased nNOS production of neuronal NO by the same NPY/SST/nNOS cells but these particular cells are spared the damaging effects of METH (Thiriet et al., 2005; Zhu et al., 2006).

The NO mediated effect on METH damage may be due to interactions with glutamate-induced oxygen species that form peroxynitrite (Pacher et al., 2007). This reactive substance can damage axon terminals (Imam et al., 2001a). For example, using 3-nitrotyrosine as a marker of NO toxicity, Imam et al. (2001a) found METH treatment increased NO and subsequently increased 3-nitrotyrosine. The same group also demonstrated that NO and peroxinitrite knocknout mice have reduced expression of "pro-apoptotic" and increased expression of "anti-apoptotic" proteins. This expression profile is opposite of what is normally seen in the striatum in response to METH treatment (Imam et al., 2001b).

In later studies, Imam et al. (2005) also found that animals with increased *Nurr 1* protein involved in TH expression and subsequently DA synthesis, had increased nNOS, and the 3-nitrotyrosine that are used as markers of NO mediated METH damage. Multiple studies have demonstrated that NO inhibition reduced neural damage (Di Monte et al., 1996: Eyerman and Yamamoto, 2007; Itzhak and Ali, 1996; Sheng et al., 1996). In a recent study in which nNOS was inhibited, VMAT-2 protein oxidation and the altered trafficking that normally accompanies METH were reduced (Eyerman and Yamamoto, 2007). These results also corroborated data demonstrating protection from METH damage and cell death in nNOS knockout mice or mice overexpressing free radical scavengers (Cadet et al., 1994b; Imam et al., 2001; Itzhak et al., 1998). For example, evidence that a NO mediated toxicity separate from thermoregulatory changes or direct DA release may be involved in damage, was observed in the Di Monte et al. (1996) study. They prevented the production of nNOS by treating mice with nNOS inhibitor 7-nitroindazole along with METH. This treatment prevented the loss of METH-induced DA

and TH immunostain, even as temperature, DA release and the incidence of death increased in the METH-treated animals.

D. Disparity in the time course of cell death

As the numerous studies described above indicate, reports of both striatal and cortical neuronal damage and cell death in animals given METH have been overwhelming (Eisch et al., 1998; Deng et al., 2001; Krasnova and Cadet, 2009 review; Pu et al., 1996; Zhu et al., 2006;). The duration of death however, varies from study to study. For example, using a TUNEL immunohistochemistry assay, our lab previously demonstrated peak striatal cell death twenty-four hours after a neurotoxic dose of METH (Zhu et al., 2006). There were few apoptotic cells at forty-eight hours but significant nissl staining suggested a larger quantity of nuclei than would be expected after loss of approximately a fourth of striatal neurons (Zhu et al., 2006). This led to questions regarding the possibility that cells proliferate in response to METH damage and then also undergo apoptosis.

Regardless of the method of METH administration, studies of METH-induced cell death have established that it peaks between one and three days after administration (see table 1). However, published reports show varying duration of cell death. For example, as a measure of cortical damage, Eisch et al. (1998) found peak fluoro-jade staining in cells with apoptotic morphology three days after METH treatment. Although fainter and much less in number than at three days, fluoro-jade stained nuclei with apoptotic morphology were also observed up to twenty-one days after METH treatment. Additionally, Sonsalla et al. (1996) found that administering the binge dose of METH

induced cell loss over a period of five to eight days (summarized in table 1). These data suggest a protracted phase of cell that needed to be investigated, and was one of the reasons the specific studies in this thesis were undertaken. Despite the numerous animal models, understanding of the mechanisms or time course of events following toxic METH exposure is still limited. The need for more effective treatment methods for human users underscores the gap in our current knowledge, but a review of findings in humans is a step toward that understanding.

Table 1

Summary of previous studies demonstrating METH-induced cell death in rodents

Treatment regimen	Neural structure	Time after injection	Measure of cell death	Reference
40mg/kg single injection	Olfactory bulb	1 week	Increased TUNEL positive cells	Deng et al., 2007
30 mg/kg single injection	Striatum	24 hours	TUNEL positive projection neurons ChAT and PV interneurons	Zhu et al., 2006
10 mg/kg injections at 2 hour intervals for a total of 4 injections	Striatum	3 days	TUNEL positive enkephalin projection neurons	Thiriet et al., 2005
5 mg/kg injections at 2 hour intervals for a total of 4 injections	Parietal cortex	7 days	Increased TUNEL positive cells	Ladenheim et al., 2000
40 mg/kg single injections	Striatum, hippocampus, cortex, indusium griseum, medial habenular nucleus	3 days	Increased TUNEL positive cells	Deng et al., 2001
10mg/kg injections at 2-hour intervals for a total of 4 injections.	Substantia nigra	5 and 8 days	Decreased cresyl violet staining of TH positive cells	Sonsalla et al., 1996
4mg/kg injections at 2 hour intervals for a total of 4 injections	Parietal cortex	3, 7, 14 and 21 days	Increased fluoro-jade stain with apoptotic cell morphology	Eisch et al., 1998

Note. The duration of cell death in the striatum by others shows that it peaks at 3 days. We previously found cell death peaks at 24 hours with our treatment regimen (Zhu et al., 2006). ChAT, choline acetyl transferase; PV, parvalbumin; TH, tyrosine hydroxylase; TUNEL, Terminal deoxynucleotidyl transferase dUTP nick end labeling.

E. The human data

The clinical consequences of METH use and ethical considerations have made animal models an attractive method for studying its effects on neural systems. However, a number of recent studies have been done that used post-mortem brains of human METH users, brain images of both active and detoxified users, as well as individuals prenatally exposed to the drug (Chung et al., 2010; Kim et al., 2005; McCann et al., 1998; Thompson et al., 2004; Volkow et al., 2001a; 2001b; Wilson et al., 1996,). Some of these studies have included cognitive or neuropsychological behavioral assessment. Although they demonstrate partial recovery, some results raise an important concern regarding METH-induced effects in what appears to be permanent structural and metabolic brain changes. For example, Wilson et al. (1996) neurochemically assessed the post-mortem brains of METH-exposed individuals and found decreased striatal DA terminal markers such at DAT compared to non-exposed brains. VMAT levels however, appeared normal in the METH groups, which is suggestive of a partial recovery.

Positron emission tomography (PET) imaging also revealed DAT loss in METH users that correlated with duration of drug use (McCann et al., 1998; Sekine, et al., 2001; Volkow et al., 2001a, b). Additionally a PET study by Johanson et al. (2006) found 10% decreases in striatal VMAT2 in former users who had abused METH for approximately 10 years. Even though participants in Volkow et al. (2001a) study had been abstinent for periods ranging from 2 weeks to up to 3 years, high cortical but low subcortical glucose metabolism (a marker for neural activity) were seen in these detoxified users compared to controls. In the same group of subjects, lower dopamine 2 receptors (D2R) in the striatum were also found, and it correlated with greater DA turnover in the orbitofrontal cortex

(Volkow et al., 2001d). Similar alterations in striatal and cortical DA activity are implicated in schizophrenia (Howes et al., 2007; O'Donnell and Grace, 1998 review) and this neural disease shares some of the behavioral symptoms seen with high dose METH exposure (see Kita et al., 2009 review). However a distinguishing feature of METH is the level of cell death and axon injury after toxic exposure to the drug.

Studies of neuronal integrity measured with proton magnetic resonance spectroscopy (MRS) revealed abnormalities of metabolite distribution suggestive of axonal injury, neuronal loss and glial upregulation (Ernst et al., 2000; Nordhal et al., 2002; 2005; Sailasuta et al., 2010). For example, normal cortical, but decreased basal ganglia N-acetyl aspartate and creatine (respectively markers for neuronal integrity and energy metabolism) were found in METH subjects compared to non-using controls (Ernst et al., 2000). In the Ernst et al. (2000) study they also observed the presence of substances typically found in glial cells, such as; choline-containing compounds and myoinositol in cortical grey matter. The abnormal levels of these metabolites correlated with lifetime METH use. Similar metabolite abnormalities were also found in the cingulate and visual cortex of current and both recent and long abstinent METH users (Nordhal et al., 2002; 2005)

Glutamate increases coupled with decreased N-acetylaspartate in the frontal white matter have also been found in humans exposed to METH (Sailasuta et al., 2010). These results in humans corroborated animal models showing evidence of glutamate involvement in METH-induced terminal toxicity and damage to DA systems. Moreover, in METH exposed children, brain metabolite changes were seen in which basal ganglia creatine levels increased and N-acetyl-aspartate in frontal white matter decreased. These

metabolite changes are often observed when glia upregulation accompanies neural damage and dysfunction (Smith et al., 2001). The results from these imaging studies support evidence for increased gliogenesis, metabolic dysfunction and neuronal loss, which may explain some of the cognitive- behavioral differences observed in individuals exposed to METH.

Additional studies using magnetic resonance imaging (MRI) revealed structural abnormalities in both active and detoxified METH users, and some of these changes were found to correlate with cognitive performance. For example, along with performance deficits on word-recall tests, Thompson et al. (2004) observed decreases in the volume of the cingulate gyrus, subgenual cortex, and the hippocampus along with increased frontal white matter and the right lateral ventricle of active users. This is suggestive of axonal and or dendritic growth in some areas as well as cell loss. Interestingly, children exposed to METH in utero had smaller striatal and hippocampi volume compared to non-exposed children (Chang et al., 2004), while abstinent adult users had changes in the shape and thickness of the corpus callosum (Oh et al., 2005).

The publication of two definitive studies in 2005 demonstrated that structural changes in abstinent METH users were correlated with cognitive performance. Chang et al. (2005) found enlargement of the striatum and globus pallidus in some abstinent METH users compared to controls. METH subjects with the smallest striatal volumes had the greatest neuropsychological deficits and longer duration of use. These data suggest the possibility that enlarged basal ganglia structures like the striatum and globus pallidus may be involved in recovery or compensation for neuropsychological deficits after METH. As previously mentioned, these hypotheses need further testing because an

alternative hypothesis is that the structural alterations may contribute to the long-term deficits. However, the alternative is less likely if increased volume accompany normalized behavior. Additionally, imaging studies by Jernigan et al. (2005) found that striatal and parietal cortex volumes were enlarged in abstinent METH users compared to drug naïve controls. The younger individuals however, had larger striatal volume increases, and those with the largest volume increases in the parietal cortex performed more poorly on cognitive tasks. Thus, it seems enlarged cortex in contrast to enlarged striatum may be involved in poor cognitive outcome for adults.

A reasonable explanation for the various alterations in neural structures, particularly the enlarged striatal volume, could be the presence of new striatal glia or neurons. Glia would hypothetically increase in response to the acute cell death and damage, as would neuronal cells that attempt to replace and even exceed in number those lost during the acute phase of METH-induced cell death, if such events were to be considered compensation. Even if some of these new cells themselves may be lost through cell death, excessive cell genesis would alter the volume of the affected neural structure. These processes need not be mutually exclusive to other compensatory processes. Compensation may occur via non-damaged long resident cells in a given structure by synaptic plasticity and axonal growth. However compensation may also occur via generation of new cells but additional evidence for cytogenesis as a METH specific response to damage is lacking.

Chang et al. (2005) and Oh et al. (2005) have suggested both gliogenesis and compensatory sprouting of surviving fibers as possible reasons for the increased volume observed in their studies. The swelling and inflammatory response of glia is an acute

effect and would not be expected after long-term abstinence. However, a change in the number of glia cells is likely since new glia have been found in response to other types of damage in the striatum (Mao et al., 2001); and thus, may also explain the altered volume of neural structures. MRS, MRI and PET studies in humans described above, do suggest gliogenesis in long-term effects of METH in the cortex. However, the return to normalized behaviors in some adults may also include neuron replacement. Since the striatum is damaged and enlarged in abstinent METH exposed adults, studies that employ assays to observe the type of new cells that are generated are important for clarifying these issues. The striatum is a structure that is clearly vulnerable to METH damage but the same neurochemistry that influences this vulnerability may contribute to the likelihood of cytogenesis. Animal models again provide a more accessible means for studying these issues.

III. Striatal neurochemistry: Vulnerability to damage with potential for cytogenesis

A. Glutamate from the cortex and thalamus.

Based on the reports of cell death and altered neural structures, it is obvious that, basal ganglia monoaminergic systems are particularly vulnerable to METH damage (Axt and Molliver, 1991; Hotchkiss and Gibb, 1980; Seiden et al., 1975). For example, the basal ganglia nucleus, the caudate-putamen (striatum) suffers significant neurotoxic effects of METH as measured by loss of the terminal markers tyrosine hydroxylase (TH) and DA transporters (DAT) (Ricaurte et al., 1980; Schmidt and Gibb, 1985; Wagner et al., 1980). Additionally, previously described neuron cell death also occurs in this structure. The

striatum is the major dopaminergic input area of the basal ganglia (Weiner et al., 1991) and plays a role in voluntary motor activity and cognition (Graybiel et al., 1994; Knowlton, 2002; Squire, 2004). Striatal function also involves the activity of multiple neurotransmitter systems that have been implicated in METH damage. For example, the striatum receives dopaminergic afferents from the substantia nigra to its dorsal areas and from the ventral tegmental area (VTA) to its ventral areas. Additionally, the striatum also receives excitatory glutamate input and colecystokinin from the cortex and the thalamus (Walaas, 1981; Záborszky et al., 1985). Thus, when METH induces DA overflow, a significant amount of DA is released into the striatum and damaging biochemical cascades that involve other transmitters and substances become active.

B. Intrinsic striatal cells

Cells intrinsic to the striatum include gamma aminobutryic acid (GABA) spiny projection neurons, which account for over 90 percent of striatal neurons. There are also GABA and acetylcholine (ACh) aspiny interneurons that account for less than 10% of striatal neurons (Kawaguchi, 1997). GABA spiny projection neurons synthesize the neuropeptides SP, dynorphin and enkephalin. These projection neurons send axons via the "direct pathway" (SP, dynorphin) to the substantia nigra and the globus pallidus-internal or via the "indirect pathway" (enkephalin) to the globus pallidus-external and subthalamic nucleus. When GABA (with SP and dynorphin) is released from the striatum via the direct pathway, it inhibits the substantia nigra and globus pallidus-internal, which normally inhibits the thalamus. Subsequently, the activated thalamus stimulates the cortex, which responds by activating motor activity and sending glutamate to the striatum. On the other hand, via the "indirect pathway" projection neurons release GABA

(enkephalin) to the globus pallidus-external that acts on the subthalamic nucleus of the basal ganglia. This action stimulates the substantia nigra and globus pallidus internal. Subsequently, the stimulated substantia nigra/globus pallidus-internal inhibits the thalamus and subsequent cortical release of glutamate to reduce motor activity. Basal ganglia D1 and D2 receptor activity is believed to modulate the direct and indirect pathways, respectively (Stocco et al., 2010). Therefore, striatal projection neurons modulate basal ganglia output and subsequently enhance or inhibit cortical and thalamic activity, glutamate release and influence behaviors to promote or inhibit motor learning (Hasenöhrl, et al., 2000). Furthermore, both enkephalin and SP are thought to play a role in recovery of motor function after drug-induced sensitization (Steiner and Gerfen, 1998).

The other neuronal cells types in the striatum consist of several types of aspiny interneurons (Kawaguchi et al., 1995). Although small in number, the interneurons are very important in regulating the activity of projection neurons, and subsequently, basal ganglia output (Kreitzer, 2009). For example, the largest interneuron cell type is the ACh neuron. Striatal ACh cells immunostain for the enzyme choline acetycholine transferase (ChAT), and receive inputs from the cortex, thalamus and the collaterals of striatal projection cells. Their targets include other striatal interneurons and projection neurons, exciting the former and inhibiting the latter (Tepper and Bolam, 2004). ACh interneurons account for 1 to 3 % of striatal neurons and contain most of the striatal dopamine 2 (D2R) and ACh muscarinic receptors. To a lesser extent but as important for METH mode of action is the fact that ACh cells also contain dopamine 1 receptors (D1R), NMDA, glutamate 1 (Glu1R) and 2 (Glu2R), as well as, the neurokinin receptors (NK-1R) for the neuropeptide SP (Kawaguchi et al., 1995). These striatal interneurons are involved in

modulating both thalamic "feed forward" information to other striatal compartments, and feedback integration of the direct and indirect pathways (Bolam et al., 1984; Kawaguchi, 1997; Kreitzer, 2009; Saka et al., 2002). Thus, striatal ACh neurons are hypothesized to be the "associative" cells of the striatum (Kawaguchi et al., 1995), and normal activity is necessary for procedural learning on a T-maze task (Kitabatake et al., 2003).

The other class of striatal interneuron contains GABA but with several subtypes. They receive inputs from the cortex and target projection neurons in an inhibitory manner. One type of GABAergic interneuron contains the calcium binding protein parvalbumin (PV) that accounts for approximately .7 % of striatal neurons. These PV cells receive inputs from the cortex (Tepper, et al., 2008). PV interneurons contain most of the striatal glutamate 2, 3 and 4 receptor (GluR) subtypes, along with twenty percent of the striatal D2Rs (Kawaguchi et al., 1995). Despite their relatively small numbers compared to other striatal neurons, they are very important for sensorimotor integration. For example, they are involved in "feed forward" inhibition from the cortex to various striatal regions and can also alter functioning of the spiny projection neurons (Koos and Tepper, 1999). Reduced numbers of striatal PV interneurons are associated with procedural learning deficits (Marrone et al., 2006).

Another GABAergic subtype, are calretinin cells that immunostain for the enzyme glutamic acid decarboxylase (GAD_{67}). These cells are also cholinergic and immunostain for ChAT (Holt et al., 1999). Jayanthi et al. (2004) found significant loss of this cell type within 7 days after METH, which suggest the possibility that motor activity that require the function of these cells may be altered the first week after METH exposure. Studies have shown that a small percentage of the calretinin cells also contain

PV (Figueredo-Cardenas et al., 1996; Holt et al., 1999). Reduced calretinin cell density is found to be associated with dystonia, a movement disorder believed to be due to striatal disinhibition, in a rodent model of Huntington's disease (Hamann et al., 2005). However, little is known about the physiological properties of this cell type.

An additional striatal interneuron containing GABA is involved in nitric oxide (NO) synthesis. As mentioned earlier, these NO producing cells also contain somatostatin (SST) and neuropeptide Y (NPY), otherwise known as NOS/SST/NPY cells that account for 1-2% of striatal neurons (Kawaguchi et al., 1995). These cells express NK-1 and D1 but not D2 receptors. They receive inputs from the cortex and target projection neurons as well as other interneurons. Via NO, these interneurons are thought to regulate striatal ACh, GABA and glutamate (Kawaguchi, 1997; Le Moine et al., 1994; McKinney and Kent, 1994). Interestingly, of the striatal neurons lost to METH, Zhu et al., (2006) found that 45% were the PV containing GABA interneurons in the dorsal striatum, followed by 29% of the ChAT/calretinin immunostained cholinergic cells, along with 21% DARPP-32 projection neurons. The nNOS/SST/NPY cells were resistant to METH damage and follow up studies have implicated SP and nNOS in METH-induced cell death (Wang et al., 2008). In contrast to SP and nNOS, NPY has been found to protect from METH-induced striatal apoptosis and its mRNA is increased after METH treatment (Thieret et al., 2005). Furthermore, NPY promotes proliferation and adult neurogenesis under normal and injury conditions in the SVZ and the hippocampus (Agasse et al., 2008; Decressac et al., 2009; Howell et al., 2007; Laskowski et al., 2007).

Our lab is currently investigating the role of SST in protection from METH damage. It is reasonable to hypothesize that SST and NPY may counteract the damage

due to SP and nNOS activity, but convincing evidence remains to be determined. However, since NPY has been shown to play a permissive role in adult neurogenesis and is released by the same cells that respond to SP, a reasonable expectation of neurogenesis in response to METH-induced damage can be made. Therefore, experiments that measure not only proliferation, but also whether proliferating cells differentiate into the PV or ChAT neuron subtype as a compensatory response to METH-induced apoptosis became a focus of our studies. Striatal neurons are summarized in table 2.

Table 2

Intrinsic striatal neuron phenotypes

Cell phenotype Transmitters/enzymes	Receptors	Function
	Aspiny interneurons	
GABA medium size; contains PV and GAD_{67}	D2, GluR1, GluR2, 3 and 4 Potassium channel	Fast spikes. Feed forward inhibition from cortex and synchronization of inhibitory cell activity.
GABA medium size; contains calretinin, and GAD_{67}	ND	ND
ACh Large interneuron; contains ChAT and DARPP-32	D1, D2, m1, m2, m4, Glu1, Glu 4, $NMDAR^2$, NK-15-HT_2 Trk-A, δ opioid, GAP,	Feed forward modulation from thalamus and feedback integration of striatal projection neurons.
SST/NO/NPY interneuron; contains NADPH-diaphorase, NPY, GAD_{67} and ACE	D1, M1, M4, NMDA-R1 NMDA-R2B, NK-1, $GABA_A$ $\alpha 2^a$, Calbindin	Low threshold spikes. Feed forward modulation from and DA inhibition of the cortex. Regulation of local blood-flow.
	Medium spiny projection neurons	
GABA, SP/dynorphin neurons to GPe, GPI and SNpr, some to SNpc; contains DARPP-32	μ opioid, GluR-2, GluR3, NMDA-R1, NMDAR-2A, NMDAR -2B. D1 receptor	Integrate cortical inputs Regulation of direct pathway Phasic inhibition of dopamine cells and basal ganglia output.
GABA enkephalin calbindin neurons to GPe; contains DARPP-32	μ opioid, GluR-2, GluR3, NMDA-R1, NMDAR-2A, NMDAR -2B, D2R	Integrate cortical inputs Regulation of indirect pathway.

Note. Adapted from tables found in *Kawaguchi et al. (1995)* and *Kawaguchi (1997).* ACE, acetylcholine esterase; GPe, globus pallidus external, GPi, globus pallidus internal, NADPH, nicotinamide adenine dinucleotide phosphate; nd, not described. SNpr Substantia nigra par reticulata; SNpc, substantia nigra par compacta.

IV Cytogenesis in response to neural damage

A. Proliferative zones in the adult brain

As the previously cited works indicate, most studies that look at METH effects in the striatum have primarily focused on terminal damage and mechanisms of cell death. Behaviorally, some studies have looked at psychomotor and cognitive changes (see Kita et al., 2009 review). However, significant evidence for a proliferative response to various types of injury in the adult brain exists (see Litchenwalner and Parent, 2006 review) but has not been studied in the context of METH-induced damage. For example, proliferation in the subventricular zone (SVZ) that borders the striatum or the subgranular layer of the hippocampus dentate gyrus (SGZ) occurs under normal physiological conditions in the adult brain (Sohur et al., 2006). This process allows for constant replacement of hippocampus and olfactory bulb neurons as a part of physiological activity. Both the SVZ and SGZ are considered germinal zones. Increased proliferation also occurs in these areas after cortical aspiration (Szele and Chesselet, 1996) and transection (Willis et al., 1976); inflammation-induced demyelination (Calza et al., 1998), stroke (Arvidsson et al., 2002; Dihne et al.,2001; Jin et al., 2001; 2003; Parent et al., 2002a; 2002b; Takasawa et al., 2002 and Zhang et al., 2001) and finally, excitotoxin or psychostimulant-induced damage (Collin et al., 2005; Mao and Wang, 2001; Mao et al., 2001; Tande et al., 2006).

B. Cytogenesis after ischemia-induced damage

It appears from many studies of damage-induced proliferation that the fate of new cells depend on the cause and location of damage; sometimes even the species under consideration (Arvidsson et al., 2002; Collin et al., 2005; Dihné et al., 2001; Jin et al.,

2001; 2003; Mao and Wang 2001, Mao et al., 2001; Parent et al., 2002b; Takasawa et al., 2002; Tande et al., 2006; Van Kampen and Robertson, 2005, 2005). For example, in a focal ischemia injury model, Jin et al. (2001) demonstrated a proliferative response to neural damage in the SVZ and SGZ over a two-day period in rats. They also saw that within three weeks a significant number of the new cells were no longer present. Although the remaining new cells expressed nascent migratory neuron marker doublecortin (DCX), they did not express mature neuron marker neuron nuclear protein (NeuN), suggesting the new cells did not mature to neuron phenotypes. The same group (Jin et al., 2003) also found proliferating neural precursors migrate to the stroke-damaged rat cortex and striatum.

Also using a focal ischemic model, Takasawa et al. (2002) found increased proliferation of progenitors in the SGZ areas of the rat hippocampus within one week. Twenty-eight days later a significant number of these new cells failed to survive. Of the remaining cells at twenty-eight days, 80% expressed mature neuron marker NeuN, and a few expressed glial marker glial fibrillary acidic protein (GFAP). Zhang et al. (2001) also used an ischemic model but they failed to observe proliferative changes in the dentate gyrus. However, they observed peak proliferation after seven days in the SVZ and cortex. Many of these cells immunostained for the polysialylated form of the neuronal cell adhesion molecule (PSA-NCAM), suggesting they could be neurons. A few cells also stained for astrocytic marker GFAP, and SVZ proliferation corresponded with increased neural progenitors in the olfactory bulb and cortex twenty-eight days after treatment. However, many of the new cells failed to survive, and none of the surviving new cells expressed mature neuron markers. Parent et al. (2002b) however, found increased

neurogenesis in the rat SVZ with neuroblasts extending into the striatum between 10 and 21 days after focal ischemia. By 35 days they found new cells with mature projection neuron markers in the striatum, suggesting this area is amenable endogenous neuron replacement by SVZ precursors after injury.

C. Cytogenesis after excitotoxin and psychostimulant damage

In contrast to the ischemic model of injury-induced proliferation, several studies have measured proliferation after treatment with excitotoxins and psychostimulants (Collin et al., 2005; Dihne et al., 2001; Mao and Wang, 2001; Mao et al., 2001; Tande et al., 2006). For example, Dihné et al. (2001) examined proliferation in the striatum after lesioning these areas with quinolinic acid. They found apoptosis as well as cell proliferation in response to the striatal damage. However, only newly generated glial cells were observed. Additionally, Mao and Wang (2001) found increased proliferation of S100B-positive astroglia in response to a toxic insult of-methyl-4-phenyl-1, 2,3,6-tetrahydropyridine (MPTP) in the striatum, while Collin et al. (2005) found neurogenesis of DARPP-32 containing striatal projection neurons, as well as, PV and NPY interneurons after quinolinic acid-induced striatal lesions.

Unlike the SVZ and SGZ derived progenitors seen in the earlier mentioned experiments, the striatum is not normally considered a source for neural progenitors in the adult brain, and is thus termed a non-germinal area (Greenberg and Jin, 2007; Lie et al., 2004 for reviews) The stroke studies provide evidence that cells in the SVZ migrate to the site of injury and differentiate into neuronal precursors or glial phenotypes. However, Bédard et al. (2002) provided evidence that dividing cells in the normal

monkey striatum can differentiate into mature neurons, while other studies further confirmed that the rat striatum has a dormant population of progenitors that can be altered under various conditions (Mao and Wang, 2001; Parent et al., 2002b). Furthermore, it has been suggested that astroglia in non-germinal areas may retain progenitor properties that become activated under different environmental conditions and promote cell genesis (see Boda and Buffo, 2010 review).

Mao and Wang (2001) performed one of the few studies on the effects of amphetamines on striatal cytogenesis in rats. However, without the drug they observed low level BrdU staining as a measure of proliferation within 24 hours of BrdU injections. Three weeks later the new cells expressed S100B marker for mature astrocytes in the striatum. When they administered D-amphetamine in a dose that produces behavioral changes, the Mao group actually saw a transient decrease in striatal BrdU staining but no effects in the dentate gyrus or SVZ. This suggested that the possibility exists for dormant progenitor cells in the striatum that can proliferate and differentiate into astrocytes. An additional suggestion from this study is that striatal cytogenesis may be inhibited with administration of the dopamine agonist D-amphetamine.

Interestingly, in another study, Mao et al. (2001) found robust striatal astrogliogenesis and a few new neurons two months after MPTP induced nigro-striatal lesions in mice. Additionally, Kay and Blum (2000) used the same treatment in mice and also and found astrocytes in the striatum. It should be noted that like METH, MPTP lesion depletes striatal dopamine. In contrast to the studies by the Mao group, a study by Collin et al. (2005) found proliferating cells that mature as neurons, express projection neuron marker DARPP-32 and interneuron markers NPY and PV in the injured adult rat

striatum. This result was revealed after treatment with excitotoxic quinolinic acid. Others have also observed new neurons in response to damage in a non-germinal area of monkeys and rats (Bédard, et al., 2002; Van Kampen and Eckman, 2006; Van Kampen et al., 2004; Van Kampen and Robertson, 2005).

Zhao et al. (2003) found newly generated DA neurons under normal physiological conditions in the substantia nigra, a basal ganglia nucleus that provides DA input to the striatum and is considered a non-germinal area. More interesting are the series of studies after substantia nigra lesions by the Van Kampen group working with a rodent model of Parkinson disease. In their studies, the substantia nigra was lesioned with 6-OHDA followed by treatment with D3 receptor agonist 7-hydroxy-N, N-di-n-propyl-2-aminotetralin (7-OH-DPAT). Van Kampen and colleagues observed increased SVZ proliferation and neurogenesis in the striatum (Van Kampen et al., 2004) and the substantia nigra (Van Kampen and Robertson, 2005). Additionally, they suggested the new cells did not derive from the SVZ progenitors due to lack of migratory markers and the wide distribution of the cells. Intriguingly, behavioral recovery of motor tasks accompanied maturation of new substantia nigra cells after the 6-OHDA-induced lesion (Van Kampen and Eckman, 2006).

It is also notable that 6-OHDA is produced in the striatum after METH treatment (Seiden and Vosmer, 1984), which suggests striatal cytogenesis and neurogenesis may increase after METH damage. However, because D3 agonist was given to the experimental animals in the Van Kampen studies, it appears that the damage-induced rather than physiological striatal and substantia nigral neurogenesis requires treatment with additional substances to promote survival of the new cells. However, as the Parent et

al. (2002b) and Mao and Wang (2001) studies suggests, another route for cell genesis-induced recovery, is for progenitors in the germinal SVZ to divide via alterations in DA receptor activity (Winner et al., 2009). These dividing progenitors then migrate to the injured area where they may incorporate into the local circuits. Therefore, studies that examine adult neurogenesis in normally non-germinal structures should test for both migratory and non-migratory progenitors. A summary of cytogenesis after striatal injury in rodents is presented in table 3.

Table 3

Cytogenesis after striatal injury in rodents

Mode of injury	Proliferation	New cell fate in the striatum	Reference
Focal ischemia in rats	Increased SVZ neuroblasts extending into striatum at 10 and 21 days	Projection neurons at 35 days	Parent et al., (2002a)
Quinolinic acid striatal lesion in rats	Increased in the striatum 3-5 days	Microglia by 5 days but some with apoptotic marker TUNEL at 10 days. Astrocytes by 30 days	Dihné et al., (2001)
MPTP striatal lesion in mice	Eight-fold increase in the dorsal striatum at 3 days	S100B astrocytes by 10 days that survive to 60 days.	Mao et al., (2001)
Quinolinic acid striatal lesion in rats	Increased in the SVZ	At 6 weeks DARPP-32 projection neurons, NPY and parvalbumin interneurons	Collin et al., 2005
6-OHDA in rats	Increased in SVZ and striatum within 3 days	After 2 weeks, GFAP for astrocytes and TuJ1 (Beta III tubulin) for neuron progenitor	Van Kampen et al., (2004)
MPTP nigrostriatal lesion in mice	Increased in the striatum 3-14 days	GFAP astrocytes and Mac-1 microglia.	Kay and Blum, 2000.

Note. 6-OHDA, 6-hydroxydopamine; MPTP, 1-methyl-4phenly-1, 2,3,6-tetrahydropyridine; SVZ, subventricular zone; NPY, neuropeptide Y; DARPP-32, dopamine- and cAMP-regulated neuronal phospho protein of 32 kilo daltons.

D. Dopamine involvement in cytogenesis

The works previously cited all establish that excessive DA overflow is damaging to neural tissue but an elevation of D3 receptors is seen in the DA depleted striatum (Van

Kampen and Stoessl, 2003). DA receptors may be important for cytogenesis in neural damaged structures. Several lines of evidence, including the Van Kampen studies have also suggested that DA is involved in proliferation and subsequent neurogenesis in both the developing and adult brain. For example, it is thought that progenitor cell proliferation in the developing striatum is activated by D1 receptors, and inhibited by D2 receptors, though some studies show the opposite in the adult brain (see, Borta and Hoglinger, 2007 review).

In the neurogenic SVZ of the adult brain, there is a significant amount of D3 receptors. This receptor subtype belongs to the D2 receptor family and thus is sensitive to substances that act on D2 receptors (Diaz et al., 1997). In addition, it appears from the work by Diaz et al. that certain progenitor cells in the developing and adult brain respond specifically to DA. For example, migrating "A cells" from the SVZ called neuroblasts; end up as mature neurons in circuits of the olfactory bulb. Migrating neuroblasts predominantly express D1 receptors (Hoglinger et al., 2004). The "A cells" are derived from "C cells" in the SVZ, and "C cells" in turn, derive from special GFAP expressing SVZ progenitors called "B cells". B cells are astrocytes that produce both neuron and glial cell types (see reviews by Boda and Buffo, 2010; Borta and Hoglinger, 2007). C-cells have D2-like/D3 receptors and receive strong substantia nigra DA innervation in the SVZ. These studies suggest that D2 receptors may promote multipotent progenitor cell proliferation while D1 receptors promote the neuron fate determination of migrating neuroblasts. These studies also suggest that METH should influence striatal cytogenesis because of the increased DA overflow and subsequent depletion that accompanies this substance.

An issue with this hypothesis is that studies that pharmacologically manipulate DA activity and measure cell genesis have so far provided contradictory results. D2 receptors have been shown to either increase, decrease, or have no effect on proliferation and subsequent neurogenesis. For example, Milosevic et al. (2007) found no effect on proliferation, survival or differentiation using rodent or human progenitor cells in response to in vitro D2/D3 receptor stimulation. The Milosevic group like the Van Kampen group used the DA agonist 7-OH-DPAT to enhance proliferation. In contrast, treatment of cultured precursors or adult mice with D2 agonist bromocriptine and apomorphine increased proliferation, while D2 antagonist sulpiride or lesion inducing 6-OHDA decreased proliferation (Coronas et al., 2004; Hoglinger et al., 2004). The latter is interesting in light of studies previously described by the Van Kampen group (2005), which suggested that D2/D3 receptor subtype agonists enhance neurogenesis after a 6-OHDA lesion. Hoglinger et al. (2004) also found, the D1 agonist SKF 38393 had no effect on neurospheres suggesting specific DA receptor influences on proliferation.

A study by Yang et al. (2008) provided further support for the findings of the Caronas et al. (2004) and Höglinger et al. (2004) studies. Yang and colleagues demonstrated that astrocyte derived cytokine ciliary neurotrophic factor (CTNF) act via D2 dependent processes to increase proliferation. Although this was an in vitro study, they also demonstrated in vivo that the selective D2/D3 receptor agonist quinpirole increased proliferation in wildtype mice. Knockout mice lacking CTNF did not show increased proliferation. Furthermore, when Yang et al. (2008) depleted substantia nigra DA with a 6-OHDA lesion, then treated the animals with a D2 agonist, the wildtypes had increased migratory progenitor cells but no effect was observed in DA depleted

knockouts. This suggested that DA acting on D2 receptors induces cytogenesis in normal animals.

In contrast, Wakade et al. (2002) and Kippin et al. (2005) used in vivo only studies to show that D2 receptor antagonist increased proliferation and maturation of progenitor cells in the adult. For example, Wakade et al. (2002) treated rats with either chronic saline, or one of the D2 receptor antagonists: risperadone, olanzapine or haloperidol. Olanzapine and haloperidol treated animals had significantly more SVZ proliferation compared to controls, and surprisingly, risperidone animals did not show this increase. Twenty-one days after treatment new cells were positive for the mature neuron marker NeuN. It is notable that even though all three drugs have high affinity for D2 receptors they also act on adrenergic, sigma and serotonergic receptors (Blin, 1999). The latter also influences neurogenesis. For example, serotonin agonists used to treat depression have been shown to increase adult neurogenesis in the dentate gyrus and SVZ (Bansar et al., 2004), thus its blockade by the drugs used in the Wakade study could have been a confounding issue.

Kippin et al. (2005), revealed that in rats, increased proliferation of neural progenitors results in cells that become forebrain neurons in response to chronic haloperidol administration. The results were also consistent with the group's in-vitro experiment in which cultured cells from rats were exposed to haloperidol. Kippin et al. (2005) then treated D2R knockout and wildtype mice with haloperidol or saline. Wildtypes that received D2 receptor antagonist had significantly increased proliferation and subsequent maturation to new neurons compared to saline or D2R knockout animals;

suggesting that D2 receptor inhibition but not receptor absence is necessary for neurogenesis in the adult.

Further confirmation that D2 inhibition, rather than stimulation, induces neurogenesis in the injured adult brain comes from two studies by the Winner group. Winner et al. (2006) unilaterally damaged the medial forebrain bundle DA neurons by injecting 6-OHDA into the substantia nigra. This caused near complete SVZ and striatal DA depletion and region specific effects on neurogenesis. For example, they found a 25% decrease in SVZ cells expressing cell cycle marker PCNA. However, greater expression of the cell signal involved in DA cell fate (PAX-6) was observed in the rostral SVZ and rostral migratory stream (RMS) that transports new cells to the olfactory bulb. The PAX-6 positive RMS cells also co-expressed migratory neural progenitor marker DCX. Although the granule cell layer of the olfactory bulb had less proliferation two weeks after the lesion, this normalized by six weeks. In the glomerular layer, however, there was an increase in the number of new cells. A majority of the new glomerular cells were immunopositive for mature neuron marker NeuN as well as TH, at both the two and six-week time points after lesions, indicating the new cells were dopaminergic. This suggest that even though there may be decreased SVZ proliferation in response to loss of DA, there may be increased potential for progenitor cells to adopt a neuronal fate in other areas of the adult brain after DA loss.

The same group (Winner et al., 2009) again used a 6-OHDA-lesion model of Parkinson's disease but with a chronic 10-day regimen of the D2R agonist pramipexole. This treatment regimen induced greater SVZ progenitor proliferation in rats. Four weeks after cessation of the D2 R agonist, animals had greater olfactory bulb maturation of DA

neurons compared to controls. The increased DA neurogenesis also accompanied recovered psychomotor performance measured in the open-field. In the same study they also demonstrated that D2 and D3 receptors are present on progenitors cultured from the rat SVZ (Winner et al., 2009). This suggest that D2 activation is necessary for increased progenitor proliferation, but with the data from their previous study (Winner et al., 2006), subsequent lack of D2 stimulation increases the potential for neuronal fate in the injured adult brain. These actions may thus explain the contradictory results from many studies of the effects of DA on cytogenesis.

The striatum is rich in both D1 and D2 receptors (Weiner et al., 1991). Thus, it is reasonable to hypothesize that the initial METH-induced dopamine overflow may be accompanied by proliferation of dormant striatal progenitors, while subsequent METH induced DA depletion may increase the likelihood that new cells mature and adopt a neuron phenotype. Alternatively, in response to damage, progenitors that derive from the SVZ can proliferate then migrate to the damaged striatum, and with DA depletion are more likely to adopt a neuronal fate. Since METH action includes both striatal dopamine overflow then depletion, the working assumption in undertaking the studies described in later chapters is that METH might in some way influence the generation of new cells within the striatum. Therefore, it was not enough to show proliferation in response to METH damage, but determination of the phenotypic fate of the new cells. Additionally determination of whether behaviors improve over the same time course of cell maturation would suggest a process for recovery.

E. Identifying new cells.

Thymidine analog 3'5' bromodeoxyuridine (BrdU) has been reliably used to identify the time of birth of a cell. During the S-phase of cell replication, if BrdU is present it will be incorporated into the DNA (figure 1). Cell birth can later be visualized via immunohistochemistry with an antibody to BrdU (Gratzner, 1982). Knowing when BrdU was administered provides the birthdate of new cells. The cells can then be accurately quantified using unbiased stereological techniques proposed by West et al., (1992) and modified by Peterson (1999) and Mouton (2002).

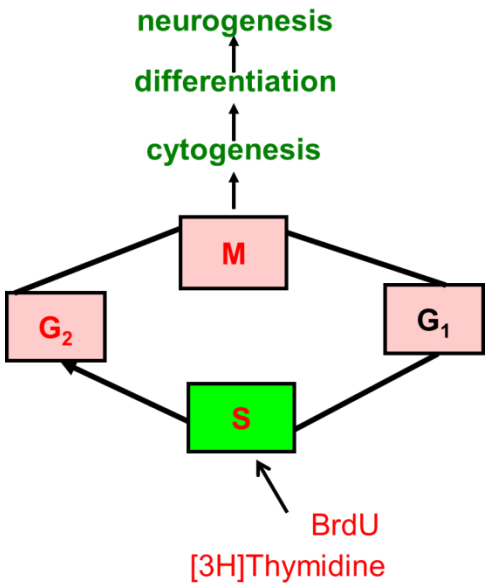

Figure 1. 3H thymidine analog 3'5' bromodeoxy uridine (BrdU) is incorporated into DNA during S-phase of mitosis (A). Note: BrdU can be incorporated during DNA repair. However, according to Bauer and Patterson (2005) and Taupin (2007), fewer nucleosides are present to incorporate BrdU, and immunostain to identify repair with BrdU are almost undetectable when using proliferation protocols.

All BrdU positive nuclei, which can clearly be seen to have divided is another level of ensuring accurate counts of new cells (Cooper-Kuhn and Kuhn, 2002). Nuclei displaying condensed pigmentation, with a shrunken, fragmented round or crescent shaped nuclei consistent with pyknosis/apoptosis are described as being in the process of process of dying (Kerr et al., 1972; Soriano et al., 1993). According to Zeigler and Groscurth (2004), nuclei with swollen disintegrating nuclei and large vacuole that occur when membranes are disrupted in necrosis, are also dying cells. Therefore, morphologically pyknotic or necrotic BrdU positive nuclei would not be counted as surviving cells. Since labeled thymidine analogs have long been used to study the birth of new cells in the adult brain (Bacci and Gown, 1993; Bayer, 1983; Cooper-Kuhn and Kuhn, 2002), there are established methods for measuring METH induced cytogenesis.

F. Issues with BrdU co-localization studies of new cells

A potential issue with co-localization studies involves the use of overlays as evidence of the coexistence of two or more markers within same neuron. At times two or three neurons can be stacked on top of each other in the *z* –plane of the section yielding false positive results. In order to avoid this kind of error, co-localization must be verified with data obtained from *z*-scanning and orthogonal rotation of the z-stacks, using the confocal microscope and immunofluorescent histochemical staining (Cooper- Kuhn et al., 2002; Taupin, 2007). When used in conjunction with unbiased stereology, histochemical techniques provide more accurate estimates of neurogenesis within a given area. There is some criticism regarding BrdU incorporation during DNA repair. However, using proliferation/neurogenesis protocols, BrdU immunostaining is undetectable in

DNA repair, because only some nucleosides are hypothesized to be replicated in contrast to the entire DNA for proliferation (Bauer and Patterson, 2005; Taupin, 2007)

Of the possible neuron phenotypes to assess, two main reasons exist for examining whether the population of any surviving new cells are PV and ChAT positive interneurons; 1. A small but significant portion of striatal GABA cells are aspiny interneurons that express PV and another small but significant population of striatal interneurons is cholinergic cells immunopositive for ChAT (Gerfen, 1992; Kawaguchi, et al., 1995). 2. Previous studies have found that most of the cells lost during the acute phase of METH-induced cell death were the GABA-PV and ChAT positive interneurons (Zhu et al., 2006). Although, previous studies by Betarbet et al. (1997) revealed increased GABA synthesizing enzyme GAD_{67} in the striatum after excitotoxic injury, they did not look for co-localization with a mitotic marker. Co-label of GAD_{67} with a mitotic marker such as BrdU, would have given some indication of whether new GABA cells were being produced in response to damage, as opposed to just increased synthesis of GAD_{67}. Furthermore, quantifying PV rather than GAD_{67} neurons was important for assessing functional recovery in the current work because reduced PVcell numbers in the striatum accompany diminished procedural learning (Marrone et al., 2006). This type of behavior is the topic of the next section.

V. The Striatum and Behavior

A. Motor and procedural learning

Striatal involvement in motor function and cognition makes studies of METH damage and potential recovery in this area important for improving patient outcome. For

example, the function of the striatum in what is termed “habit,” “procedural,” or, “egocentric” learning and memory, been extensively studied (Albertin, et al., 2000; Botreau and Gisquet-Verrier, 2010; De Leonibus et al., 2003b; 2005; Packard et al., 1989; Tremblay and Schultz, 1998; Whishaw, et al., 1987). The striatum is necessary for stimulus-response association when learning a maze task (Knowlton et al., 1996; Packard, et al., 1989; Packard and Knowlton, 2002). The use of an internally generated series of movements that lead to the food reward on a maze task (i.e. turn left after eight steps) is considered an “egocentric response“ or procedural learning (Restle, 1957; Tolman et al., 1946). In contrast, using spatial cues in the environment (i.e. turn right at checkered image) to locate a food reward is a form of declarative memory called “place,” or “allocentric learning” (Packard and McGaugh, 1996; Squire, 2004).

The “place” strategy is thought to be under hippocampal control, while the “response” strategy requires the striatum (Squire, 2004). Animals often shift from a hippocampus-based cue or place strategy to a striatum-based response strategy once a task becomes habitual. If forced to use a striatal strategy while learning, deficits accompany striatal lesions (Packard et al., 1989; Packard and McGaugh, 1996; See Packard, 1999 review). For example, Packard et al. (1989) revealed that lesions of the striatum resulted in disruption of a procedural task but left hippocampus-dependent declarative task acquisition intact. Thus, even though the hippocampus is often the target structure in studies of spatial memory, the striatum is also used to acquire a spatial task (De Leonibus et al., 2005; Yin and Knowlton, 2004).

As previously described, the effects of METH are thought to begin with alterations in DA activity, particularly in the striatum (Kita et al., 2009 review).

Numerous studies have shown that striatal DA signaling promotes both motor and cognitive processes (Darvas and Palmiter, 2010; De Leonibus et al., 2003b; Featherstone and McDonald, 2004; Hollerman et al., 2000; Hollerman and Schultz, 1998; Nakamura and Hikosaka, 2006a; O' Doherty et al., 2004; Schultz et al., 1989; Wolterink et al., 1993). For example, after MPTP-induced DA depletion in the monkey striatum, Schultz et al. (1989) observed deficits in task reaction times and eye-arm movement. Furthermore, mice genetically deficient in DA perform poorly on motor as well as spatial learning tasks, but performance is restored to near normal levels when only the dorsal striatum is treated with a dopamine agonist (Darvas and Palmiter, 2010).

It should be noted that reward based spatial learning using the "response" or egocentric strategy is accompanied by striatal ACh release, and additional neurotransmitter systems may be involved (Kitabatake et al., 2003; Pych, et al., 2005a, 2005b). For example, mice with decreased immunostaining for ChAT, NE and 5-HT neurons in the striatum show impaired spatial learning, and the neurochemical and behavioral outcome was worse in aged mice (Stemmelin et al., 2000). Additionally, ablation of striatal ACh interneurons impairs T-maze learning but not performance on a rotarod task or habituated open-field activity (Kitabatake et al., 2003); suggesting a differential role of ACh interneuron in motor activity and habit learning. Furthermore, a reduction of striatal PV interneurons was observed in genetically modified mice deficient in reelin protein (Marrone et al., 2006). These mice also had spatial learning deficits. Reelin protein is involved in synaptic plasticity and neurogenesis (Hartfuss et al., 2003; Weeber et al., 2002); suggesting a lack of this protein may result in deficient PV interneuron formation in striatal circuits.

In contrast to the ACh and PV effects on learning, asphyxia-induced interneuron loss in the mouse striatum during the perinatal period, resulted in few motor deficits at six weeks of age (Van de Berg et al., 2003). These results from the Van de Berg group suggested recovery from the perinatal PV interneuron loss. However, individuals with Tourette's syndrome, an inherited disorder in which voluntary motor activity is disrupted, have decreased numbers of both PV and ACh interneuron phenotype in the striatum (Kataoka et al., 2010). Because METH decreases PV and ChAT interneurons, studies that measure motor and learning performance along with compensatory processes in adults are needed. Motor activity and maze learning after METH treatment provides a reliable avenue for such studies. One can expect that motor and learning performance would be disrupted in adult animals after METH. However, if new neurons are then generated in response to the damage, and functionally, this cytogenesis is a compensation for cell loss, performance of motor and striatum-dependent learning tasks should improve as new cells mature.

B. Efects of METH on behaviors that require the striatum

The behavioral consequence of a neurotoxic dose of METH includes increased psychomotor activity during the early acute phase (Itzhak and Ali, 2002) but also long-term decreases in some types of motor behaviors (Boger et al., 2007; 2009). For example, although amphetamines initially increased open-field locomotor activity (Hall et al., 2008), the long term effect has been shown to be a reduction in this behavior. Boger et al. (2007) observed motor deficits in two- and- a- half- month old mice treated with METH. The mice used in the study had partial deletion of the glial derived neurotropic factor gene, and subgroups were tested at times ranging from ten weeks to a year after

treatment. These animals also had reduced locomotor activity at the late-post treatment times along with altered immunoreactivity of TH and DA metabolites in the striatum. Therefore, long-term motor effects of METH treatment include less motor activity, which should be a separate measure from anxiety on open-field tasks after striatal damage.

METH also impairs appetitive conditioning necessary for normal performance on some cognitive and motor tasks (Achat-Mendes et al., 2005; Izquierdo, et al., 2010; Krasnova et al., 2009). However, studies of the cognitive effects in the aftermath of METH also revealed that performance depends on the post-METH time that the task is measured. For example, in humans, Simon et al. (2010) found deficits during the early abstinent period in former METH users compared to controls but with some improvement one month later. In rodents, beginning one day after a neurotoxic regimen of METH, Marshall et al. (2007) observed object recognition deficits up to three weeks after treatment. Krasnova et al. (2009) observed no psychomotor deficits in mice tested in the open field ten days after METH. However, open field performance worsened as the animals aged because deficits were present at three and five months. Interestingly, DA was depleted at ten days but partially recovered by the three and five-month time point; suggesting that it is not just the lack of DA, specifically, that is driving psychomotor deficits. In contrast, deficits in DA turnover and spatial maze task performance were observed in rodents during the early post-METH period, followed by 80% recovery in striatal DA turnover and no maze learning deficits two to six months after METH (Friedman et al., 1998). The current work proposes that the cytogenesis may also play a role in this recovery. Cytogenesis-associated behavioral recovery can be inferred from studies that look at the behavioral changes over the same time-course of the proliferation

and differentiation of any newly generated striatal cells following a neurotoxic dose of METH.

Interestingly, two studies that employed the T-maze to test spatial learning in METH-treated rodents revealed no difference from controls in maze task acquisition four to seven weeks after treatment (Daberkow et al., 2007; 2008). These results provided additional evidence that there is functional recovery of spatial learning as early four weeks after METH. Alternative interpretations are that the task did not require the specific striatal function disrupted by METH or the disruption occurred at earlier time points and other unmeasured neuroadaptations are responsible for performance equivalent to controls. For these reasons, more studies of behavior at both early and later post-METH times are necessary. With the evidence available for the functional role of the dorsal striatum in maze learning tasks (De Leonibus et al., 2005; Ragozzino et al., 2001), the behavioral studies conducted for the current work was an important addition to understanding the possible function of neurochemical changes in the striatum after METH.

C. Issues with testing motor performance and learning

An important consideration when conducting studies that disrupt motor systems is that performance of some learning tasks can be affected (De Leonibus et al., 2005; 2007; Dunham and Miya, 1957; Gerald and Gupta, 1977; Jones and Roberts, 1968a; 1968b; Reiter and McPhail, 1982). Performance can also be affected by psychomotor changes such as anxiety (Denenberg, 1969; Kuczenski & Segal, 1997; Richards et al., 1993; Whimbey and Denenberg, 1967; White et al., 2006). Therefore, it is important to use

multiple measures in order to dissociate motor deficits from learning deficits. The rotarod, open-field and T-maze have been used to test a variety of behavioral performance in rodents with specific tasks measures for dissociating motor activity, anxiety and learning (Crawley, 2007).

The rotarod for example, has long been used to measure motor performance parameters such as coordination and balance (Jones and Roberts, 1968a; 1968b). Tests with an automatic rotarod involve placing rodents on a rotating cylinder at fixed or variable speeds and the latency to fall off the rod is the measured outcome (Barlow et al., 1996). Although damage to the cerebellum can affect rotarod performance, animals with damaged striatum also perform poorly (Kalonia et al., 2009). Furthermore, normal signaling in the striatum is critical for motor skill needed to do well on a rotarod task (Bureau et al., 2010).

Rodent behavior in an open-field is used to measure two dimensions of psychomotor performance: "emotionality" (anxiety) and stereotyped "exploration" or movement/motor activity (Reiter and MacPhail, 1982; Whimbey and Denenberg, 1967). For example, rodents have a natural tendency to thigmotaxic behaviors, in which they spend more time closer to the walls, periphery zone or corners of the open-field than the central zone (Simon et al., 1994). Dopamine agonist such as cocaine and amphetamines increase thigmotaxis and increases are thought to indicate anxiety (Simon et al., 1994). Freezing in an anxiety-inducing situation such as being placed in the center of an open-field is also common in mice (Whimbey and Denenberg, 1967). However, motor system-induced changes may result in increased freezing that is not due to anxiety. For example, failures to explore or move in the open-field (freezing) due various types of motor

dysfunctions have been described by Reiter and MacPhail (1982). Therefore, animals treated with substances or are genetically modified such that motor function is disrupted, may not move as often as control animals, despite accounting for anxiety (Crawley, 2007; Reiter and McPhail, 1982). For these reasons center and periphery zone activity should be assessed in conjunction with measures of distance traveled and ambulation activity in the open-field.

IV. Proposed model and specific Aims (hypotheses).

A. Model

Based on all the previously cited works, the proposed model of events following a neurotoxic exposure to METH includes early acute effects (twelve-twenty-four hours), late acute effects (twenty-four to forty-eight hours), and long-term effects (weeks after). Early acute effects previously reported are DA overflow and increased striatal glutamate and NO activity, accompanied by increases in stereotyped motor behaviors and activation of damaging molecular pathways. Late acute effects previously reported are: cell death, dopamine depletion and decreased psychomotor activity, although there appears to be a window between twelve and twenty-four hours where both early and late acute effects may occur (see Krasnova and Cadet, 2009 review). The hypothesis proposed was that cytogenesis follows late acute effects, and the long-term effects were expected to include striatal volume changes that accompany survival and death of the new population of cells. Additionally, new cells that survive would express mature neuron markers as well as glia cells (see figure 1 for model). Recovery of any previously lost interneuron type would be considered evidence of the potential for neurochemical recovery. Along with proposed

neurochemical recovery, motor and habit learning behaviors that require the striatum would be expected to improve over the time course of new cell maturation. An alternative hypothesis was that no cytogenesis would result and thus a theoretical neurochemical recovery of interneuron phenotype would be zero.

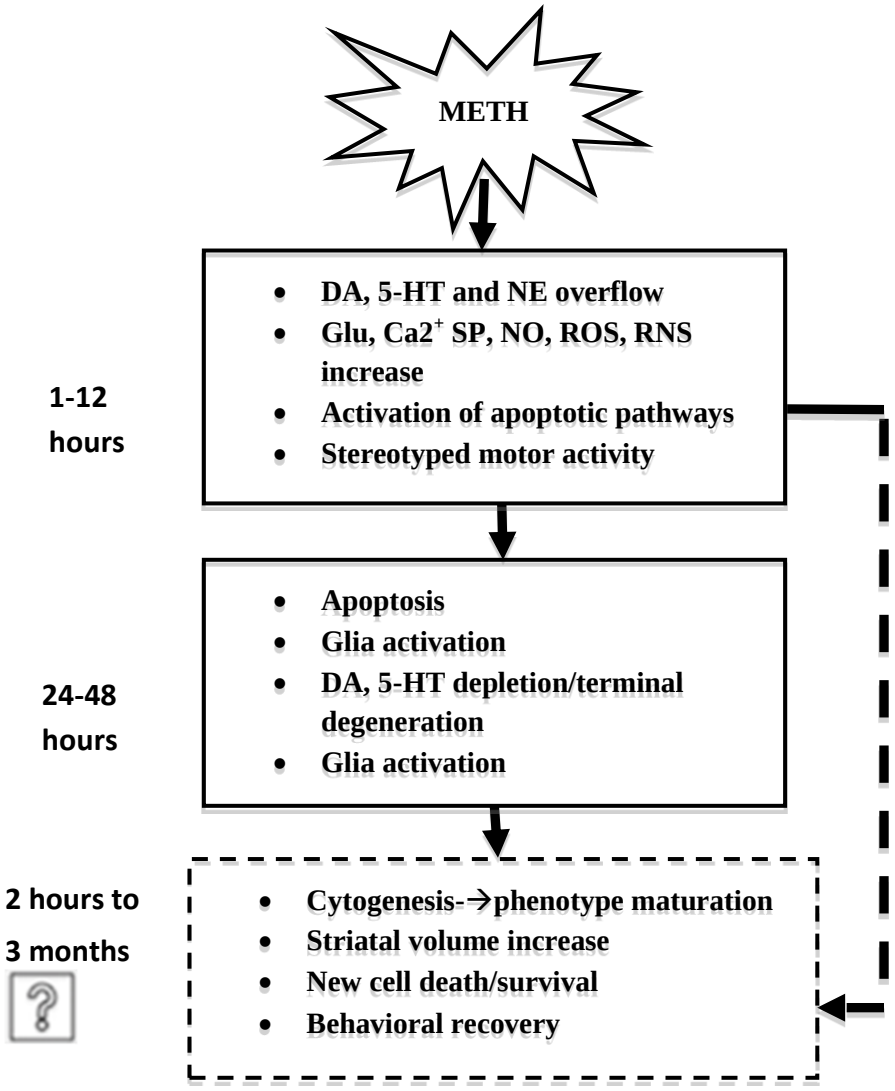

Figure 2. Proposed model of striatal events after a neurotoxic dose of METH. Previously reported events are indicated by solid rectangles. Hypothesized events investigated in the current work are indicated within the broken rectangle. Note: gap between 12 and 24 hrs. Some studies show DA depletion as early as 12 hours in primates and rats (See Krasnova and Cadet, 2009). Findings from our lab with the same treatment regimen used with mice in the current work shows that degeneration occurs between 24 hours and 3 days after METH (Zhu et al., 2005; 2006).

Because there is significant striatal damage in response to METH and increased striatal volume that accompany partial behavioral recovery, to test the cytogenesis hypothesis, it was necessary to determine whether the model was correct. *The working hypothesis that was tested is that cytogenesis follows acute methamphetamine cell loss and the function of cytogenesis and subsequent new cell maturation serves in part, as a means for recovery that can be demonstrated by behavioral outcome.*

B. Specific Aims.

1. Specific Aim I was to determine if cytogenesis occurs in the striatum in response to METH-induced cell death. Three experiments were designed. In each experiment, mice were exposed to a neurotoxic bolus dose of METH previously demonstrated to cause DA depletion and cell death in the striatum, and several parameters of cytogenesis were measured.

For Aim 1A**,** the time course of cell proliferation was assessed after METH or saline exposure by using BrdU to label dividing cells at various post-treatment times ranging from two hours to twenty-one days. Within five hours of BrdU injection, striatal tissue was collected for processing via anti-BrdU immunohistochemistry. BrdU-positive nuclei were then visualized with histochemical assays for light and fluorescent microscopy and quantified using unbiased stereology. Significant proliferation (defined as increased BrdU-positive nuclei) was expected in METH-treated mice after 30-mg/kg single injection compared to saline-injected mice.

For Aim 1B, survival of newly generated cells in the striatum of METH-treated mice were assessed using the same methods of METH exposure, histochemical visualization and quantification techniques, except no additional mice were treated with saline and BrdU was injected in all mice at the peak of proliferation determined from the time course in aim 1A. Subgroups of animals survived to one of several post-METH times (2.5 days, 1 week, 2 weeks, 4 weeks, 8 weeks, and 12 weeks), at which point they were sacrificed and striatal tissue collected for use in histochemical assays. The baseline variable for comparison was BrdU incorporation at the peak proliferation time in aim 1A. The outcome variables measured in this experiment were percent of baseline BrdU-nuclei that had no morphological features of a dying cell and were defined as surviving nuclei. BrdU nuclei that had pyknotic or necrotic morphology as per Kerr et al. (1972) and Soriano et al. (1993) were defined as dying. Many new cells were expected to die via pyknosis and/or necrosis but some non-pyknotic and non-necrotic cells were expected to remain at various post-treatment times.

For Aim 1C, striatal volume was measured in a subset of BrdU-stained tissue from Aim 1B to compare with matched tissue from average volume of saline control mice from Aim 1A (baseline volume). The variable measured was percent difference in volume from baseline. Striatal volume was expected to increase in conjunction with new cell generation.

2. Specific Aim 2 tested the hypothesis of neurochemical recovery via the mechanism of cytogenesis. Recovery was defined as surviving new cells in the

mouse striatum that differentiate from progenitors to phenotypes consisting of astroglia, microglia, and neurons. Of particular interest were two neuron sub-populations known to undergo the most apoptosis during acute METH damage (ChAT and PV interneurons). To fulfill this aim, a series of three experiments were carried out in a subset of tissue from the survival experiments in aim 1B. Analysis accounted for the same post-METH time course used in Aim1B (2.5 days, 1 week, 2 weeks, 4 weeks, 8 weeks and 12 weeks). A double-label immunohistochemistry assay was done to visualize phenotypes for progenitors, glia and neurons. A percentage of the non-pyknotic and non-necrotic BrdU-positive nuclei were expected to co-label with markers for neural progenitors within the first two weeks, and mature glial and neuronal markers at later post-METH times. In part, as a measure of neurochemical recovery, two neuron subtypes that underwent apoptosis in response to METH were only assessed at 8 and 12 weeks when new neurons were expected to mature.

For Aim 2A, progenitor cells were identified using double label immunohistochemistry for BrdU-positive nuclei co-localized with the following histochemical markers: anti-nestin, and anti- βIII-tubulin for neural progenitor populations and anti-double cortin (DCX) for migratory progenitors. Variables assessed were the percent of BrdU-positive nuclei co-labeled with each progenitor marker over the same time course as aim 1B (2.5 days to 12 weeks). Quantification was done using a modified version of unbiased stereology adjusted for manual and partially computerized counts as described by (Mouton, 2002; Peterson, 1999; West et al., 1991). As an indication of cytogenesis rather than just

DNA repair, progenitor markers were expected during the early post-METH times.

For Aim 2B, glial cells were identified using double-label immunohistochemistry for BrdU-positive nuclei co-localized with the following histochemical markers: anti-S100B for astrocytes and anti-IB4 for microglia. Variables assessed were the percent of BrdU-positive nuclei co-labeled with each glial marker. S100B was used instead of GFAP to identify astrocytes for several reasons. S100B is primarily expressed by astrocytes and is involved alterations of the cytoskeleton, cell proliferation and differentiation, as well as protection from and promotion of damage under various neural injury conditions (Rothermundt et al., 2003). Additionally, newly generated cells expressing S100B were previously found following excitotoxic lesion to the striatum (Mao et al., 2001). Quantification was done in the same manner as Aim 2A. In brief: a partially manual and partially computerized version of unbiased stereological techniques adjusted as described by (Mouton, 2002; Peterson, 1999; West et al., 1991). Mature glia were expected at later post-METH times.

For Aim 2C, new neuronal cells were assessed by using immunohistochemistry for BrdU-positive nuclei co-localized with the following histochemical markers: anti-neuronal nuclear protein (NeuN) for mature neurons, anti-parvalbumin (PV) for parvalbumin containing GABA interneurons, and anti-choline acetyl transferase (ChAT) for ACh containing interneurons. The time course measured for NeuN was the same as Aim 2A but different for PV and ChAT. Since the interest was in recovery rather than a time course of

differentiation of these two cell types, measures were taken only at the time point where the most BrdU-positive mature neurons were likely present (8 and 12 weeks post-METH). Variables assessed were percent of BrdU positive cells co-localized with each neuron marker (NeuN, PV, ChAT). Since recovery was predicted for interneurons, the difference was expected to be significantly greater than zero.

3. **Specific Aim 3 tested the hypothesis that behaviors requiring striatal function change as a measure of recovery in the following manner: Deficiencies observed during early post-METH time, then improvement as the new cells mature over the same time course as neurochemical studies in Aim 2 (2.5 days to 12 weeks).** To test this hypothesis, three experiments were proposed: motor performance on the rotarod, psychomotor activity in the open-field and spatial learning on the T-maze designed to test for striatal function. METH-treated mice were expected to reveal deficits during the early post treatment times (2.5 days to 2 weeks) but recover at later post-treatment time when new cells were hypothesized to mature (4-12 weeks).

For Aim 3A, motor coordination on a rotating rod was assessed in all of the adult male mice before injections. Animals then received either METH or saline injections and sub groups from each treatment condition again received the rotarod test at one of several post-treatment times corresponding to the survival study time course (2.5 days, 1 week, 2 weeks, 4 weeks, 8 weeks and 12 weeks). The average latency to fall off the rotarod was the variable measured. ANOVAs assessed pre and post-treatment performance in both groups. METH animals were

expected to perform poorly during early post-METH tests but improve new cells matured.

For Aim 3B, psychomotor performance and anxiety in the open-field were assessed in groups of mice receiving either METH or saline. One untreated group of mice was tested for comparison with METH or saline treated animals to control for injection effects. Test times following injection corresponded to the twelve-week survival time course in Aim 2 (2.5 days, 1 week, 2 weeks, 4 weeks, 8 weeks, and 12 weeks). At the various post-treatment time points, mice were placed individually in an automated open-field chamber for five minutes. The variables assessed were software-generated scores from photobeam breaks that measured motor activity (ambulation, distance traveled, and movement) and anxiety (number of entries, freezing time and time spent) in the center and periphery of the open-field. METH-treated mice were expected to show early deficits but improvement over time as new cells mature.

For Aim 3C, learning was assessed over the time course that new cells differentiate into striatal neuron phenotypes that were lost during acute METH damage. Learning protocols began two weeks after treatment to allow the mice to recover from the acute METH effects, and have sufficient time to regain appetite before having food restricted. This was important because the spatial task is appetitive and METH reduces appetite. At the same time, the mice needed to be sufficiently motivated to eat the food reward used during maze training. Thus at the designated time after METH or saline treatment, food availability was decreased in order to facilitate weight reduction to 85% of free-feeding levels.

Once target weight was reached, mice were trained to enter the non-preferred arm of a T-maze for food reward. Variables measured were percent correct arm entry per daily training sessions (learning progress), number of days of training sessions to criterion, average latency to correct arm entry per trial at criterion (latency), and the strategy (striatal or hippocampal) used to perform the task at criterion. The latter was based on a probe trial in which the T-maze was rotated 180 degrees. METH treated mice were expected to perform poorly at time points closer to injection time but improve at later time points when new cells mature. Statistical analysis involved a series of tests depending on the variable being measured and is described in the materials and methods section. Experimental design is summarized in table 4.

Table 4

Summary of experimental design to test hypotheses for each Specific Aim.

Aim and # of animals	Drug condition	Test	Time course	variables
		Aim 1		
1A N=5-7	METH or Saline	proliferation	2hrs-21 days	# of BrdU nuclei
1B N=7	METH compared to baseline METH at 1.5 days	survival, pyknosis necrosis	2.5 days-12 weeks	% BrdU nuclei
1C N=5-7	METH compared to saline baseline	volume	2.5 days-12weeks	% change in volume.
		Aim 2		
2A N=4	METH	progenitor cells	2.5 days-12weeks	% BrdU with ßIII-tubulin, nestin or DCX,
2B N=4	METH	glia	2.5 days-12weeks	%BrdU with IB4 or S100B
2C N=4	METH	neurons	2.5 days-12weeks	%BrdU with NeuN
		interneurons	8 and 12 weeks	%Brdu with ChAT or PV
		Aim 3		
3A N=6	METH, Saline, or no treatment	rotarod	2.5days-12weeks	Latency to fall
3B N= 6	METH, Saline, or no treatment	open-field	2.5days-12weeks	distance; ambulation; movement; entries; time and freezing
3C N=4-8	METH or Saline	T-maze	2-12 weeks	% correct arm entries; days to Criterion; task latency per trial and strategy

Note. Drug treatments were 30 mg/kg METH in 200µl saline or 200µl saline injected interperitoneal. N, number of animals per treatment group for each time-point tested.

C. Materials and methods

1. Animal care and use.

All procedures involving animals were performed in accordance with the *National Institutes of Health Guide for the Care and Use of Laboratory Animals* and were approved by the Institutional Animal Care and Use Committee of Hunter College of the City University of New York. Male Institute of Cancer Research mice (Taconic, Germantown, NY) between 11 to 12 weeks of age were housed individually on a 12-h light/dark cycle with food and water available *ad libitum* unless otherwise noted.

2. Drug preparation and treatment

For all experiments that required drug treatments, (+/-) Methamphetamine hydrochloride (Sigma, St. Louis, MO) was dissolved in 10 mM phosphate-buffered saline; pH 7.4 (PBS). Groups of mice were injected intraperitoneal with either saline or one bolus METH dose (30 mg/kg of body weight) in a volume of 200 μL. Sacrifice and striatal tissue collection were done by anesthetizing each animal with a 1:3 mixture of ketamine/acepromazine (100mg/kg of body weight) then transcardially perfused with 25ml of PBS followed by 25ml of 4% paraformaldehyde in PBS. Brains were dissected out and immediately post-fixed for 12 hours in 4% paraformaldehyde at 4 °C, followed by cryoprotection in 30% sucrose in PBS solution at 4 °C for forty-eight hours. Tissue sections were then stored at -80 °C until use in immunohistochemistry assays.

In addition to drug conditions for proliferation experiments (Aim 1A), 100 mg/kg of the mitotic marker BrdU from Sigma (St. Louis, MO) was injected at one of the following post-METH or saline injection time: 2, 24, 36 hours and 2, 3, 4, 5, 6, 7, 14 or 21 days. Sacrifice and tissue collection were done within five hours of BrdU injections

using the transcardial perfusion method. Five hours was chosen to allow for cells undergoing mitosis to incorporate BrdU into the DNA. For survival (Aim 1B and 1C), phenotype (Aim 2), and behavior (Aim 3*)* experiments, BrdU was injected thirty-six hours after the METH injection. This time point was chosen based on peak BrdU staining determined in Aim 1A. Subgroups of phenotype study mice were randomly assigned to survive until one of the following post-injection times: 2.5 days, 1 week, 2 weeks, 4 weeks, 8 weeks and 12 weeks. 2.5 days was chosen as the earliest point for phenotype experiments because it was twenty-four hours after peak proliferation. Twenty-four hours is sufficient time for mitotic cells to complete the cell cycle (cytogenesis). At the designated survival time point, mice were sacrificed via the same transcardial perfusion method described in the preceding paragraph. Striatal tissue sections were collected and prepared for BrdU immunohistochemistry. For behavior studies, however, mice were not sacrificed at those post-treatment times. Instead, subgroups of mice were randomly chosen to begin post-treatment behavior tests at the time points corresponding to phenotype study of Aim 2 (2.5 days, 1 week, 2 weeks, 4 weeks 8 weeks, 12 weeks) or an adjusted time course for T-maze learning task (2 weeks, 4 weeks 8 weeks, 12 weeks).

3. Histochemistry assays for visualization of BrdU-positive nuclei

The same tissue collection method was used for both proliferation and survival immunohistochemistry assays. Coronal sections from each striatal hemisphere were cut at 40μm thickness and serially collected from the striatum between bregma - 0.30 and 1.4 mm. Every sixth sample per striata was collected into one of six adjacent sample wells per mouse, for approximately thirty-six striatal samples per hemisphere. For each immunohistochemical assay, we used two adjacent wells of samples per mouse from the

ipsilateral hemisphere. One well was used for peroxidase + 3,3'-Diaminobenzidine (DAB) assays for light microscopy and the other for immunofluorescence assays

For light microscopy immunostained BrdU-positive cells were visualized using the Vectastain ®ABC peroxidase method with DAB. Sections were first washed in PBS and antigen unmasking accomplished by incubation in a 1:1 solution of formamide and 4X SSC for two hours at 65^{o}C, then followed by 30 minutes in 2N HCL at 37^{o}C. Samples were then rinsed with 0.1 M boric acid pH 8.5 at room temperature for 10 minutes. Endogenous peroxidases were quenched in 0.3% H_2O_2 for five minutes. Non-specific binding was blocked according to instructions of the Vectastain® ABC elite sheep kit (Vector Labs, Burlingame CA), followed by overnight incubation in primary antibody consisting of 1:500 sheep-anti-BrdU (Novus Biologicals, Littleton, CO) at 4^{o}C. Staining was visualized with Impact DAB® substrate reaction (Vector Labs, Burlingame, CA). Sections were then washed and mounted on coded superfrost glass slides. Dehydration and clearing were done with two-minute incubations in a 50% solution of xylene in ethanol followed by 100% xylene. Slides were cover slipped with VectorMount™ permanent mounting medium (Vector labs, Burlingame CA) and stored until unbiased stereological quantification was done.

Fluorescent immunostaining was visualized as follows: PBS wash, followed by incubation in 65^{o}C solution of 1:1 formamide in 4X SSC for two hours, then incubation in 2N HCL at 37^{o}C for thirty minutes. Following a ten-minute rinse in 0.1M boric acid at pH 8.5, non-specific binding sites were blocked with 5% donkey serum in 0.2% triton X and PBS at room temperature for an hour. Sections were then incubated in primary antibody 1:500 sheep anti-BrdU (Novus biologicals, Littleton, CO) in 1% normal donkey

serum overnight at 4^{o}C. After two PBS washes, sections were incubated for one hour in secondary antibody; 1:500 FITC donkey anti-sheep (Novus biologicals, Littleton, CO) at room temperature. After two PBS washes, tissue sections were mounted on superfrost glass slides. They were then sealed and cover slipped with Vectorshield hard set^{TM} mounting medium for fluorescence (Vector laboratories, Burlingame CA). Each slide was then coded and images taken via Leica TCS SP2 confocal microscope (Leica Microsystems, Germany) for use in partial manual and computerized stereological quantification to compare with full computerized stereology for accuracy of counts using each method.

4. Histochemistry for BrdU-positive phenotype markers

All primaries were incubated at least overnight at 4^{o}C. Labeling was done with BrdU antigen retrieval steps for fluorescence as described for survival study. However, additional steps specific to the second label per phenotype were done.

For progenitor phenotypes (ß3Tub, DCX, nestin), and microglia (IB4), an amplification protocol was used according to the TSA-CY3 kit N5000 ® (Perkin Elmer, Waltham, MA) before BrdU immunolabeling. Protocol proceeded according to the following: Two quick PBS rinses followed by 1M citric acid in dH_2O at 100^{o}C for 8 minutes were done before two additional PBS rinses. When using mouse based primary antibodies with the TSA protocol, i.e. mouse anti-beta III tubulin and mouse anti-nestin, the one hour block step was done in MOM IgG. Overnight primary antibody incubation solution required Vector Labs' basic MOM kit BMK2200® (Burlingame, CA) according to kit instructions. The antibody dilutions used with MOM diluent for overnight incubation were 1:2500 mouse anti-beta III-Tubulin (Millipore); 1:5000 mouse anti-

nestin (Millipore). For doublecortin (DCX) after citric acid step in TSA protocol, and PBS rinse, a blocking step was done with tissue incubation in 3% normal donkey serum in .3% triton X-PBS for one hour, followed by primary antibody solution of 1:2000 goat anti-DCX, (Santa Cruz Biotech, Santa Cruz CA) in 1% donkey serum solution. On the second day for mouse based antibodies, three quick PBS washes were followed by one-hour incubation in secondary antibody solution of 4ul/ml biotin-anti Mouse IgG from the MOM kit (Vector labs). For DCX, biotinylated-anti-goat IgG from Vector Elite ABC kit was used according to instructions, (Vector labs, Burlingame, CA). Visualization of all the progenitor markers and microglia were done with 1:1000 Cy3 conjugate to secondary antibody. Cy3 was according to TSA kit instructions (Perkin Elmer, Waltham, MA) for an hour, followed by ten-minute incubation in a solution of 0.1% trypsin in 0.01M tris buffer and 0.1 $CaCl_2$ at room temperature. After trypsin step, two quick washes were followed by 2N HCL incubation for thirty minutes at room temperature. 3 PBS washes preceded a one- hour blocking step in normal donkey serum and overnight incubation in 1:500 sheep anti-BrdU solution. On the third day of the assay, BrdU visualization commenced with FITC secondary antibody as previously described in single label immunofluorescence assay.

Isolectin B4 conjugated to horseradish peroxidase was used in a modified TSA protocol to label microglia as follows: Two PBS washes followed by a 0.01M citric acid incubation step was done. Following citric acid step, incubation was done in 3% H_2O_2 at room temperature for five minutes to quench endogenous peroxidase. Two washes in 1% Tx-PBS followed peroxidase quench step then primary antibody incubation. Primary antibody dilutions were 1: 2500 IB4-HRP (Sigma, St. Louis, MO) in 1% triton X-PBS

overnight at 4^{o}C. TSA protocol then commenced in the normal manner per 1:1000 Cy3 from TSA kit.

Mature phenotype markers: For NeuN, S100B, ChAT, and PV, the BrdU immunofluorescence assay was done first according to steps previously described. On the second day after BrdU visualization with sheep-anti-BrdU conjugated to FITC, three washes were done followed by one- hour blocking step and incubation in second primary antibody. For NeuN and PV, blocking was with MOM kit IgG from (Vector labs, Burlingame CA). Five minutes in MOM diluent was followed by incubation in primary antibodies: 1:1000 Mouse anti-NeuN (Novus Biologicals, Littleton CO) or 1:500 mouse anti-PV, (Millipore, Billerica, CA) over night at 4^{o}C. For S100B and ChAT, blocking was done in 3% normal donkey serum in 0.2% tritonX in PBS. After blocking step, primary incubation in 1:500 goat anti-ChAT (Millipore, Billerica, MA) or 1:500 rabbit anti-S100B (Novus biologicals, Littleton CO). NeuN and PV were visualized using secondary antibody 1:1000 CY3 goat anti-mouse (Millipore, Bellerica CA) in 1% NGS in 0.2% triton X PBS. However, S100B was visualized with 1:1000 CY3 goat anti-rabbit (Millipore) in 1% NGS in 0.2% triton X PBS. After block with donkey serum, ChAT was visualized using secondary antibody dilution 1:500 Cy3 donkey anti-goat (Millipore) in 1% donkey serum in 0.2% TxPBS. All secondary antibody incubation was for an hour. All tissue sections were mounted on coded superfrost glass slides and cover slipped with vectashield hardset mounting medium for fluorescence (Vecta labs, H-1400, Burlingame, CA). Reagents used in histochemical protocols are summarized in table 5 and 6.

Table 5. Aim 1 ***Summary of reagents used for BrdU histochemistry***

Assay	Antigen retrieval	Block	Primary AB	Block	Secondary AB
DAB-peroxidase	1:1 formamide + 4X SSC.2hrs @ 65^{o}C 2N HCL 30 minutes @37^{o}C 1M Boric Acid pH 8. 10 minutes @ RT	0.3% H_2O_2 at RT Vectastain ® ABC elite sheep kit per instructions	1:500 sheep-anti-BrdU 4^{o} C, ON	ABC Elite Kit	Impact DAB® substrate reaction per kit instructions
Immunofluorescence	1:1 formamide + 4X SSC.2hrs @ 65^{o}C 2N HCL …30 minutes @37^{o}C 1M Boric Acid….10 minutes	5% NDS serum in Triton X+ PBS for 1 hours @ RT	1:500 sheep-anti-BrdU in normal 1% NDS @ 4^{o}C ON	----------	1:1000 Fit C donkey anti sheep in 1% NDS @ RT for 1 hour

Table 5 Summary of reagents and dilutions used in Aim 1. Two different staining assays were used; DAB and fluorescent to measure accuracy of manual vs. computerized stereology. NDS, normal donkey serum; ON, overnight; RT, room temperature.

Table 6

Summary of reagents used for phenotype histochemistry

Marker	Antigen retrieval	Block	Primary AB	Block	Secondary AB
ßIII-tub	1M Citric Acid 8min @ 100°C TSA-CY3 Kit Perkin Elmer # N5000	Vector basic MOM kit BMK2200 for 1 hour	1:2500 mouse anti-beta III-tubulin 24hrs @4 °C	4ul/ml biotin-anti Mouse IgG from the MOM kit for 1hour.	1:1000 TSA CY3 conjugated with anti-mouse IgG per kit instructions 1% trypsin in .01M tris buffer and 0.1 $CaCl_2$
DCX	1M citric acid for 8min @ 100°C TSA-CY3 Kit Perkin Elmer # N5000	3% NDS in 3% triton X+PBS for 1 hour	1:2000 goat anti-DCX in 1% NDS 24 hrs @ 4 °C	----------	biotinylated-anti-goat IgG from Vector Elite ABC kit conjugated to TSA Cy3 per kit instructions
Nestin	1M citric acid for 8min @ 100°C TSA-CY3 Kit Perkin Elmer # N5000	Vector basic MOM kit BMK2200 for 1 hour	1:5000 mouse anti-nestin 24 hrs@ 4 °C	4ul/ml biotin-anti Mouse IgG from the MOM 1hour	1:1000 TSA CY3 conjugated with anti-mouse IgG per kit instructions 1% trypsin in .01M tris buffer and 0.1 $CaCl_2$

Continues on next page

Table 6

Summary of reagents for phenotype histochemistry continued.

Marker	Antigen retrieval	Block	Primary AB	Block	Secondary AB
IB4	1M citric acid for 8min @ 100°C TSA-CY3 Kit (Perkin Elmer # N5000)	3% H_2O_2 for 5 mins 0.1% TX PBS @ RT for 1 hr	1: 2500 IB4-HRP in 1%triton X +PBS	----------	1:1000 TSA CY3 per kit instructions 1% trypsin in .01M tris buffer and 0.1 $CaCl_2$
NeuN	Per BrdU protocol	Vector MOM IgG and diluent from sheep kit	1:1000 Mouse anti-NeuN in MOM diluent	3 % NGS in 0.2%Tx-PBS for 1 hour	1:1000 CY3 goat anti-mouse in 1% NGS +PBS
ChAT	Per BrdU protocol	3% NDS in 0.2% tritonX in PBS	1:500 Gt-X-ChAT in 1% DK serum +0.2% Tx+PBS	----------	Cy3 DK Anti-Goat in 1% DK serum + 0.2% Tx + PBS
PV	Per BrdU protocol	Vector MOM IgG and diluent from sheep kit	1:500 mouse anti-PV in MOM diluent	3 % NGS serum in .2%Tx-PBS for 1 hour	1:1000 CY3 goat anti-mouse in 1% NGS + PBS

Table 6 Reagents used for phenotype staining in conjunction with BrdU immunofluorescent staining (see table 5). BrdU assay preceded S100B, NeuN, ChAT, PV and S100B protocol, but followed βIII-tubulin, DCX, nestin and IB4 staining. DK, donkey serum; NDS, normal donkey serum; NGS, normal goat serum.

5. Behavior Assays

Motor performance on the rotarod was measured over the same time course as the surviving new phenotypes in Aim 2. The apparatus used was an ENV-575M five station mouse Rota-Rod (Med associates, Georgia, VT). Rotarod performance is known to correlate with the level of striatal cell death (Haelewyn et al., 2007). For this reason, METH animals tested during the early post-treatment time were expected to perform poorly. If cytogenesis was an indication a neurochemical recovery underlying motor activity under striatal control, METH-treated animals were expected to show better performance on the rotarod task as new cells mature. However, because unfamiliarity with the apparatus may result in animals performing poorly the first time tested, pre-injection latency to fall off the rotating rod was measured in each mouse in a three-minute fixed (20 rpm) and a three-minute variable (2-20 rpm) speed test given five minutes apart.

After pre-injection trials to get baseline performance, matched groups of animals were semi-randomly assigned to receive either METH or saline injections then tested again at one of six post-injection times over the twelve-week period. In order to counter balance the groups and avoid bias toward high or low performers in one drug condition at a given post-treatment time, animals were assigned to groups according to the following: If six animals had an average latency score of fifty seconds and another six had a latency score of a hundred and eighty seconds, one animal from each score group was randomly assigned to receive METH or Saline injections and tested at one of the six post-treatment test time. Post-treatment tests in the subgroups of animals were done using the same pre-treatment fixed and variable speed rotarod test at either 2.5 days, 1 week, 2

weeks, 4 weeks, 8 weeks and 12 weeks after METH or saline injections with the average of the two trials used as one score. Because of early METH-induced deaths in some animals that may have disrupted matching, analysis consisted of only 6 animals per drug condition per post-treatment times. Testing was done in the home-cage room by an individual blind to the drug treatment condition of the animals.

For, psychomotor performance and anxiety in the open-field, determination of anxiety or motor deficits were done to see if these behaviors could later affect maze-learning tasks. Performance in the open-field was assessed in groups of animals receiving either METH or saline at the same time course as rotarod tasks. The tasks were based on Whimbey and Denenberg's (1967) interpretation of two dimensions of open-field behavior. One dimension measured emotionality (here defined as "anxiety") and the other measured exploration (here defined as "movement" or "motor") activities. The open-field apparatus used was a Kinder Scientific SmartFrame™ activity chamber, with 32 infrared photobeam detectors configured with 16 in the X and 16 in the Y orientation of the chamber. The dimensions of the open-field were 32" x 16' x 32". Because the novelty of the open-field provides an approximation of anxiety, injected mice were tested only once, and thus, did not receive a pre-treatment test. Instead, a separate group of untreated animals were used to measure baseline performance as a control group for injection effects different from METH or saline treatment. The same animals used on the rotarod protocols were used for the open-field assays. Open-field testing was done in a room different form normal housing, thus animals were habituated to the testing facility for at least thirty minutes before the start of a trial.

At the time of the test, each animal was individually placed in the center of the automated open-field chamber for five minutes. If there were motor deficits, mice were expected to spend less time ambulating or performing movement activities. Therefore, motor performance variables were total ambulation, total movement and total distance traveled in the open field. Anxious mice were expected to spend more time in the periphery and less in the center or more time freezing in general. Therefore variables for anxiety were the number of entries, the total time spent and the total time freezing in each of two designated zones of the open field. METH animals were expected to have movement deficits during the early post-treatment times but some recovery at later times corresponding to time course of new cell maturation observed in the neurochemical studies.

Learning a T-maze task was assessed over the time course that new cells differentiate and neuronal phenotype become evident in animals treated with METH or saline. However, since METH may affect appetite while it is in the bloodstream, and after clearance results in exhaustion (Dean, 2004), waiting at least a week after drug treatment allowed the animals time to recover from the physiologically stressful conditions before being placed on limited food availability.

Maze-learning tasks are appetitive in that animals receive a food reward for performing the task correctly. Reduced food availability over the training period, allowed the animals to be sufficiently motivated to get the food reward (Tolman et al., 1946). Approximately a week before training began, daily food availability was reduced until 85% of free feeding weight was achieved. A pilot study demonstrated that 15% weight reduction requires approximately seven days of restriction to three grams of food daily

(data not shown) after METH treatment. Once training on the actual task began, weight was maintained between 85 and 90% of free feeding levels.

Training was done in a designated room separate from normal housing. A thirty-minute habituation to the testing area was done before each session. In order to encourage striatal rather than hippocampal strategy to solve the task, the testing room had minimal spatial cues and testing was done in dim light. The apparatus was cleaned with 75% alcohol in distilled water solution between trials to avoid odor cues for solving the task. The apparatus was a black metal elevated radial arm maze modified to reflect T-maze configuration for use in this experiment. The dimensions of each arm of the T-maze was 15" x 5" x 2" adapted from the Deacon and Rawlings (2006) but with longer arms and shorter walls. The behavior protocol was adapted from a combination of two studies: Yin and Knowlton (2004) and De Leonibus et al., (2005). In brief: animals were allowed a 5-minute habituation trial in which food was available everywhere on the maze and the preferred arm was determined from the number of entries into a given arm. Food reward consisted of Maypo™ brand maple syrup flavored instant oatmeal moistened with water. Animals were then trained to enter the non-preferred arm and avoid the preferred arm. The variables measured were: the number of correct arm entries per training session, latency to enter the correct arm, the number of daily session to criterion, and the strategy used at criterion. If an animal did not leave the start area of the T-maze within ninety seconds, the trial ended immediately with no food reward and counted as an error.

Training sessions were done in blocks of five trials per session. No more than two sessions were done daily because METH treated animals were found to tire easily and stopped responding after the 10^{th} trial daily. Eighty percent (4/5) correct arm entries per

session, in two consecutive sessions was the designated task acquisition criterion. Once this criterion was met, a probe trial was done in which the T-maze was rotated 180 degrees to see if a striatal or hippocampus based strategy was used. If the mouse entered the arm that was always baited, even though it was spatially displaced 180 degrees, it was using ego-centric or procedural (striatal) strategy to acquire the reward. If the mouse went to the place where the arm was on the same side of the room they were trained to go, they were using an allocentric or place (hippocampus) strategy, though they would fail to get the reward on that trial.

6. Quantification for neurochemical and behavioral assays

For all histochemical assays (proliferation, survival, volume and phenotype) slides were coded and two different individuals blind to the treatment conditions performed counts to determine the number of BrdU nuclei and striatal volume estimates using Stereologer ™ (Stereology Resource Center; Chester, MD) unbiased stereology software for MAC. Hardware component of the stereology system included a Leica DM 2500 microscope (Leica Microsystems, Germany) attached to a Prior optiscan II motorized XYZ stage system (Prior Scientific, MA), a Sony CCD video camera and a MAC pro computer with the settings described below. A cross section of the striatum (example in figure 2) from one hemisphere per striata was outlined in 5X magnification for each tissue sample. This outline allowed for an estimate of the area of the structure in which cells were counted. Counts of BrdU nuclei were done at 100 X magnification. The optical fractionator in Stereologer ™ was used with a cavalieri estimator for separate counts of the mean number of BrdU-positive nuclei for the following: morphologically intact but visibly mitotic (proliferation), intact (survival), morphologically pyknotic

(apoptosis) and morphologically necrotic nuclei that fell within the inclusion lines of the sampling frame. Sampling frame area was 50 mm^2 and the frame moved in steps automatically set at (x-step · y-step = 100 μm^2) in a raster pattern. Approximately 200 frames of striatal tissue per animal were counted with the first and last 2 μm excluded from analysis. Therefore, the average section thickness analyzed was approximately 15 μm per section. For all groups, Stereologer ™ estimated sampling error (CE) was well within acceptable range of less than 0.1.

For proliferation experiment mean BrdU positive nuclei were quantified for approximately 7 METH and 5 saline treated mice at each of the following post-drug time; 2 hours, 24 hours, 36 hours; 1 day, 2 days, 3 days, 4 days, 5 days, 6 days, 7 days, 14 days, and 21 days. Proliferating cells were defined as BrdU-positive nuclei that morphologically appeared to have divided.

For survival experiment, non-pyknotic or non-necrotic, pyknotic and necrotic BrdU-positive nuclei counts and striatal volume were estimated by stereologer for 6-7 mice at each of the following post-METH times: 2.5 days, 1 week, 2 weeks, 4 weeks, 8 weeks and 12 weeks. Surviving cells were morphologically BrdU-positive nuclei with normal nuclear morphology (intact and not shrunken and fragmented or swollen, with vacuole as seen in pyknosis and necrosis, respectively). Apoptosis was defined as intensely stained BrdU-positive round or crescent shaped clumps of nuclei fragments that occur during karyopyknosis. Necrosis was defined as enlarged BrdU-positive nuclei with vacuoles, and/or fragmented membrane. As an extra level of confirmation for necrotic morphology, tissue stained with ßIII-tubulin from Aim 2A was also morphologically examined for disrupted membrane components that occur when cells swell and lyse as

they undergo necrosis. The estimated striatal volume was automatically calculated concurrently with counts using the region point probe of stereologer.

For phenotype experiments, fluorescent signals were detected using a Leica TCS ™ confocal microscope and corresponding Leica software system (Leica microsystems, Heidelberg, Germany). FITC and CY-3 signals corresponded to single wavelength laser line 488 (green) and 568(red), respectively. The striatum was divided into four regions corresponding to dorsal medial (DM), dorsal lateral (DL), ventromedial (VM) and ventrolateral (VL). Z-stack images from each striatal region were taken in four animals per group, six tissue sections per animal (see figure 3 for schematic of tissue section). To avoid cross detection between the signals, the pinhole setting was less than 2μm and z-stacks between fifteen and thirty μm thick were recorded sequentially between frames at 100X in a raster pattern per series. Confirmation of co-label was done by reconstruction and orthogonal rotation of the images using the Leica confocal software in "view "and also "analysis" mode. Using the equation for estimating volume by stereology (Mouton, 2002) the estimated volume of 4 striatal sections per animal was [$V=T(\sum A)$] where "T" is the average section thickness and "A" is the surface area. Leica TCS software quantified both figures. Average surface area of striatum quantified per region was 1.5 mm^2

To determine the proportion of cells with BrdU positive nuclei that were also positive for the second marker of interest, a modification of the stereology technique for the confocal microscope as described by Peterson (1999) was employed as follows: Using the quantification mode in the Leica software a sampling frame measuring an area of 50 mm^2 per z-stack with inclusion and exclusion lines was drawn on the computer

monitor and counts were taken at 100X magnification after outlining the striatum at 5X. Only cells that fell within the inclusion area of each sampling frame and clearly visible within the z-axis were counted. Partially visible nuclei or those that touched the exclusion lines of the sampling frame were not counted. Separate counts of BrdU-positive and BrdU-co-labeled nuclei from the same tissue sections were taken from 4 mice per time point (2.5 days, 1 week, 2 weeks, 4 weeks, 8 weeks and 12 weeks). These procedures provided the mean counts per animal within an average Leica defined area of 1.5 mm^2. After stereological quantification was complete, the total BrdU-positive nuclei per animal and the total phenotype immunostained cell co-labeled with BrdU were used to calculate percentage BrdU-nuclei co-labeled. Once phenotype percentages were done, coding was revealed for statistical analysis.

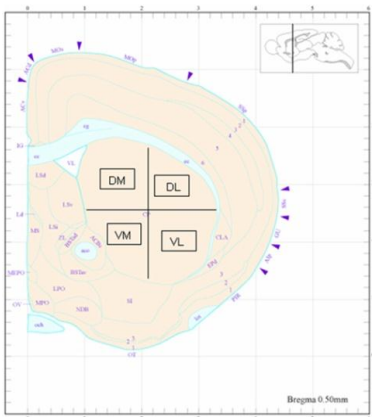

Figure 3. Quantifying new cells. Schematic representation of a striatal cross section at .50 mm from bregma that was used for quantification of BrdU incorporation. Quantification of proliferation, survival and volume were done for the entire area of the striatum borderd by the corpus callosum, ventricle and anterior commisure. Nucleus accumbens was not inculded. For phenotype studies counts were done from each labeled subregion. DM, dorsomedial; DL, dorsolateral, VM,ventromedial and VL, ventrolateral. The total of a given phenotype within an average of 1.5 mm^2 was used to determine percentages. Schmatic modified from (Hof et al., 2000).

For rotarod performance, the latency to fall of the rod was generated automatically by the timer on the apparatus. Since each test consisted of a fixed and variable speed trial, the two scores were averaged to give one outcome variable "latency to fall" off the rotarod. This score was used in the statistical analysis of rotarod performance.

For open field performance, behaviors were automatically scored by motor monitor™ quantification software (Kinder scientific, Poway, CA), based on the break in photobeam on the opposite side of the chamber. The behaviors quantified were photobeam breaks corresponding to X and Y ambulation, basic and fine movement, distance traveled, number of entries, time spent freezing and total time spent in the periphery versus the center of the open-field. The software was set to quantify behaviors in one-minute blocks over the five-minute trial. However there was little difference in behaviors between the first minute and the last minute of the trial. Thus the behavior totals over the five minutes were used in the analysis. Movement behaviors quantified were: the sum of X and Y ambulation for "ambulation" values; the sum of the basic and fine movements for "total movement" and the sum of distance traveled in the periphery and center for the total "distance traveled" values. The anxiety measures were, the number of entries into the center and periphery, the time spent freezing in center and periphery and the total time spent in the center and the periphery. Thus there were two values, center and periphery for each anxiety measure used in statistical analysis.

7. Statistical analysis

For all statistical analysis, $p < .05$ was considered significantly different. Analysis was done with Graphpad Prism software (San Diego, CA) except for multi-factor ANOVA in the open field. For multi-factor analysis SPSS 18 software (IBM, Somers, NY) was used.

For proliferation experiment, the dependent variable was the mean number of BrdU-positive nuclei. A two-way ANOVA was done to compare the mean number of BrdU-positive nuclei for each treatment condition (METH or saline) at each post-treatment time. Post-hoc analysis was done using Bonferonni multiple comparisons test of significant differences between groups at each time point.

For survival experiments baseline was set to the mean BrdU-positive nuclei present at the peak proliferation time point in METH-treated animals from proliferation study (100% at 36 hours or 1.5 day time point). Using stereologer™, separate counts were done for each of the three morphological variables. Calculation of the percent difference between baseline and each morphological variable was then done to get three outcome variables. The morphological variables were percent surviving BrdU-positive nuclei with non-pyknotic and non-necrotic morphology (survival analysis), percent BrdU-positive nuclei with pyknotic morphology, and percent BrdU-positive nuclei with necrotic morphology. A separate one-way ANOVA was done for each of the three variables to compare differences per post-METH survival time (2.5days, 1 week, 2 weeks, 4 weeks 8 weeks, and 12 weeks). Significant F-values for the ANOVA were

followed by Bonferroni multiple comparisons post-hoc test to compare significant differences between mice at each post-METH time.

For percent change in volume analysis, the raw volume score at each post-treatment time was estimated by stereologer then compared to the average volume from saline treated mice in the proliferation experiment for calculation of percent change. The average volume for all saline comprised a baseline of 0% change. The percent volume change compared to saline in METH-treated mice was measured at 2.5 days, 1 week, 2 weeks, 4 weeks, 8 weeks and 12 weeks after drug treatment. Statistical analysis was done using a one-way ANOVA with Bonferonni post-hoc test for significant differences between groups of mice at each post-METH time.

For phenotype experiments, there were several outcome variables corresponding to the percentage of BrdU-positive nuclei co-labeled with a given phenotype marker. The phenotype markers were beta III-tub, nestin, DCX, IB4, S100B, NeuN, PV and ChAT. With the exception of PV and ChAT, statistical analysis was done using a one-way ANOVA followed by trend analysis and Bonferroni post-hoc to determine the differences in percent of a given phenotype at various times after METH-treatment (2.5 days-12 weeks). For PV and ChAT, two separate one-way ANOVAs compared each phenotype to the alternative hypothesis value of zero striatal interneurons generated. This was done because the amount of these two interneuron types in the striatum is low compared to other striatal neurons and it was important to know if they were significantly different from zero as a measure of neurochemical recovery at the time when most of the new NeuN positive neurons were present. Significant one-way ANOVA was followed by Dunnett's post-hoc test.

For motor coordination on the rotarod, the variable analyzed was the average latency to fall off the rotarod. It was important to analyze the pre-injection performance separately to ensure that the latencies to fall were relatively the same regardless of what group the mice were subsequently assigned for the post-treatment tests. This was done with a two-way ANOVA for pre-treatment performance per assigned treatment group and post-test time. Non-significant pre-treatment result was followed by post-treatment analysis. Post-treatment comparisons for the mean latency to fall off the rotating rod for the post-injection condition per time point (2.5 days to 12 weeks) were done with a two-way ANOVA. For significant interaction and simple effects, Bonferroni post-hoc was done to determine differences between treatment conditions per post-treatment time.

Motor performance and anxiety in the open field were analyzed in a series of multi-factor ANOVAs. Three movement variables and three anxiety variables were measured. Movement variables were total ambulation, total movement, and total distance traveled. Each movement variable was analyzed separately with a two-way ANOVA. There were three levels of the drug treatment factor (no-injections, METH or saline injections), and 6 levels of the post-test time factor (2.5 days, 1 week, 2 weeks, 4 weeks, 8 weeks, 12 weeks). Statistically significant interaction and simple effects were followed by Bonferroni multiple comparison post-hoc tests. Anxiety variables were the number of entries, time spent freezing and total time spent in each of the two locations (periphery and center) of the open field. Each anxiety variable was analyzed separately with a multi-factor ANOVA. There were two levels of the location factor (periphery versus center), 3 levels of the drug-treatment factor (no-injection, METH and saline) in addition to the six levels of the post-treatment time factor (2.5days, 1 week, 2 weeks, 4 weeks, 8

weeks, and 12 weeks). For significant interaction effects, each anxiety measure was split by open-field location (center and periphery) and planned contrasts by two-way ANOVA were done for interaction effects between drug condition X time tested, drug condition alone or time alone were done for each anxiety measure. Significant results were followed up by post-hoc analysis using Bonferroni multiple comparison tests to determine simple effect differences per time point.

For learning on the T-maze, scores per training session were recorded for correct arm entries and the latency to perform the task. Calculated variables were the percent correct entries per daily training session (learning progress), number of training days to criterion, the average latency to enter the correct arm per session and the strategy used to perform the task at criterion responding. Since a session was five trials, chance performance was set at three out of five (60%) correct arm entries per session and included in the learning progress analysis. Separate one-way ANOVAs for each post-treatment training time (2 weeks, 4 weeks, 8 weeks, and 12 weeks post-treatment) was used for percent correct arm entries over a ten-day training period. Two-way ANOVAs were used for the number of training days to criterion and latency to correct arm per trial at criterion. Pearson's correlation was used to determine the relationship between strategy used at criterion, days of training to criterion and latency to correct arm entry. Fisher's exact test was used to assess differences in number of animals in each treatment group that used either the hippocampus or striatal strategy.

Chapter 2

Cytogenesis after METH: A role in altered striatal volume and the disparity in the time course of METH-induced cell death?

VII. Results

A. Effects of METH on measures of proliferation (BrdU incorporation).

Fluorescent green nuclei can be seen 36 hours post-METH throughout the striatum of a METH-treated animal (Figure 4B) and in the subventricular zone of controls (Figure 4A). The latter structure supports neurogenesis in the adult brain. BrdU-positive cells that appear to have divided are observable throughout the striatum (Figure 4C). Statistical analysis with a two-way ANOVA revealed significant interaction effects of drug treatment x time on the mean number of nuclei that incorporated Brdu *[F* (10, 110) = 47.9, $p < .001$]. This accounted for 34% of the variance. A significant effect of drug treatment *[F* (1, 110) = 88.8, $p < .001$] was observed but it only accounted for 6 % of the variance. This small contribution to the variance was probably because there was no difference between mice in the saline treated group over the entire study time course, and a narrow time frame of BrdU incorporation in METH-treated mice. This was confirmed with a significant effect of time [*F* (10, 110) = 47.2, $p < .001$]. Post-hoc analysis showed these effects were due to robust BrdU incorporation between the 24 and 48-hour time points in METH-treated mice. The difference between mean number of BrdU-positive nuclei in saline and METH animals at 24 hours was significant [*MD*=139603, $p < .01$]. The greatest difference was at 36 hours [MD = .01 $x10^6$, $p < .001$]. Although the difference was smaller at 48 hours, it was still significant [*MD*= 211513, $p < .001$]. Significant differences in the mean number of BrdU-positive nuclei between groups of

METH-treated only animals were observed at 2 hours compared to 36 ($p < .0001$) and 48 hours ($p < .001$), as well as at 24 hours compared to 36 hours ($p < .0001$) and 48 hours ($p < .001$). No difference between the two types of treatments (saline or METH) or between groups of METH animals at any of the other times was observed.

B. Survival of new cells

1. Non-pyknotic and non-necrotic morphology (intact nuclei).

One-way ANOVA revealed a significant number of the BrdU-positive nuclei generated at thirty-six hours post-METH failed to survive within the twelve weeks measured [F (6,36)=, 4.03, $p < .004$]. This accounted for 40% of the variance depending on the post-METH time [Figure 5]. Post-hoc analysis showed that at one and two weeks post-METH, there were no significant differences in the number of striatal BrdU-positive nuclei compared to thirty-six hours post-METH. However, at four, eight and twelve weeks after METH the surviving cells were significantly less than nuclei observed at peak BrdU incorporation [MD=49.3% $p<0.05$]; [MD=49. 7%, $p < .01$] and [MD=61.6%, $p < .001$], respectively.

2. Pyknotic morphology

Morphological analysis and one-way ANOVA showed that newly generated cells are undergoing apoptosis as evidenced by the BrdU-positive nuclei with pyknotic morphology (Figure 6). Approximately 40% of the total BrdU-positive nuclei underwent apoptosis as measured by pyknotic morphology by twelve weeks and was significant [F

(6, 35) =7.517, p = .0001] accounting for 56% of the variance. Cell loss was a protracted process. The highest numbers of BrdU-positive nuclei with pyknotic morphology were observed at two, four and eight weeks post-METH. Post-hoc analysis showed the differences at two, four and eight weeks were significant [*MD*= 7.9, p=. 01]; [*MD*=10.7, p< .001], and [*MD*=10.0, p< .001], respectively.

3. Necrotic morphology

A population of the BrdU-positive cells displayed fragmented cell morphology including swelling and fragmentation of the membrane and vacuolization shown in figure 7. At every time point after METH a significant percentage of BrdU-positive cells displayed a necrotic morphology, one-way ANOVA [F (6, 35) = 7.693, p< .001]. By twelve weeks post-METH, approximately 30% of the newly generated cells were lost by necrosis.

C. Effects of METH on striatal volume

METH treatment had a significant effect on the striatal volume as seen in figure 8. METH-treated mice had significantly larger striatal volume than baseline in saline control mice. Two-way ANOVA [F (1,72) = 17.22, p< .001]. Note that the enlargement of the striatum normalizes to near saline-injected controls by twelve weeks post-METH but was still significantly different (p< .001) at every post-METH time point.

D. Figures summarizing Aim 1 results

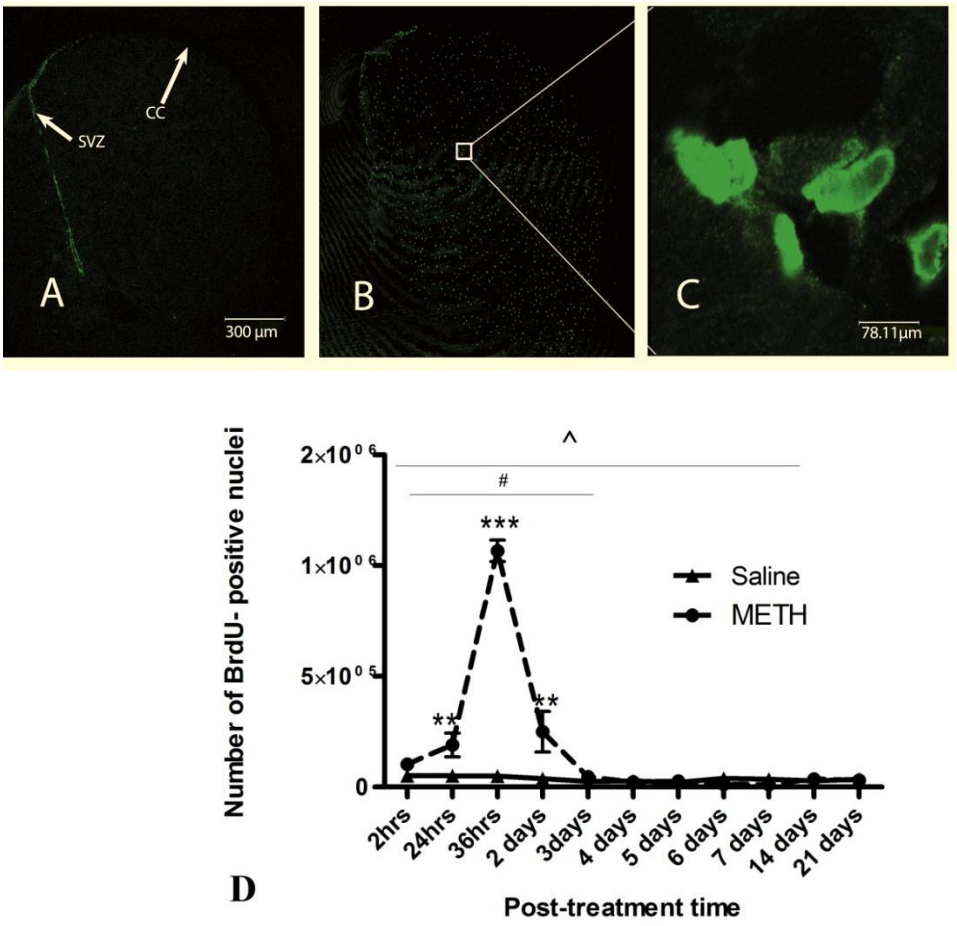

Figure 4. BrdU incorporation as a measure of proliferation (cytogenesis). Top panel (A-C) histology with anti-BrdU conjugated to FitC 36 hours after injections. No BrdU incorporation in the mouse striatum was observed after saline (Panel A), but robust BrdU incorporation after METH injections (Panel B) was observed at 36 hours. scale bar = 300µm. Cells can be seen to divide within the striatum (Panel C), scale bar 78.1µm. Quantification with unbiased stereology revealed significant BrdU incorporation between 24 and 48 hours after METH injections (broken line). After 48 hours and by 21 days proliferation declined to saline control levels (Panel D). Two-way ANOVA. ^ indicates significant two-way interaction effects between drug treatment and post-treatment time; # indicates significant effect of drug treatment; ** p<.01, ***, p<.001. n= 5 saline and 7 METH animals per time point.

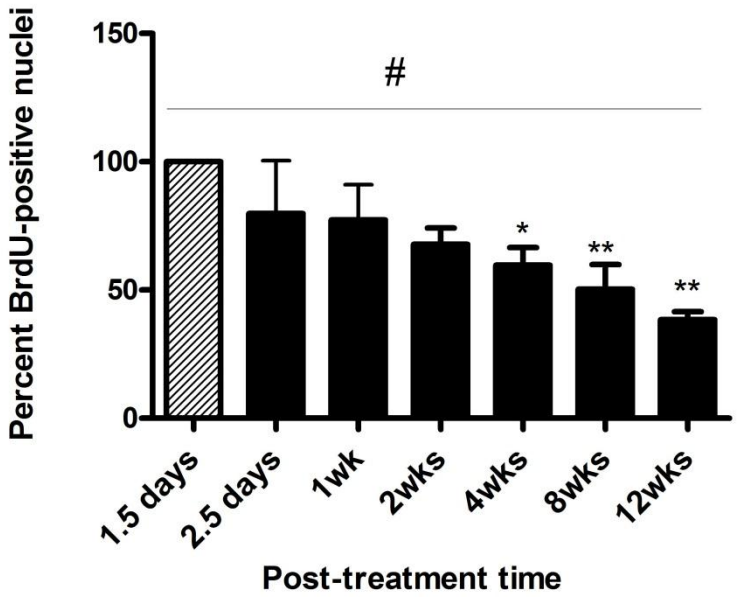

Figure 5. Percent survival of BrdU-positive with morphologically intact nuclei (non-pyknotic or non-necrotic) is observed over a time course of 12 weeks. There was a protracted loss of BrdU-positive nuclei over the entire time course but significant decline occurred at 4, 8 and 12 weeks after METH injections. Approximately 30% of new cells remained at 12 weeks. # indicates significant one-way ANOVA; * $p<0.05$ and ** $p<0.01$. n= 7 animals analyzed per time point. Note at 1.5 days the average BrdU-positive nuclei correspond to 100% of cells that proliferated thus no error is included.

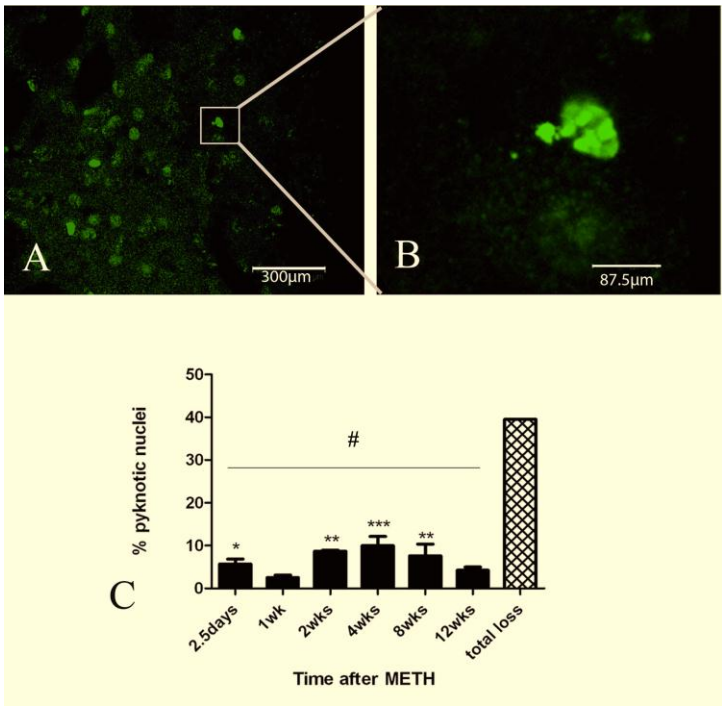

Figure 6. BrdU-labeled nuclei with pyknotic morphology. Cells with pyknotic morphology are shown at two weeks after METH in the striatum (Panel A), scale bar =300µm. A magnified area from panel A shows a fragmented nucleus as occurs during karyopyknosis in apoptotic cell death (Panel B), scale bar =37.6µm. Protracted cell loss by pyknosis occurred from 2.5 days to 12 weeks. Post-hoc demonstrated significant loss at 2, 4 and 8 weeks that totaled 39% of the new cells. # indicates significant one-way ANOVA; * $p<.05$; **, $p<.01$ and ***, $p<.001$ (Panel C). n=6 animals analyzed per time point. Note the total loss is sum of the average pyknotic nuclei from each time point thus standard error for the total loss data set is not present.

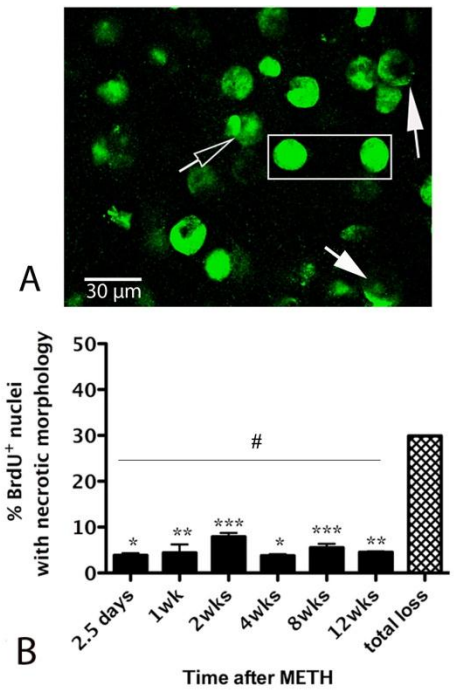

Figure 7. BrdU-labeled nuclei with necrotic morphology. Cells with necrotic morphology shown at two weeks after METH (panel A). White solid arrow shows an example of BrdU-positive disintegrated nucleus of a necrotic cell. Hollow arrow is an example of pyknotic nucleus in the same tissue sample, and white rectangle indicates intact nuclei that survived, scale bar = 30µm**.** There was a protracted loss with significant differences compared to baseline at every time point, for a total loss of 29% by necrosis (panel B). # indicates significant one-way ANOVA; *, $p<0.05$; ** $p<0.01$ and ***, $p<0.001$; n=6 animals per time-point.

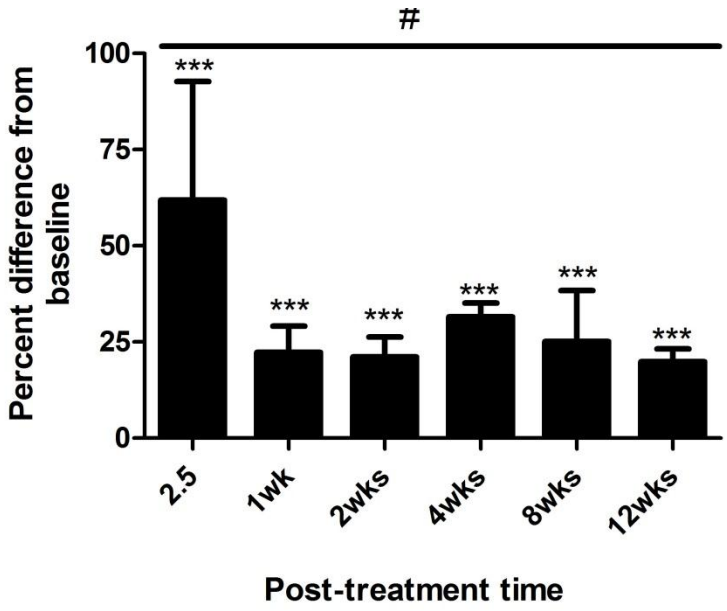

Figure 8. **Striatal Volume.** Quantification of the percent change in striatal volume for mice given METH compared to baseline mice (average of saline mice from proliferation study). Striatal volume in METH treated animals increased over the entire time course. The greatest volume increase was at 2.5 days with an average of 58.7%. Volume declined by 12 weeks to near control levels but on average still larger than control animals. This corresponds to the birth, the death and survival of some new cells; n=7 animals analyzed per time point. # indicates significant effect of drug treatment in two-way ANOVA; ***, $p<0.001$

E. Aim 1 Discussion

The results presented here demonstrate that a neurotoxic dose of METH induces cytogenesis that results in two phases of cell death in the striatum. First, previously reported by Zhu et al (2005), there is an acute phase of resident cell death that occurs 24 hours post-METH. At this time point after treatment, approximately 25 % of striatal neurons undergo apoptosis. Secondly, as reported here, cell proliferation occurs between 24-48 hours post-METH (12 hours after the peak of acute resident cell death), followed

by a protracted phase of apoptosis and necrosis of the newly generated cells extending over 12 weeks. The proliferative response is in agreement with multiple studies demonstrating cell proliferation in response to excitotoxic lesion in the adult brain (Gould and Tanapat, 1997; Dihne et al., 2001). However, a protracted phase of cell death consisting of the newly generated striatal cells in the aftermath of METH is novel and provides opportunities to study the long-term effects of METH.

Of particular relevance to the results reported here, are published results demonstrating that d-amphetamine and MPTP affect striatal cytogenesis. In contrast to our results, acute exposure to d-amphetamine (10 mg/kg) suppressed spontaneous BrdU incorporation (cytogenesis) in the striatum of rats (Mao and Wang, 2001). Unlike the present study, BrdU was given 1, 24 and 48 hours after the single injection of d-amphetamine and cells in one plane of the striatum were counted (Mao and Wang, 2001). We gave the mice an injection of METH (30 mg/kg) followed by BrdU at various times after METH. We observed some BrdU incorporation at 2, 24 and 48 hours, but the robust peak of BrdU incorporation occurred at 36 hours post-METH (1.5 days). We observed low levels of spontaneous BrdU incorporation in the mouse striatum. In the present study we counted BrdU incorporation using automated unbiased stereology in all rostral-caudal planes of the caudate-putamen. In contrast to d-amphetamine, exposure to systemic MPTP (25 mg/kg, once daily for five days) augmented BrdU incorporation into striatal cells and the newly generated cells survived for up to 60 days (Mao et al., 2001). It was not determined in the above studies if d-amphetamine and MPTP exposure resulted in loss of striatal neurons. In our study the robust incorporation of BrdU occurs 12 hours

after the peak of METH-induced apoptosis (Zhu et al., 2009), and approximately 30% of the newly generated cells survive up to 12 weeks post-METH.

The acute effect of METH has been reported to include dopamine overflow in the striatum followed by dopamine depletion and toxicity (for review see Yamamoto and Bankson, 2005; Krasnova and Cadet, 2009). Although we did not measure these aspects of METH, the timing of proliferation is interesting when these studies are considered. Some studies have shown that dopamine depletion persists up to 6 months (Seiden et al., 1975) and 4 years (Woolverton et al., 1989) after METH treatment in non-human primates. However, Cass and Manning (1999) showed partial DA recovery at 6 months post-METH in rats. They also found full recovery measured as evoked dopamine overflow and striatal tissue levels of dopamine by 12 months post-METH in rats. Since we measured survival of the new cells up to 3 months, it is to be determined if the newly generated cells contribute to the kind of dopaminergic recovery noted in the Cass and Manning study. An interesting factor in the data reported here is that cytogenesis occurs within a 12 hour window after previously reported loss of striatal neurons and acute dopamine depletion begins (Zhu et al., 2005). Published studies demonstrate that D2/D3 receptors are involved in proliferation and neurogenesis as well as gliogenesis in both developing and adult brain (Diaz et al., 1997: Van Kampen et al., 2004, 2005; Winner et al., 2009). Our results suggest that METH-induced striatal dopaminergic changes may play a role in the induction of cytogenesis observed in the present study but needs further investigation.

The protracted cell death induced by METH is different from the initial phase of cell loss occurring within the first 24 hours after METH. This initial phase involves the

loss of approximately 25% of striatal neurons that include DARPP-32 projection neurons and parvalbumin and cholinergic interneurons. The SST/NPY/NOS interneurons are resistant to METH (Zhu et al., 2006). Other laboratories have also reported the METH-induced loss of some striatal neurons using TUNEL (Deng et al., 2001) or Fluoro-Jade C (Bowyer et al. 2008). In the current work, the protracted phase of striatal cell death induced by METH is restricted to the newly generated cells.

Our results demonstrate that the production of new cells is associated with enlarged striatal morphology. This observation is particularly significant in the light of recent studies showing enlarged striatal volume in METH users (Jernigan et al., 2005; Chang et al., 2005, 2007). One study reported that subjects with enlarged putamen and globus pallidus had relatively normal cognitive performance compared to subjects with smaller striatal structures; suggesting a compensatory response (Chang et al., 2005). A recent *in vivo* imaging study reported enlargement of the striatum in rats exposed to METH (Delis et al., 2010). Our data demonstrate that the enlarged striatal volume begins to normalize over a period of three months in mice, the same amount of time associated with the bulk of protracted cell death. A human study found enlarged striatal volume (Chang et al., 2005) in recently abstinent METH users. However, a study assessing abstinent METH users drug-free for approximately two years reported normal striatal volumes (Oh et al., 2005). Our results show that the mouse striatum begins to normalize over a period of three months as most of the newly generated cells die by apoptosis and necrosis, suggesting that the enlarged striatal volumes observed in METH users may be accounted for by inflammation and the production of new cells.

In conclusion, the data demonstrate that a single high dose of METH induces the proliferation of new cells in the striatum during a narrow window occurring between 24-48 hours post-METH. The bulk of the new cells die off gradually over a period of 12 weeks that was measured. The METH-induced cytogenesis coincides with the enlargement of the striatum, which normalizes to near control levels by 12 weeks. At 12 weeks approximately 70% of the newly generated cells are lost by apoptosis and necrosis combined. Characterization of phenotype differentiation of the surviving cells is discussed in chapter 3 as a part of specific aim 2.

Chapter 3

Are the phenotypes of newly generated cells indicative of neurochemical recovery?

IX. Results.

A. Progenitor cell phenotypes.

1. BrdU-positive Nestin progenitor cells.

BrdU-positive nuclei expressing neural progenitor marker nestin were observed in the striatum (figure 9). Significantly more nestin positive cells were observed at 2.5 days and 1 week with a mean of 18.1 and 17.7% respectively. BrdU with nestin immunostain declined over the rest of the study and by 12 weeks only 4.8% remained. One-way ANOVA demonstrated that these differences were significant [F (5, 18) =6.63, p = .0012], accounting for 65 % of the variance. There was a significant linear trend for decrease over time [ß = -1.5, p< .001]. Post-hoc tests showed significant differences between early post-treatment times (2.5 days, and 1 week) when compared to later post-treatment times (8 and 12 but not 4 weeks) with, p< .05.

2. BrdU with Beta III- tubulin for progenitor cells

BrdU-positive nuclei expressing beta III-tubulin progenitor marker were observed in the striatum (figure 10). Beta III-tubulin phenotype appeared early at 2.5 days but peaked at 30% one week after METH. BrdU-positive nuclei co-labeled with beta III tubulin declined over the rest of the study time course to 6.6% at 12 weeks. One-way ANOVA showed these differences were significant over time [F (5, 18) = 11.5, p< .0001]. Post-hoc revealed significant differences between the peak at one week and

every other time point measured ($p < .01$). This was further confirmed by significant decreasing linear trend [ß=-1.07, $p = .002$].

3. BrdU with DCX for migratory progenitor cells.

BrdU-positive nuclei expressing DCX progenitor marker were only observed in the SVZ as shown in figure 11. Although it appears that extremely low DCX may have been in the striatum, orthogonal analysis with confocal microscopy demonstrated no BrdU co-label in this structure over the entire study time course.

B. Differentiation of cells to glial phenotypes

1. BrdU-co-labeled with S100B for astroglia cells

BrdU-positive nuclei were observed in the striatum with S100B co-label for astrocytes (figure 12). At 2.5 days after METH, approximately 9.8% of the BrdU-positive nuclei expressed S100B astrocyte marker. Increases in new astrocytes peaked at 16.5% peaked at two weeks after METH treatment. This peak was followed by a decline to 13.9% at 4 weeks and ended with 12.6 % at 12 weeks. One-way ANOVA revealed that these differences in astroglia were not significant over time [F (5, 18) = 1.1, $p = .39$]. There were no significant linear trends suggesting a stable or limited astrocyte differentiation [ß= 0.19, $p = .43$].

2. BrdU nuclei with IB4 for microglia cells

BrdU-positive nuclei reacting to the IB4 marker were observed in the striatum (figure 13). Cells adopted the microglia fate early, with a peak 10.3 % of BrdU nuclei co-labeled with IB4 2.5 days after METH. This peak was followed by small decline to 6.7%

by 12 weeks. Like astroglia, the percentage of new microglia over the study time course remained relatively flat after initial appearance. The lack of significant differences was shown by one-way ANOVA [F (5, 18) = .75, p = .59], with no significant linear trend [ß=0.59, p= .09].

C. Differentiation of cells to mature neuron phenotype.

1. BrdU-positive cells expressing NeuN for mature neurons

BrdU-positive nuclei co-labeled with NeuN were observed in the striatum (figure 14). The co-labeled cells were mostly present at later compared to earlier post-METH times. At 2.5 days after METH, very few (2.5%) of the BrdU- positive nuclei co-labeled with NeuN. However, there was a slow and steady increase to a peak of 13.8% at 8 weeks, which then decreased to 8.7% at 12 weeks. One-way ANOVA demonstrated that these differences were significant *[F* (5, 18) = 10.06, p = .0001] accounting for 73.6% of the variance. A significant increasing linear trend over the 12-week time course [ß= 0.907, p< .0001] further confirmed the differences. Bonferroni multiple comparisons post-hoc revealed significantly more cells adopting neuron phenotype at the 4, and 8 weeks post-METH time points, p< .01 and p< .001, respectively.

2. BrdU-positive cells expressing PV and ChAT for interneurons

A very small percentage of the BrdU-positive cells were seen to express markers for interneuron phenotypes at 8 and 12 weeks. Both phenotypes are presented on graphs in figure 15. A one-way ANOVA revealed BrdU-positive nuclei co-labeled with

ChAT was significantly different from zero [F (2, 9) = 73.04, p<.0001. New ChAT cells were 1.3% of BrdU-positive nuclei at both 8 and 12 weeks after METH. Dunnett's post-hoc test comparing each time point to zero new ChAT-positive cells generated revealed significant differences (p<.001) at both post-METH time points. BrdU-positive nuclei expressing PV were also significantly different as revealed by one-way ANOVA [F (2, 9) = 14.7, p=.001]. At 8 weeks and 12 weeks, respectively, .89% and 1.2% of the BrdU-positive nuclei were co-labeled with PV and post-hoc test revealed they were both significantly different form zero (p<.01) at each post-METH time point.

D. Figures summarizing Aim 2 results

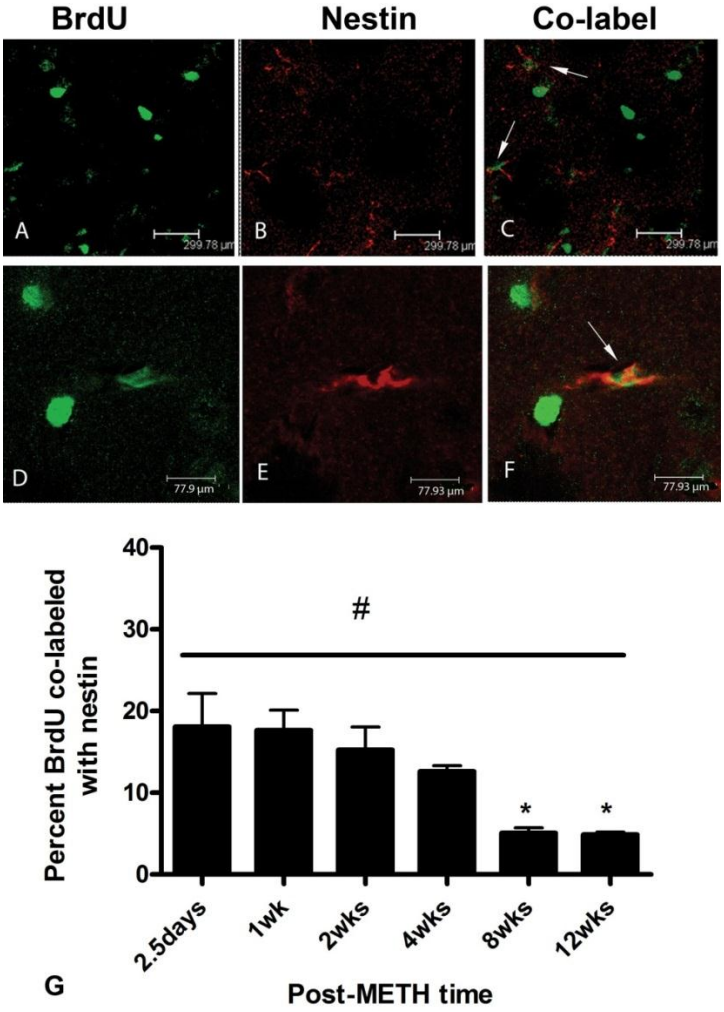

Figure 9. BrdU nuclei co-labeled with nestin. Z-stack images from representative striatal tissue sections taken 2 weeks after METH. BrdU-positive nuclei are labeled in green with FitC (panels A & D). Nestin positive progenitors are labeled with CY3 in red (panels B & E). Co-labeled cells can be seen the same tissue section indicated by white arrows, panels C & F. Top panels (A-C) scale bar 299.8= μm at 40x magnification. In the middle panels (D-F), scale bar =77.9 μm taken at 100x magnification. Significant one-way ANOVA (#) revealed the percentage of BrdU-positive nuclei co-labeled with nestin peaked between 2.5 days and 1 week. Post-hoc analysis demonstrated that new nestin progenitors declined significantly at 8 and 12 weeks compared to 2.5 days and 1 week (panel G), * $p < .05$. n=4 mice analyzed.

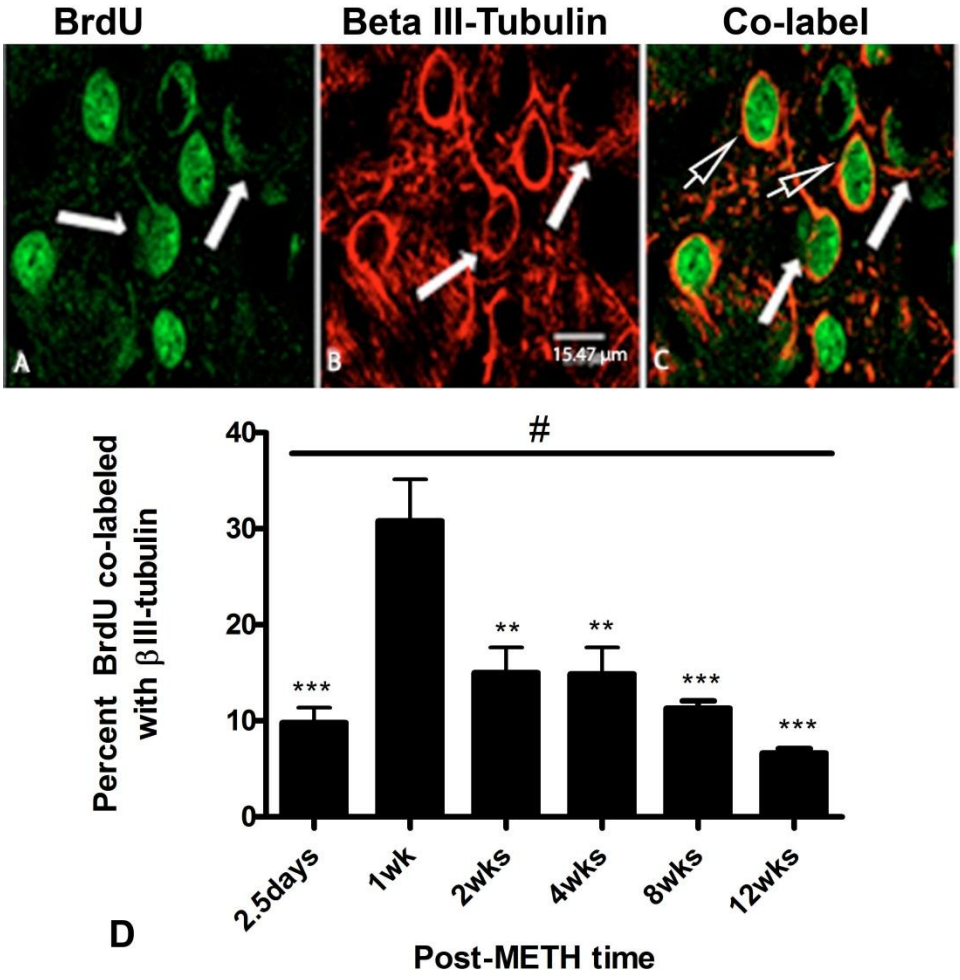

Figure 10. BrdU co-localized with ßIII-tubulin. Confocal z-stack image taken from representative striatal tissue section 1 week after METH. BrdU-positive nuclei are labeled in green with FitC (panel A) and ßIII-tubulin positive progenitors are labeled with CY3 in red (panel B). Co-labeled cells can be seen in the same striatal tissue section (panel C) identified by short hollow arrows. While solid arrows identify necrotic cells, scale bar= 15.47 µm taken at 100 x. Significant one-way ANOVA (#), revealed the percentage of BrdU-positive nuclei co-labeled with ßIII-tubulin peaked at 1 week but was significantly less at all other times after METH (panel D), ** $p < .01$, ***; $p < .001$, n=4 mice analyzed.

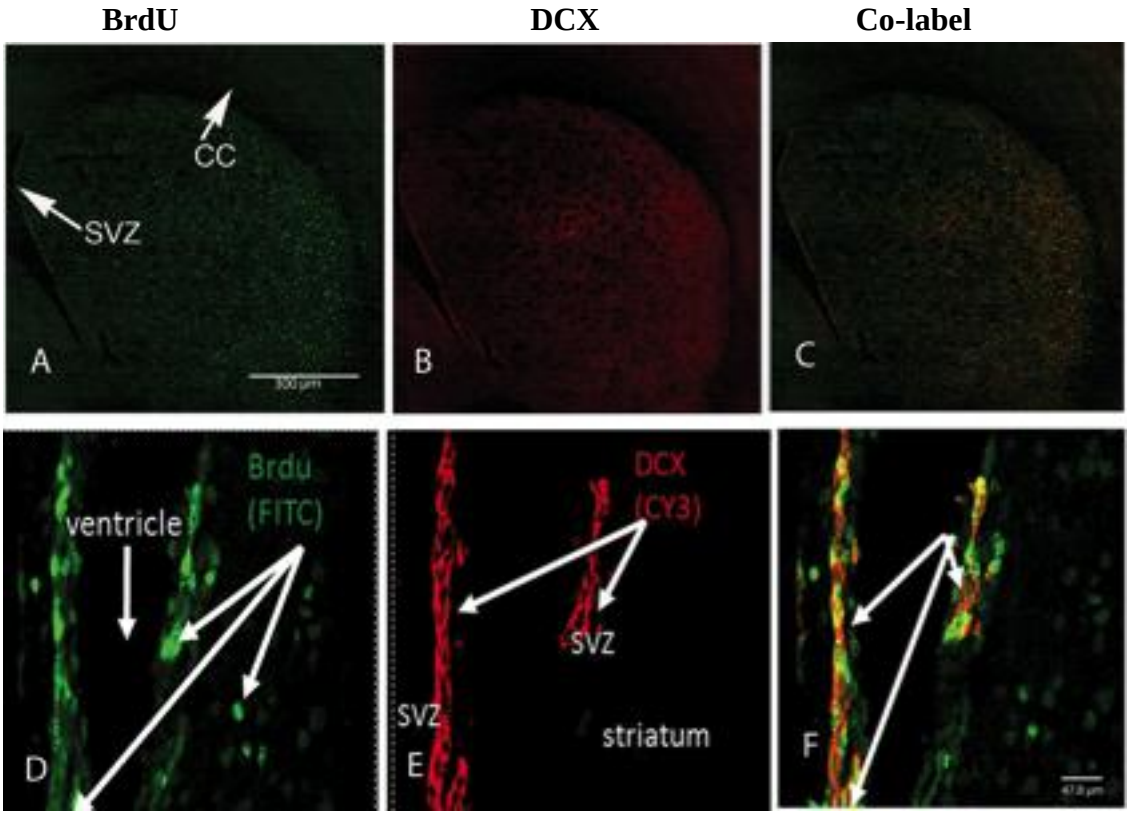

Figure 11. BrdU nuclei co-labeled with DCX. Confocal z-stack images were taken from representative striatal tissue sections at 2.5 days after METH. BrdU-positive nuclei are labeled in green with FitC (panels A and D) and DCX-positive progenitors are labeled with CY3 in red (panels B and E). No co-labeled cells can be seen in the same striatal tissue section (panel C) but are present in the SVZ (panel F) top panel scale bar 300 μm taken at 5x. Magnified SVZ image (bottom panels D-F) scale bar = 47.3 μm taken at 63 x. n=4 animals were analyzed and no co-label found. CC, corpus callosum, SVZ, subventricular zone.

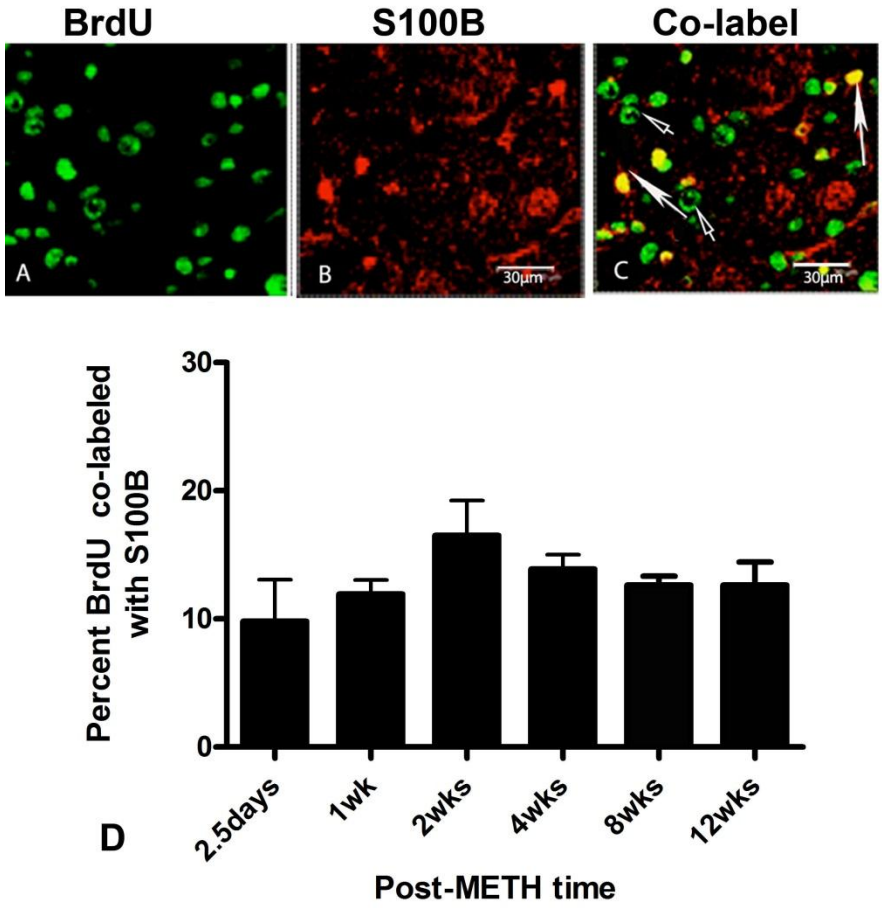

Figure 12. BrdU nuclei co-labeled with S100B. Confocal z-stack images from representative tissue section 12 weeks after METH. BrdU-positive nuclei are labeled in green with FitC (panel A) and S100B-positive astrocytes are labeled with CY3 in red (panels B). Co-labeled cells can be seen in the same tissue section (panel C) with solid white arrows showing astrocytes and hollow arrows showing dying cells; top panel scale bar= 30µm taken at 100x. One-way ANOVA revealed no significant difference between percentage of BrdU-positive nuclei co-labeled with S100B at various times after METH (panel D), n=4 mice analyzed.

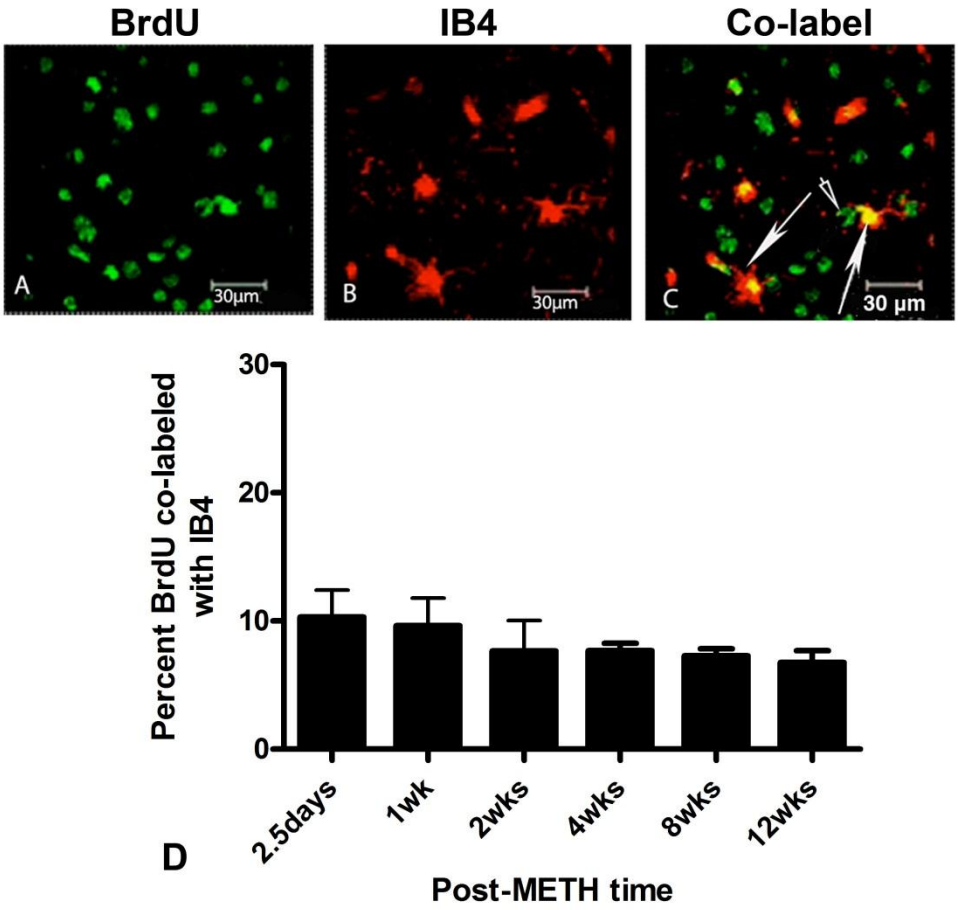

Figure 13. BrdU nuclei co-labeled with IB4. Confocal z-stack images from representative tissue section 12 weeks after METH. BrdU-positive nuclei are labeled in green with FitC (panel A) and IB4-positive microglia are labeled with CY3 in red (panel B). Co-labeled cells can be seen in the same tissue section (panel C). Long solid white arrows indicate microglia with the one on the left in an activated amoeboid form. Short hollow arrows indicate dying cells; top panel scale bar = 30µm taken at 100x. One-way ANOVA revealed no significant differences between any two post-METH time point (panel D), n=4 mice analyzed.

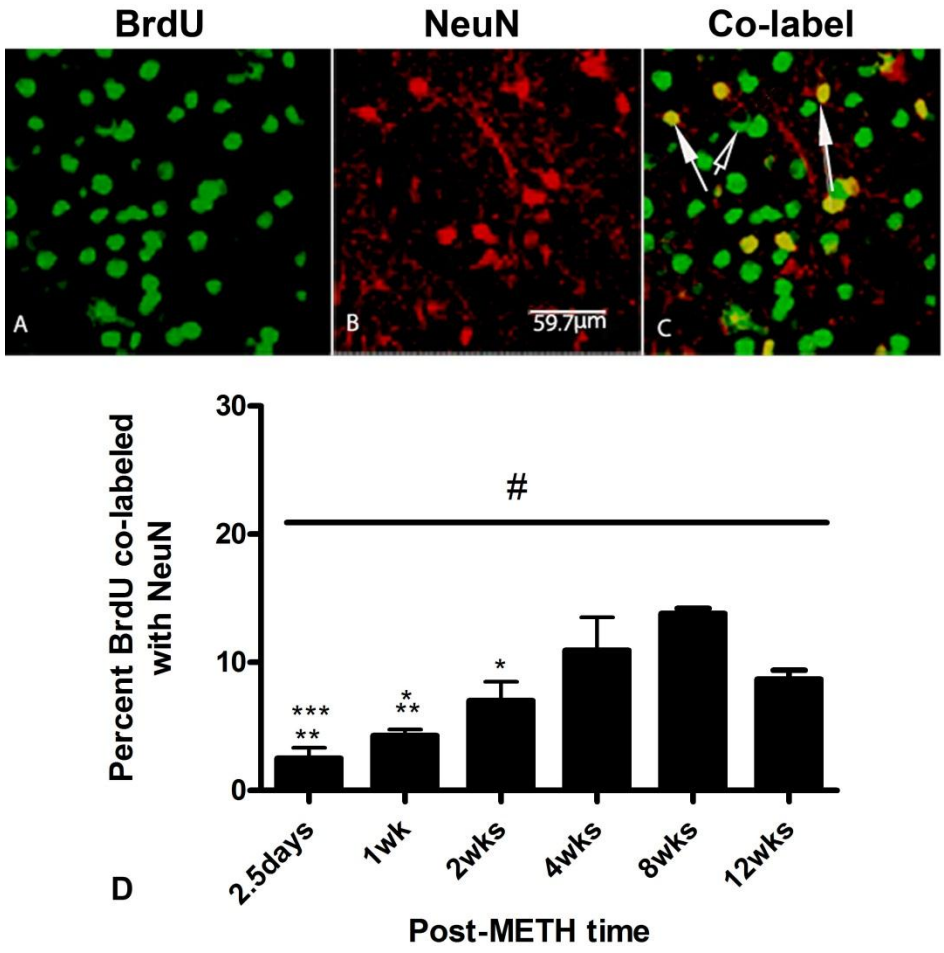

Figure 14. BrdU co-localized with NeuN. Confocal z-stack images from representative tissue section 12 weeks after METH. BrdU-positive nuclei are labeled in green with FitC (panel A) and NeuN-positive neurons are labeled with CY3 in red (panels B). Co-labeled cells can be seen in the same tissue section (panel C). Solid white arrows indicate neurons while hollow arrow shows a dying cell; top panel (A-C) scale bar = 30µm taken at 100x. Few co-labeled cells were present at 2.5 days and peak co-label was at 8 weeks. Significant one-way ANOVA (#) and post-hoc shows BrdU-positive NeuN cells significantly increased from 2.5 days to 8 weeks (panel D), * p<.05, ** p<.01, ***, p< .001; n=4 mice analyzed.

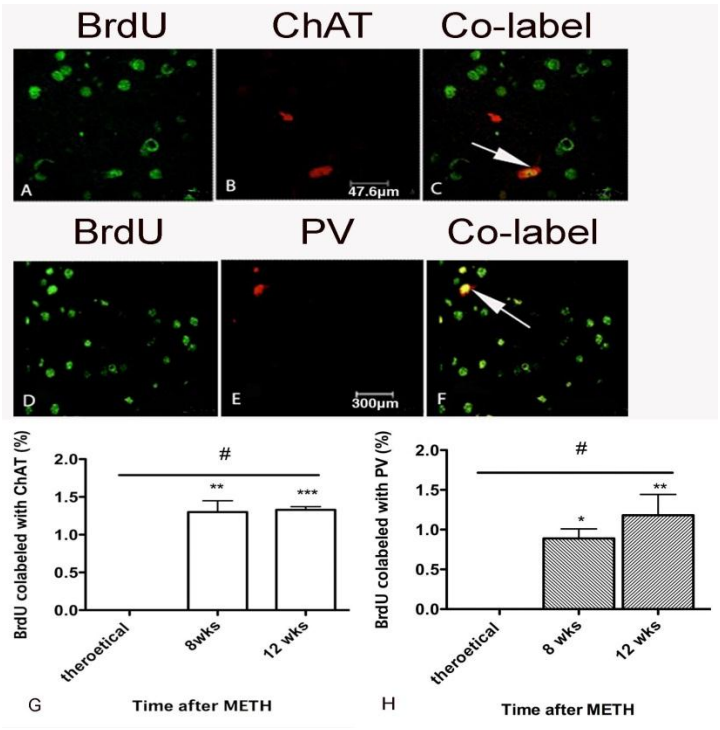

Figure 15. BrdU co-localized with ChAT and PV. Confocal z-stack image from representative tissue sections that were taken 12 weeks after METH. BrdU-positive nuclei are labeled in green with FitC (panels A and D). ChAT-positive interneurons are labeled with CY3 in red (panel B) and PV positive interneurons are also labeled with CY3 in red (panel F). Co-labeled cells can be seen in the same tissue section in panel C for BrdU+ChAT and panel in E for BrdU + PV. Arrows indicate co-labeled interneurons. Top panel for Chat (A-C), with scale bar= 47.6µm taken at 100 x. Middle panel for PV (D-F) with scale bar= 59.8µm taken at 100x. Few BrdU-positive cells with interneuron co-label can be seen. A one-way ANOVA (#) compared each phenotype to the theorized alternative hypothesis of no new interneurons generated. The low percentage of new ChAT (Panel G) and PV (Panel H) interneuron phenotypes are significantly different from zero at both 8 and 12 weeks after METH. * $p < .05$; **, $p < .01$ and ***. $p < .001$. n=4 mice analyzed.

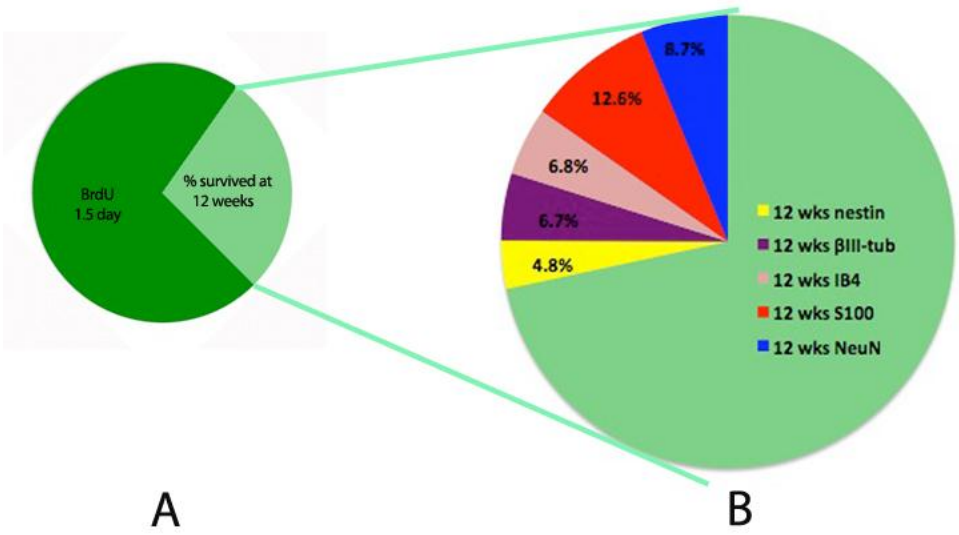

Figure 16. Pie charts representing cytogenesis and surviving proportion of new cells after a neurotoxic dose of METH. The entire pie on the left represents 100% of the BrdU nuclei present at 1.5 days with light green proportion representing approximately 38.4% of the new cells that survived to 12 weeks (A). Note that this survival could be as low as 30% surviving when taking into account the necrotic and pyknotic counts. The entire pie on the right (B) represents 100% of the surviving cells at 12 weeks (38.4% of 1.5 days) with the proportions that expressed various phenotype histochemical markers at 12 weeks. A significant proportion of the surviving cells (61.6%) remain unidentified at 12 weeks.

E. Discussion

BrdU-positive nuclei co-labeled with various phenotype markers were observed over a twelve-week time course of new cell differentiation at times after previously reported METH-induced cell death (Zhu et al, 2006). Most of the new cells first appear as neural progenitors and glial cells that show peak levels respectively within one and two weeks after METH. There were no migratory progenitors present. A significant

proportion of progenitors differentiate into mature neurons at later post-METH times, and a small subpopulation of the new cells displayed histochemical markers for interneurons.

During the early post treatment times at 2.5 days and 1 week, new cells expressed nestin and ßIII-tubulin markers for progenitor cells. Combined, these progenitors accounted for approximately 45% of the new cell phenotypes within the first week. No BrdU co-localization with DCX was observed in the striatum or a gradient of BrdU cells from the SVZ extending into the adjacent striatum. This lack of BrdU-positive nuclei co-labeled with DCX was not due to assay failure because BrdU+DCX cells were seen in the SVZ. We therefore conclude that there were no migratory progenitors and new cells did not derive from SVZ. We suggest that the new cells derive from dormant striatal progenitors.

In contrast to the prediction of glia cells appearing late after METH, most of S100B positive new astrocytes were observed early at 2 weeks and most of the new IB4 immunostained microglia were seen at 1 week. Together new glia cells accounted for approximately 25% of new cells at 2 weeks after METH. Some new cells differentiate to express NeuN histochemical marker for mature neurons mostly at 8 weeks, which accounted for approximately 14 % of the new cells. However, the proportion of new neurons declined to approximately 9% of the new cells by 12 weeks. A very small but significant proportion of new the cells were ChAT and PV immunostained interneurons at 8 and 12 weeks. Together these interneurons accounted for less than 3% of the new cells. Because we did not do triple co-localization for BrdU+ NeuN + PV or ChAT we could not say definitively what the percentage new NeuN cells were the interneuron phenotypes, but if they were, the numbers of PV and ChAT would account for 7 and 12

% NeuN cells respectively. Furthermore, many of the remaining new cells are unidentified and may be projection neurons but this requires further analysis for evidence.

These results are in agreement with suggestions of the generation of new striatal glia in response to injury (Kay and Blum, 2000). Furthermore, it supports studies that suggest a dormant population of progenitors in the mammalian striatum (Reynolds and Weiss, 1992; Magavi and Macklis, 2002; Parent et al., 2002; Bédard et al., 2002; Mao et al., 2001). For example, after identifying a low level of neurogenesis in the normal monkey striatum (Bédard et al., 2002) , the same group demonstrated in 2005 that the number of new neurons derived from striatal progenitors can be enhanced with neurogenesis promoting substances, such as brain derived neurotropic factor (BDNF). Furthermore, the new cells expressed morphological and chemical markers for striatal projection neurons. In contrast to our results, however, they did not observe new striatal interneurons. Mao and Wang (2001) also observed spontaneous cell proliferation in the rodent striatum, but none matured to express mature neuron markers.

In addition to neural progenitors and later maturation to neurons, we observed that a percentage of the new cells began expressing markers for astroglia and microglia within the first week after METH. However, the levels of new cells differentiating into glia remained flat over the 12-week period after they were generated with no significant difference in proportions. This suggests a rapid activation, as well as, a limit on the number of new cells that adopt a glial fate after METH damage. Boda and Buffo, in their 2010 review, suggested that glia in non-germinal areas like the striatum may acquire progenitor properties in response to different environmental signals and reenter the cell

cycle. However, there is a limit to the process. It appears from our results that this may indeed be the case in the striatal microenvironment after METH. Glial activation has also been shown to promote the generation, survival, and growth of new neurons, but can also contribute to bystander damage (Streit, 2002). Furthermore, glial derived neurotropic factor (GDNF) promotes striatal neurogenesis (Kobayashi et al., 2006). However, microglia can also promote further damage due to cytokines and other substances they release (Walter and Neumann, 2009, review). This suggests the necessity for a delicate balance in the levels of glia cells that are generated in response to injury and glial turnover have been shown to be restricted to a steady quantity (Kraus-Ruppert et al., 1973). Therefore, it is not surprising that glia would be generated in the injured striatum after METH exposure, or that they precede the differentiation neurons, while remaining at a limited level after initial appearance.

Our results are somewhat contradictory to Mao and Wang's (2001) finding that d-amphetamine decreased striatal gliogenesis. However, the same group demonstrated that MPTP, in contrast to d-amphetamine-induced striatal DA depletion, is accompanied by robust and rapid gliogenesis (Mao et al., 2001). The slightly different chemical structure and effect of METH compared to d-amphetamine (Shoblock et al., 2003), may account for the differences between our results and that of Mao and Wang (2001). Furthermore, glia are also needed for synaptogenesis (Allen and Barres, 2009, review). Given that our results revealed less interneurons are generated than previously lost during acute METH-induced apoptosis, synaptogenesis in surviving older cells might be a major part of the compensatory response to damage. Both compensatory processes might also require more glial cells during the early response, in order to enhance synapse formation in long

resident and new striatal neurons. Our findings are novel in that the data suggest gliogenesis that accompanies neurogenesis specifically after METH exposure.

The study taken as a whole shows a differentiation time course for neurogenesis similar to that suggested by Cooper-Kuhn and Kuhn (2002). The work by this team was in response to criticism that BrdU labeled cells might be DNA repair and not neurogenesis. However, they demonstrated, as we do here, that a proportion of cells are immunostained early with progenitor markers. Subsequently, over the progression of the study time course, BrdU labeled cells display less progenitors and more mature neuron markers. Furthermore, the level of BrdU detection is significantly higher than one would expect with the low levels of nucleosides that incorporate BrdU during repair. Bauer and Patterson (2005) revealed that high level of BrdU staining is not DNA repair because of there is too much BrdU incorporation for it to be reflective of only a few nucleosides being repaired. Moreover, and the methods of histochemical analysis for DNA repair is different from that of cell proliferation and a proliferation protocol to detect BrdU for repair resulted in near un-detectable BrdU incorporation (Bauer and Patterson, 2005; Schmitz et al., 1999; Uberti et al., 2003). Our results point to a likely proliferative event leading to neurogenesis because of the narrow timeframe in which the new cells are generated and morphologically can be seen to divide in the striatum then mature to neurons.

The generation of PV and ChAT interneurons suggests compensatory neurogenesis that may be involved in neurochemical recovery from METH damage, but within limits. With the exception of a few studies such as those by Van Kampen et al. (2004, 2005, 2006); Tandé et al. (2006), Mao et al. (2001) and Bedard et al. (2006), most

research to date have shown that new neurons derive from SVZ progenitors where they migrate to the injury site and mature to neuron and glia cell types (see, Kuhn et al., 2001 for review). Furthermore, like Kay and Blum (2000) found after lesions to the nigrostrial DA pathway with MPTP, we also found many of the new progenitors fail to survive. The low level of neurogenesis observed in the current study suggests additional substances are needed to enhance the compensation and recovery process. The Van Kampen group (2005; 2006) successfully demonstrated that a chronic two-week regimen of D3 receptor agonist previously shown to promote neurogenesis (Acheson et al, 1995; Huang, 2001), enhances neurochemical and behavioral recovery. In contrast to Hallbergson (2003) statement that new striatal neurons in response to injury "survive only a short while", we find the new neurons surviving three months after birth even though some are lost from the peak genesis time point. A longer time course would clarify whether new neurons survive long-term.

Our results are also in contrast to the Tandé group's (2006) conclusion regarding striatal neurogenesis in response to damage. They found dividing cells within the striatum after dopamine depletion induced by MPTP. These cells later expressed neuronal markers tyrosine hydroxylase (TH) and dopamine transporters (DAT). Tandé et al. also reported that the new TH positive cells were not aged over the time course of the study, implying that they were new. Similar to the data presented here, the cells they examined appeared in pairs like dividing cells, and did not show DCX immunoreactivity. However, because the cells they examined had co-localization for BrdU and TH, but not BrdU and NeuN, the authors suggested there was lack of evidence for neurogenesis. Therefore, they concluded that their results represented a phenotypic shift of resident striatal cells,

possibly even glia, into TH cells. Based on our results showing a time course of the progression of cells from progenitors to neurons within the striatum, we doubt this is a phenotypic shift, although this remains controversial. However, in the current study we found that the proportion of new glia cells remained flat, and we indeed observed NeuN co-localized with BrdU. Therefore, we report the novelty of a low level of neurogenesis following our previously reported time of appearance of METH-induced striatal cell death (Zhu et al, 2005, 2006).

Chapter 4

Do behaviors that require striatal function recover over the time course of cytogenesis in response to METH?

IX. Results.

A. Motor performance on the Rotarod

1. Pre-injection analysis of rotarod performance

Mean latencies to fall of the rotarod are presented in graphs for pre-injection and post-injection performance (figure 17). Analysis with a two-way ANOVA revealed no interaction effects between the assigned drug treatment and post-test time conditions, when tested for pre-treatment latencies to fall [F (5, 50) = .21, p= .96]. No effects of the post-treatment test time later assigned [F (5. 50) = 1.3, p = .28] was observed, or later drug-injection assigned [F (1, 50) = .28, p = .60]. Therefore, the mice were relatively matched on pre-injection performance when they were assigned to different groups.

2. Post-injection analysis of rotarod performance

Analysis of the post-injection performance by two-way ANOVA revealed that METH-injected animals performed worse on the task by scoring shorter latencies to fall off the rotarod (figure 17). Although the comparisons showed no significant interactions

between post-treatment time and the type of treatment [F (5, 50) = 1.04, p= .40], or the post-treatment time alone [F (5, 50) = 1.06, p = .*39*], a very significant effect of drug treatment [F (1, 50) =33.4, p< .001 was observed. The Bonferroni corrected post-hoc test showed that METH-treated animals fell off the rotarod significantly earlier than saline animals at twelve weeks post-injection [*MD* = -79.8 seconds, p <0.05].

B. Open-field Activities

1. Movement parameters in the open-field

a. Ambulation

For ambulation activity, the results revealed movement deficits in METH treated mice at specific times after treatment (figure 18). A two-way ANOVA revealed no significant interaction effects between drug x time tested on total ambulation [F (10, 75) = 1.5, p=. 15], nor drug condition alone [F (2, 75) = 2.4, p=12]. However, a significant effect of the post-treatment time was observed [F (5, 75) = 3.4, p< .01]. This suggested performance at one time point might be influencing the results. Bonferroni multiple comparisons post-hoc analysis revealed a significant difference in the ambulation of METH-treated mice at 2.5 days after injections compared to untreated controls [*MD* = -662, p< .01]. METH-injected mice also ambulated significantly less than saline injected mice at 2.5 days [*MD*= -546, p< .01]. There were no significant differences in ambulation between untreated animals and saline injected animals tested at any post-treatment time point.

b. Distance traveled

For distance traveled the pattern of behavior was similar to that of ambulation as seen in figure 19. Results from the two-way ANOVA revealed that although there were no interaction effects between drug treatment x time after treatment F (10, 75) =1.9, p = .06], or significant effect of the drug alone [F (5, 75) =21.4, p= .29], there was a significant effect of the post-treatment time tested [F (5, 75) = 2.7), p= .02]. Bonferroni multiple comparisons post-hoc revealed that the differences were between METH-treated mice and other treatment groups at 2.5 days. The distance traveled by METH-treated mice differed significantly from mice receiving no treatment [*MD*= 2298, p< .05], and saline treatment [*MD*=2670, p< .01] at 2.5 days. There were no significant differences between untreated and saline-injected mice tested at any post-treatment time.

c. Total movement

For total movement the pattern again suggested METH animals did not move as much compared to the untreated or saline injected mice at 2.5 days, although they recovered some frequency of movement over time (figure 20). No significant interaction effects between treatment x time tested [F (10, 75) =1.9, p= .06] or effects of drug treatment alone [F (5, 75) =2.0, p= .17] was observed. However, a significant effect of post-treatment time tested [F (2, 75) =2.6, p= .03] was observed. Bonferroni multiple comparison post-hoc revealed that at 2.5 days METH animals moved significantly less

than untreated animals [*MD*= -520, *p*< .05] and saline treated animals [*MD*=642, *p*< .01]. There were no differences between saline injected and untreated control mice.

2. Anxiety parameters in the open field (periphery versus center)

a. Number of entries

For the number of entries into the periphery versus the center zone of the open-field, untreated controls entered the periphery as often as they entered the center (figure 21). However, saline and METH injected animals entered the center more often at 2.5 days and less often at later post-treatment times compared to the one group of untreated mice. Multi-factor ANOVA revealed significant three-way interactions between location x treatment x post-treatment time [*F* (18,120) =10.6, *p*< .001]. Significant two-way interactions between location and treatment [*F* (2,120) =20.7, *p*< .001] and treatment x time [*F* (2, 5)] =14.4, *p*< .001] were also revealed. Because of these significant interactions, the data were split by location and planned analyses were done with two-way ANOVAs.

Using a two-way ANOVA revealed a very significant effect of the interaction between drug condition and time tested [*F* (10, 75) =5.3, *p*< .001]. Results also revealed a very significant effect of just the time tested [*F* (5, 75) = 13.5, *p*< .001] and just the drug condition [*F* (2, 75) = 14.6, *p*< .001] on the number of periphery entries. Bonferroni multiple comparisons post-hoc analysis confirmed that METH-injected mice had significantly less periphery entries at 2.5 days, 1 week and 2 weeks after injections (*p*< .001) compared to the one un-treated group of mice. Saline-injected mice also had

significantly less periphery zone entries at 2.5 days and 1 week, post-injection compared to the group of untreated mice ($p< 0.001$). There were no differences in periphery zone entries between saline and METH treated mice at any post-treatment time.

The planned analysis of center entries with a two-way ANOVA revealed significant interaction effects of drug treatment x post-injection time tested [F (10, 75) = 8.3, $p< .001$] for entries into the center zone. A significant effect of just the post-injection time tested [F (5, 75) =22, $p < .001$], and the type of drug treatment [F (2, 75) = 9.7, p = .002] was also revealed. Bonferroni post-hoc test results demonstrated that METH-injected mice entered the center less than the group of uninjected mice at 2, 4, and 12 weeks after treatment, with $p< .001$, $p< .05$, $p< .05$, and $p< .001$, respectively. Saline injected mice also entered the center less than the un-treated treated group of mice at 2, 4, 8, and 12 weeks with $p< .01$, $p< .01$, $p< .05$, $p < .05$, respectively. Additionally, METH-injected mice failed to enter the center as often as saline injected mice at 2.5 days after injections [MD= 33, $p< .001$].

a. Time spent freezing

The time spent freezing in the periphery versus the center are presented in graphs (figure 22). Just like the number of entries, the multi-factor ANOVA demonstrated that time spent freezing was also dependent on the location of the open-field. A significant three-way interaction effect of location x drug treatment x time tested [F (18, 120) =2.3, p = .004] was observed. Significant 2-way interaction effects of location x drug treatment [F (18, 120) = 14.4, $p< .001$] and drug treatment x time tested [F (2, 5) = 2.5, $p< .03$]

were also observed. Because of the significant 3-way interactions, planned analyses were done with two-way ANOVAs after splitting the data by location.

Planned analysis of freezing in the periphery indicated that at 2.5 days after injections, some METH treated mice were either anxious or unable to move and explore compared to the other groups of mice. There was a significant interaction effect of drug treatment x time tested on freezing behavior in the periphery [F (10, 75) = 2.5, p = .01]. There was also a significant effect of post-injection test time [F (5, 75) =1.8, p = .04], but no effect of drug treatment *[F* (2, 75) = 0.82, p=. 61] on freezing behavior. Based on the significant interaction and post-injection time effects, Bonferroni multiple comparisons post-hoc was done. METH-injected mice froze more often in the periphery at 2.5 days compared to the group of un-treated mice [*MD*=49.7, p < .01] and saline-injected mice [*MD*=49.8, p< .01]. No significant differences between the untreated group of mice and saline-injected mice were observed at post-injection times in the periphery.

Planned analysis of freezing in the center revealed no significant interaction effects between drug treatment x time tested [F (10, 75) =1.9, p= .054] on this open-field activity. Additionally, neither the post-injection time alone *[F* (5, 75) = 1.1, p= .38], nor the drug treatment *[F* (2, 75) = 2.8, p= .09] revealed significant differences. All mice avoided freezing in the center of the open-field in general.

b. Total time spent in the periphery and center

The total time spent in the periphery versus the center is presented in graphs (figure 23). As expected, all mice spent more time in the periphery than the center zone of the open-field. A multi factor ANOVA demonstrated significant 3-way interaction

effects of location x drug treatment x post-treatment time tested [F (18, 120) = 2.2 p= .005]. The results also demonstrated significant 2-way interactions between location x drug treatment [F (3, 120) =583.6, p< .001], but no significant effects of drug treatment x time tested [F (2, 5) = .41, p = .87]. Because of significant 3-way interactions, planned analyses were done with two-way ANOVAs after splitting the data by location.

A two-way ANOVA for the total time spent in the periphery confirmed no interaction effects of drug treatment x time tested for time spent in the periphery zone [F (10, 75 =1.6, p = .11]. No significant effects for just treatment time [F (5, 75) = .90, p= .48] or drug treatment [F (2, 75) =1.3, p= .31] were observed; suggesting the time spent in the center was influencing the 3-way interactions effects of time spent when the multi-factor ANOVA was done.

In contrast to time spent in the periphery, for time spent in the center, METH-treated mice avoided spent less time in the center compared to the other mice. A two-way ANOVA revealed significant interaction effects of drug treatment x time tested [F (10, 75) = 2.4, p= .01] but no significant effect of just the time tested [F (5, 75) =2.1, p= .069, or the drug treatment [F (2.75) =1.3, p = .31] alone. Bonferroni multiple comparisons post-hoc results revealed that at 12 weeks, METH-treated mice spent significantly less time in the center [MD= 46.6 seconds, p< .05] compared to saline-treated mice. There were no significant differences between groups of mice at any other post-treatment time.

The statistical results for all open-field measures that assessed “emotionality” or anxiety are summarized tables in appendix A.

C. Learning a T-maze task

1. Learning progress

Learning progress results are presented in graphs of figure 24. For training that began two weeks after treatment, one-way ANOVA revealed significant differences in the percent of correct arm entries per day of training between METH and saline injected mice, as well as, a difference from the theoretical chance performance [F (2,29) =8.3, p= .003]. Bonferroni multiple comparison post-hoc demonstrated, the mean correct response over the 10 day training period was significantly greater for saline compared to METH-treated mice [*MD*=15%, p< .01]. Saline-treated mice also performed significantly better than chance overall [*MD*= 12.7%, p<. 05]. In contrast, METH treated mice were not different than the 60% theoretical chance level in overall mean percent of correct entries [*MD*= 2.3%, p>.05]. Saline-injected also began responding above chance by the second day of training and reached criterion by day 6, compared to METH-injected animals. The latter group began responding above chance on the seventh day of training and reached criterion on day 9. All mice were responding at criterion on the 10^{th} day of training.

Learning progress in mice that began T-maze training 4 weeks after injections was the same for each treatment group, with little difference form chance when assessed by one-way ANOVA [F (2, 27) = .16, p= .90].

Learning progress in mice that began T-maze training 8 weeks after METH revealed that both METH and saline-treated mice had correct arm entries less than or equal to the theoretical chance levels. METH treated mice began responding above theoretical chance level by the 10^{th} day of treatment but a one-way ANOVA revealed there were no significant differences between saline or METH-treated mice [F (2, 27) = .18, p=.83].

Mice that began training at the 12-week post-treatment time began responding at or slightly greater than theoretical chance levels by the second day of training. METH-treated mice reached criterion of 80% correct earlier than saline-treated mice but these differences in percentage of correct arm entries were not significant [F (2, 27) = 2.2, p = .14].

2. Number of training days reach task criterion.

Days of training to reach criterion is presented on a graph (Figure 25). A two-way ANOVA revealed no significant differences overall between treatment groups for the number of days of training session. Interaction between drug treatments x post-injection training time had no significant effect [F (3, 39) =1.7, p = .19]. Type of drug alone also had no effect [F (1, 39) = .79, p = .38]; neither did post-treatment training time [F (3, 39) = .16, p = .93].

3. Latency to choose the correct arm

Latency to choose the correct arm is presented on a graph (figure 25). A two-way ANOVA revealed that the differences were not significant, F (3, 39) = 1.8, p = .16 for the interaction between drug treatment condition and time post-treatment training began.

There were also no significant drug treatment effects [F (1, 39) = .37, p= .54], or post-treatment training time effects [F (3, 39) = .01, p = .44].

4. Strategy used at criterion.

All mice did not use the same strategy once they reached criterion responding as shown in figure 27. Among the mice that began training 2 weeks after treatment, only 3 of 5 (60%) of the METH treated mice used a striatal strategy at criterion compared to 6 of 6 (100%) of the saline injected mice. For training at four weeks, 4 out of 6 (70%) of the saline and 4 out of 8 (50%) of the METH-treated mice used a striatal strategy. For training at eight weeks, 3 out of 6 (50%) saline and 2 out of 6 (30%) METH-treated mice used the striatal strategy. When training began at twelve weeks, 3 of 4 (60%) saline-treated and 4 of 6 (70%) METH-treated mice used the striatal strategy. However, results from Fisher's exact test revealed no significant differences in strategy used when training began at 2 weeks (p= .44), 4 weeks (p= .63), 8 weeks (p = 1) or 12 weeks (p=1) after injections.

5. Relationship between strategy and learning (Correlations).

It appears that the relationship between strategy and number of training days to reach criterion varied depending on the time after injections that mice began training (table 11). Pearson's correlations revealed that regardless of treatment condition, the relationship between striatal strategy and number of training days to criterion was significant at 2 weeks r (8)= -0.70, p= .02], with mice that used the striatal strategy learning the task in less time on average. At 4 weeks the relationship was the opposite [r

(12) = .60, p< 0.02], with mice that used the striatal strategy needing more training days to learn the task. In contrast, mice that began training at 8 or 12 weeks after injection did not perform in a manner that revealed a relationship between using a striatal strategy and the number of number of training days needed to reach criterion, [*r* (10)=.27, *p*=.4 and *r*(8)=.10, *p*=.77, respectively].

No relationship between strategy and latency to choose the correct arm per trial was observed. There were no significant correlations when T-maze training began at 2 weeks [r (8)=. 50, p=. 14], 4 weeks[r (12)=.34, p= .23], 8 weeks [r(10)=.13, p=.70)] or 12 weeks [(r (8)= .60, p=.66].

Note: Summary of statistical results for T-maze performance are found in Appendix B

D. Figures summarizing Aim 3 results

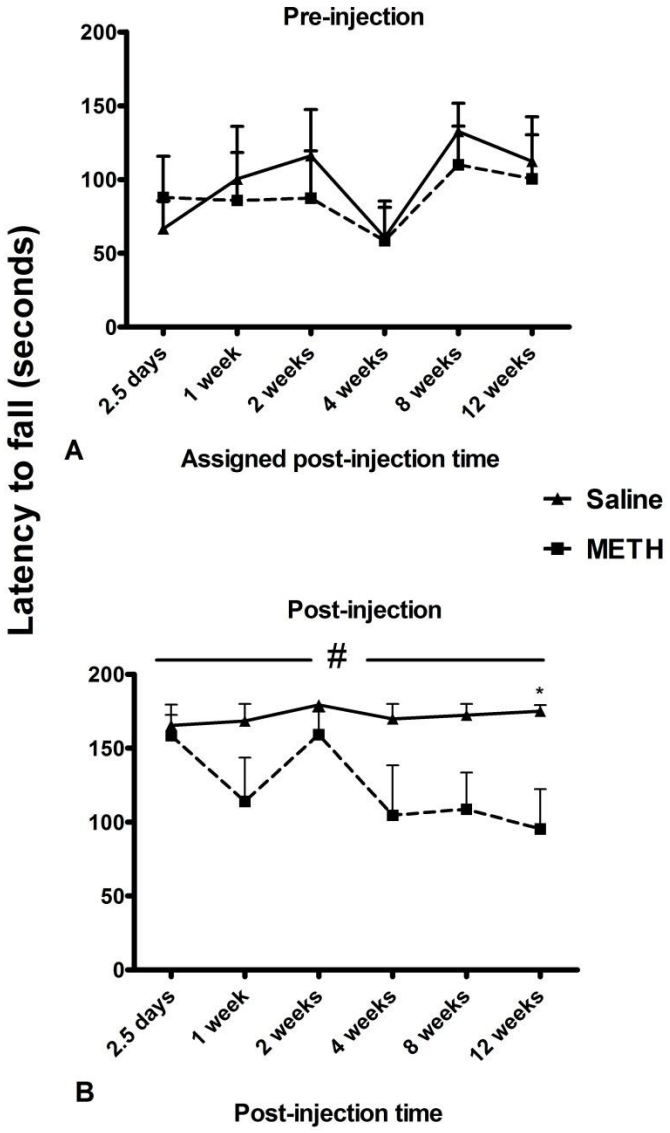

Figure 17. **Latency to fall off the rotarod**. Pre-treatment latencies to fall (panel A) were not different between animals later assigned to the METH or saline condition, as well as a given post-injection test time. In general, animals performed better after familiarity with the apparatus at post-injection times (panel B). A two-way ANOVA revealed significant effects of the drug (#) on post-treatment performance on the rotarod. METH-injected mice performed worse than saline-treated mice, and post-hoc tests revealed a significant deficit at 12 weeks. Broken lines are animals assigned to the METH group and solid lines are for animals assigned to the saline group. *, $p<0.05$ for post-hoc test result. *n*=6 per group.

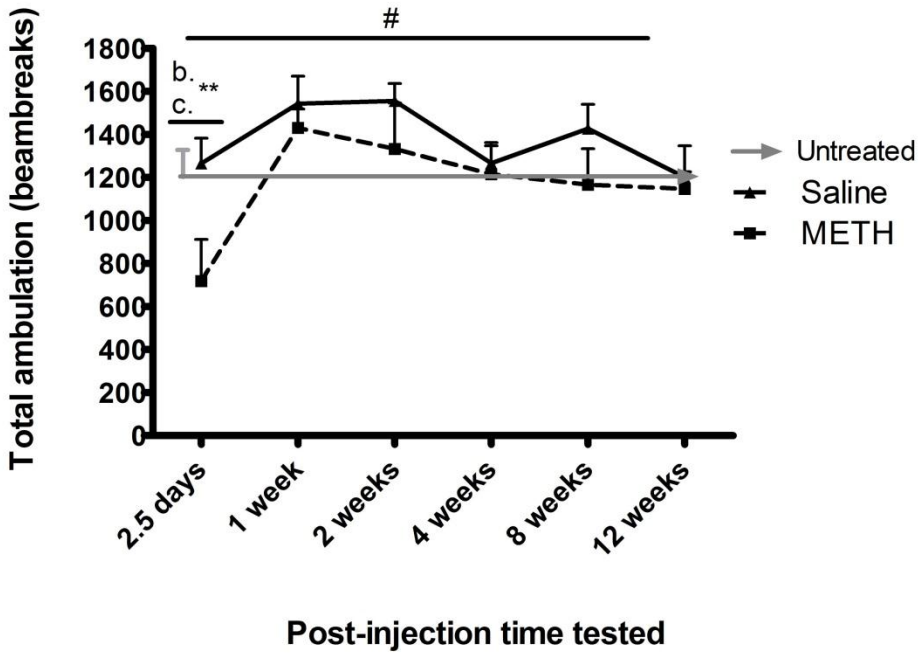

Figure 18. Ambulation in the open-field. Significant two-way ANOVA and post-hoc test revealed that mice injected with METH (broken black line), ambulated significantly less at 2.5 days compared to mice that had saline injections (solid black line) as well as one group of untreated mice (grey arrow). However, METH-treated animals recovered to saline levels of ambulation by 12 weeks. # indicates significant effect of time. b indicates post-hoc comparison between METH and untreated mice. c indicates post-hoc comparison between METH and saline treated mice. **, $p < .01$ significant differences for post-hoc test result. $n=6$ per group.

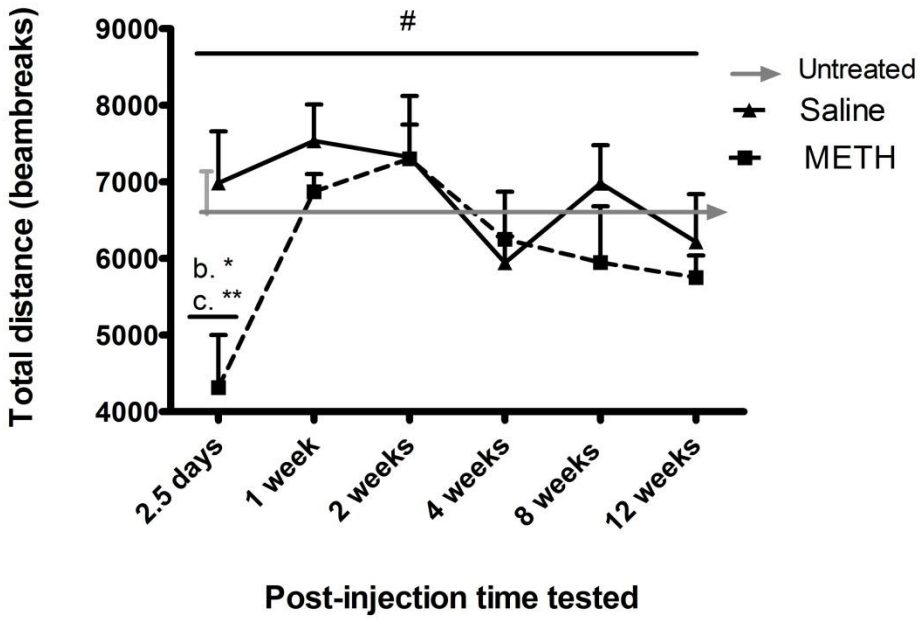

Figure 19. Distance traveled in the open-field. METH-treated mice (broken black line) traveled for a significantly less distance than the other groups of mice as assessed by two-way ANOVA. Post-hoc test revealed a significant deficit at 2.5 days for METH-treated compared to saline-treated mice (solid black line), as well as one group of mice that had no injections (grey arrow). From 1 to 12 weeks performance was the same for all groups of mice. # indicates significant effect of time. b indicates post-hoc comparison between METH and untreated mice. c indicates post-hoc comparison between METH and saline treated mice. *, $p < .05$ and **, $p < .01$ for post-hoc test results. n=6 animals per group.

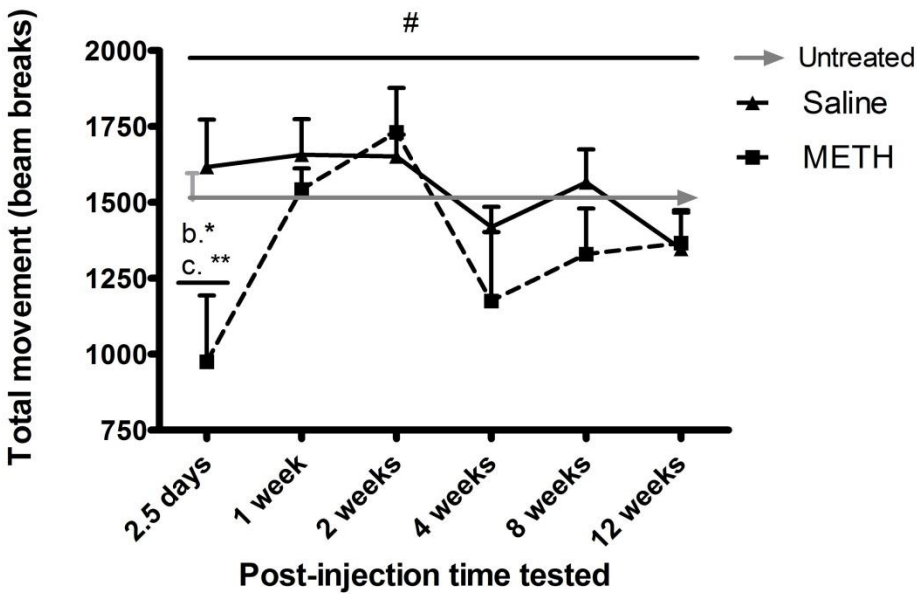

Figure 20. Total movement in the open-field. Mice injected with METH (broken black line) had significant movement deficits at 2.5 days compared to mice that received saline injections (solid black line), as well as the group of untreated mice (grey arrow). However, they recovered from 1 to 12 weeks. # indicates significant effect of time analyzed with a two-way ANOVA. b indicates post-hoc comparison between METH and untreated mice; c indicates post-hoc comparison between METH and saline-treated mice. **, $p < .01$ and *, $p < .05$ for post-hoc test results. n=6 animals per group.

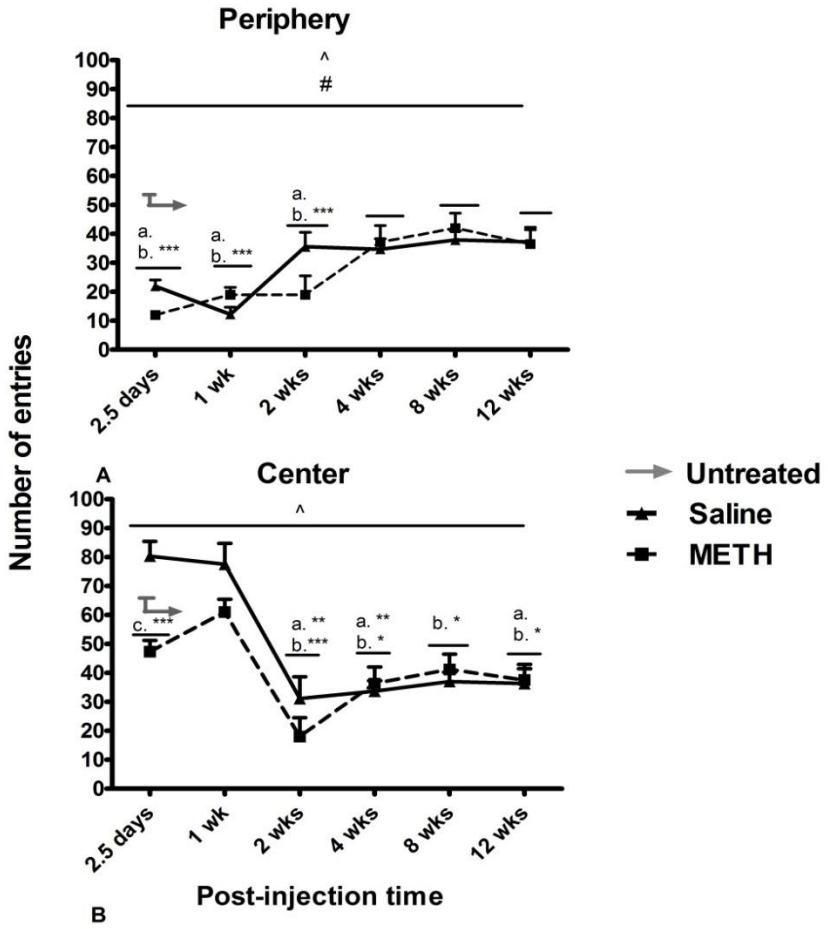

Figure 21. Entries into the periphery and center zones of the open-field. Note the closer tests were to injections (2.5 days and 1 week), the less frequent the entries into the periphery zone (panel A), and the more frequent the entries into the center zone (panel B). However, in comparison to animals that had no injection METH treated mice (broken black line) entered the periphery significantly less than untreated mice (grey arrow) at 2.5 days, 1 week and 2 weeks after injections, METH treated mice also entered the periphery significantly less than saline treated mice at 2.5 days. Saline treated mice entered the periphery less than untreated mice at 2.5 days and 1 week. For center entries, METH treated mice also entered the center significantly less than saline treated mice at 2.5 days and untreated mice at 2, 4 and 12 weeks (panel B), while saline treated mice entered the center less than untreated mice from 2 to 12 weeks. ^ indicates significant interaction effects. # indicates significant effects of time. Post-hoc: a is for comparisons between saline and untreated mice. b denotes comparisons between METH and untreated mice. c denotes comparisons between METH and saline treated mice. *p< .05; ** p< .01; *** p< .001 significant differences from post-hoc tests. n=6 animals per group.

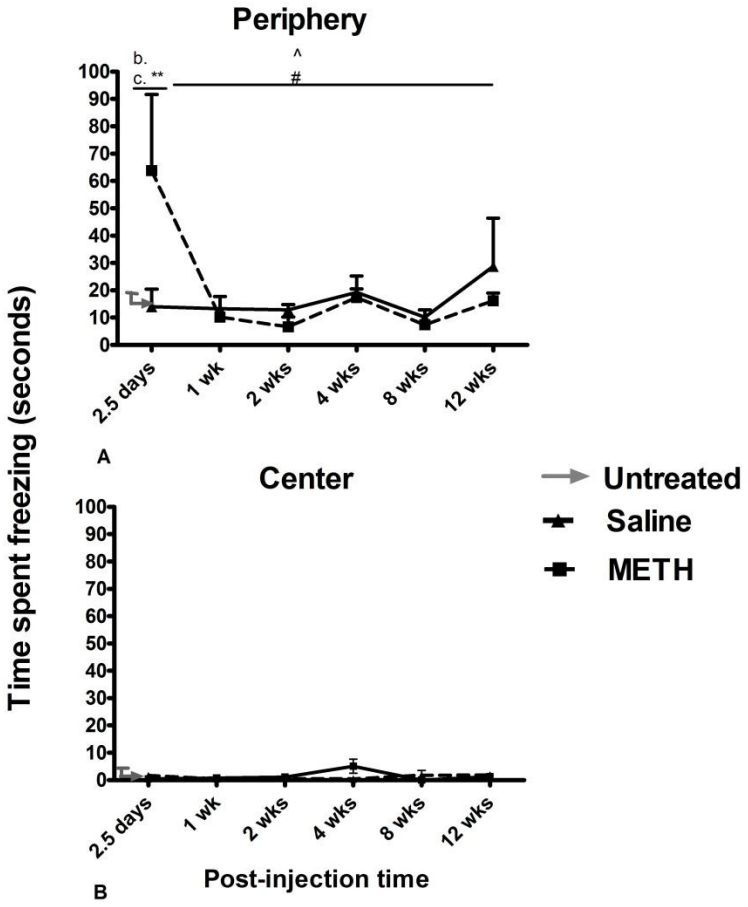

Figure 22. Freezing in the periphery and center zones of the open-field. All animals spent more time freezing in periphery zone (panel A) compared to the center zone (panel B). At 2.5 days after METH-treated mice (broken black line) froze significantly more in the periphery than saline- treated mice (solid black line) and untreated mice (grey arrow), but returned to control levels from 1 week to 12 weeks after treatment. Very little freezing occurred in the center zone of the open field and there were no significant differences between treatment groups from 1 to 12 weeks for freezing in the center. ^ indicates significant interaction effects. # indicates significant effects of time. Post-hoc results: b indicates comparisons between METH and untreated mice. c indicates comparisons between METH and saline treated mice. **, $p < .01$ for significant post-hoc results. n=6 animals per groups.

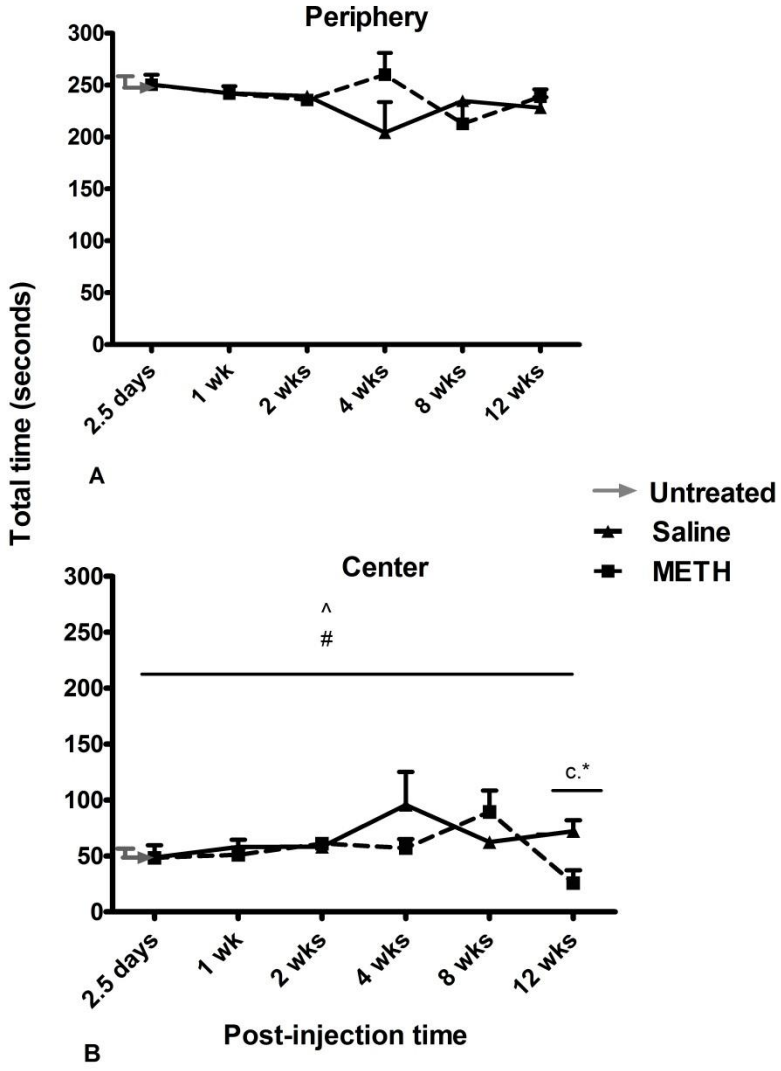

Figure 23. Total time spent in the periphery and center zones of the open-field. All animals spent significantly more time in the periphery (panel A) compared to the center (panel B) of the open field. No significant differences were seen between METH (broken black line), saline (solid black line) or untreated (grey arrow) mice in the time spent in the periphery. Time spent in the center was significantly less for METH-treated mice compared to saline-treated mice ^ is for significant interaction effects from the ANOVA. # indicates significant effect of time. c compares METH and saline treated mice on post-hoc tests. *, $p < .05$. n=6 animals per group.

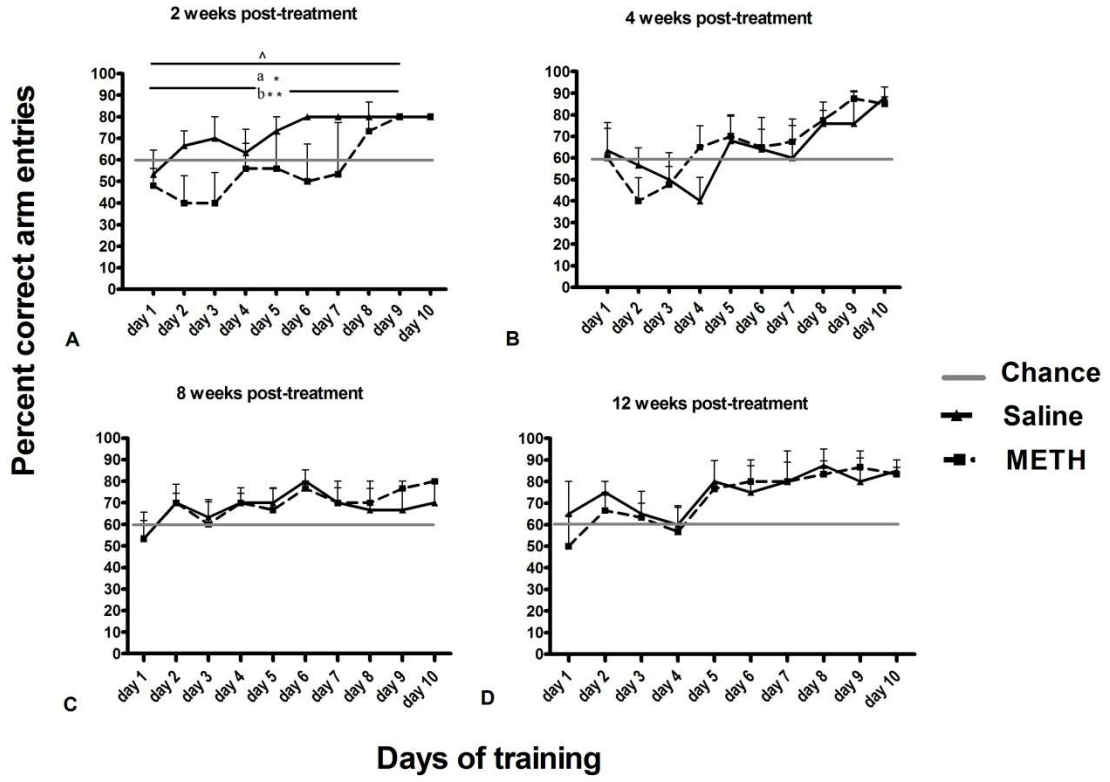

Figure 24. T-maze learning progress. Percent correct arm entries for each day of training on the T-maze when training began at various post-treatment times. METH-treated mice indicated by broken black lines. Saline treated mice indicated by solid black lines. Theoretical chance performance (3/5 or 60% correct) indicated by the grey line. All animals reached at least 80% correct performance within 10 days of training. Mice that began training 2 weeks after METH were significantly slower to learn compared to saline treated mice shown in the upper left panel (A) and no different from chance. Note animals from both the METH or saline treatment groups that began training at 4 weeks (panel B), 8 weeks (panel C) and 12 weeks (Panel D) reached criterion performance after nine days of training and were not significantly different from each other or chance. ^ indicates a significant one-way ANOVA. Post-hoc test results: a indicates significant performance difference between saline - treated mice and chance, c indicates significant differences between METH and saline treated mice at 2 week *, $p < .05$; **, $p<.01$. n=5-6 animals per group.

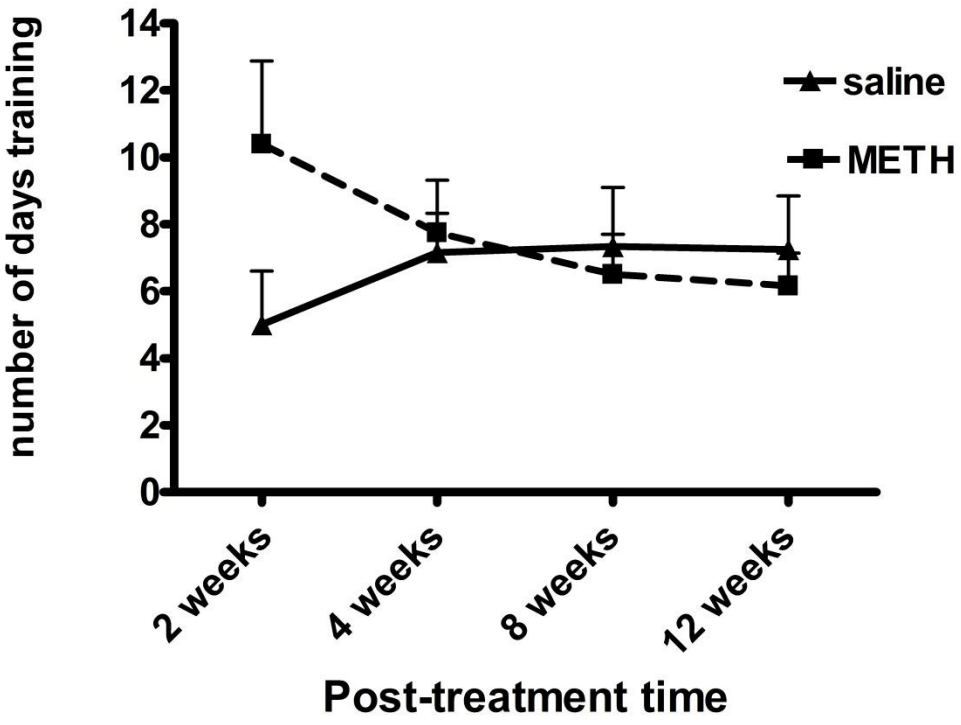

Figure 25. Number of days training to T-maze criterion response. The number of days it took METH (broken black line) or saline (solid black line) treated mice to reach criterion responding on the T-maze is presented. Mice began training at one of the following post-treatment times: 2, 4, 8 or 12 weeks after treatment. Although METH-treated animals took almost twice as long to reach criterion at 2 weeks, two-way ANOVA revealed no significant differences between the two treatment groups. *n*=5-6 animals per group**.**

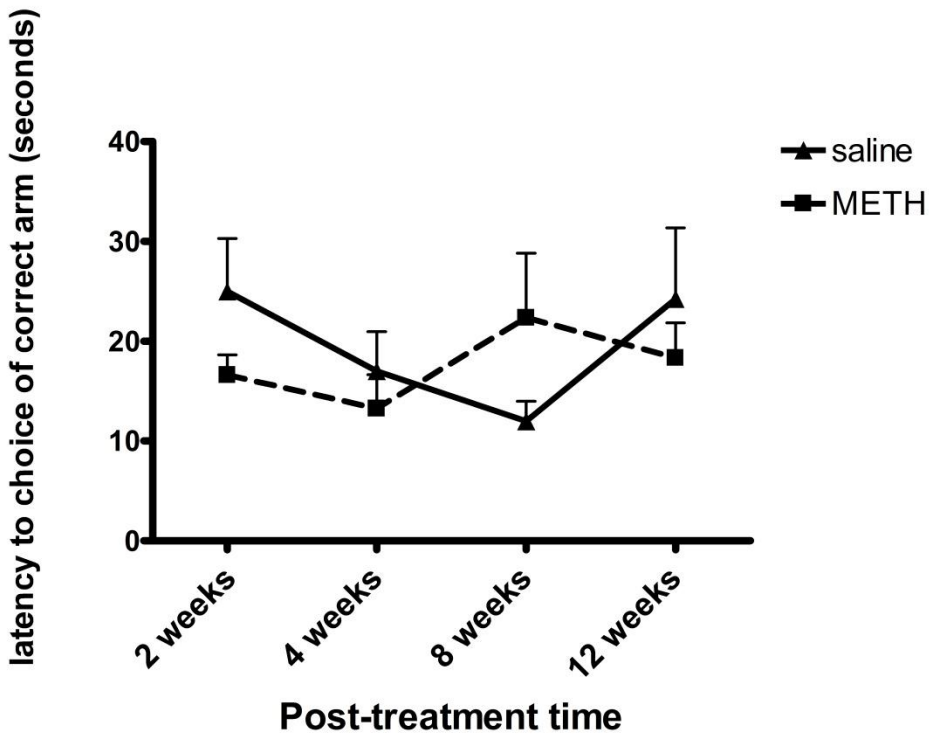

Figure 26. Average latency to choose the correct arm per trial on the T-maze. The average latency to choose the correct T-maze arm per trial was measured in METH (broken lines) or saline (solid lines) treated animals. Mice began T-maze training at either 2, 4, 8, or 12 weeks after treatment. Two-way ANOVA revealed the differences were not significant. *n*=5-6 animals per group

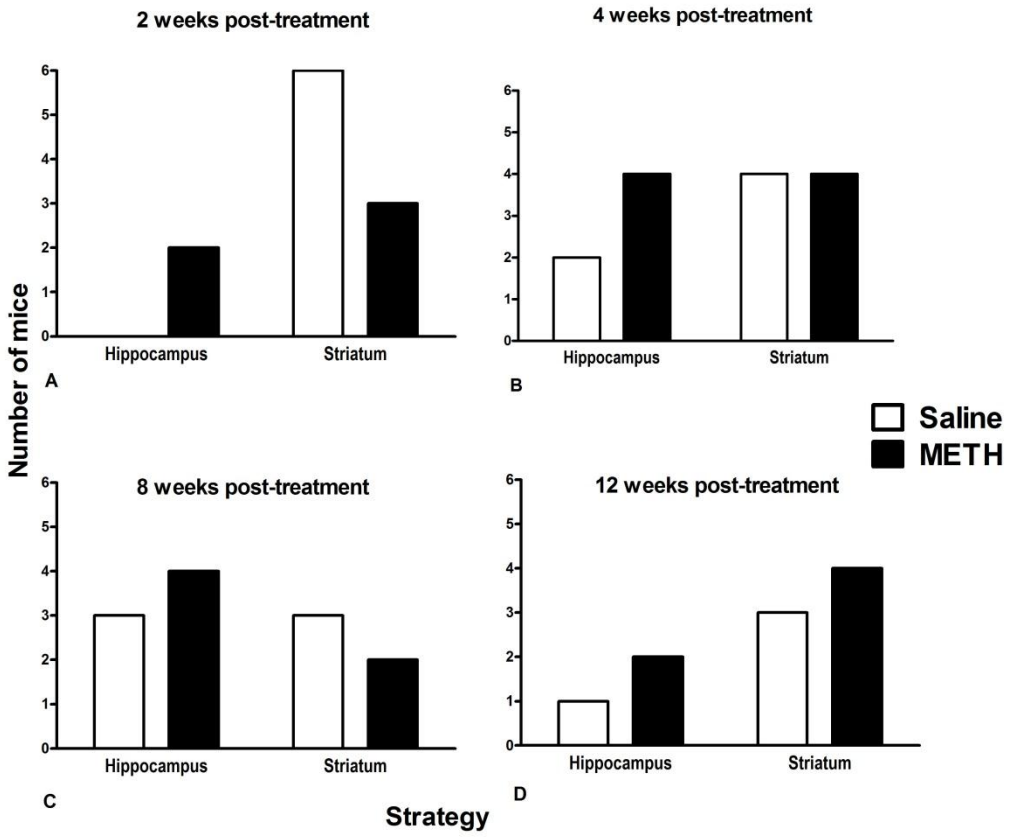

Figure 27. Number of animals using striatal or hippocampal strategy. The graphs reflect the actual number saline-treated (white columns) and METH-treated (black columns) mice that used the hippocampus or the striatum to solve the task at criterion. When training began at two weeks, all saline-treated mice used the striatal strategy compared to 3 out of 5 METH-treated mice. For training at four weeks, 4 out of 6 saline and 4 out of 8 METH-treated mice used a striatal strategy. For training at eight weeks, 3 out of 6 saline and 2 out of 6 METH-treated mice used the striatal strategy. When training began at twelve weeks, 3 of 4 saline-treated and 4 of 6 METH-treated mice used the striatal strategy. Note no standard error is presented as it is a total number of animals per strategy rather than the variability within and between groups. When assessed by Fisher's exact tests per post-treatment training time point, these differences were not significant.

E. Discussion.

Using behavioral tasks that require striatal function, METH and saline-treated mice were analyzed for motor coordination on the rotarod, two dimensions of psychomotor activity in the open-field (movement and anxiety), as well as reinforced habit learning on the T-maze. Data were collected over the same time course of METH-induced neurochemical studies reported in the previous chapters. The results suggest that METH-treated mice had persistent motor deficits as the new cells mature to neuron phenotypes, but habit learning on the T-maze recovered.

Rotarod and open-field (Motor performance when controlled for anxiety).

Performance on the rotarod without injections revealed that statistically, all the mice performed at similar levels. However, after injections, METH-treated mice had significant motor deficits compared to saline injected mice, and were worse at 12 weeks when they were approximately 6 months old. When considered with the movement parameters in the open-field, these results suggest motor performance deficits that cannot be fully accounted for by anxiety. For example, METH-treated mice failed to ambulate at 2.5 days, travel for much distance or generally move in the open-field compared to control mice. This suggested that during the time that 25% of striatal neurons are lost to apoptosis (Zhu et al, 2006) and new cells have just been generated (see chapter 2), the animals are too fatigued to move. Furthermore, METH treated mice most likely lacked the neurochemical support to more since our lab previously reported DA depletion at these post-METH times (Xu et al., 2005). In general, METH mice recovered open-field movement related behaviors to control levels by 12 weeks. This recovery contrasted with

the rotarod performance, suggesting general movement recovers but motor coordination worsens.

The results from anxiety measures in the open-field revealed that both METH and saline treated mice had fewer entries into the periphery and center compared to untreated controls. METH-treated mice entered the periphery less often than untreated mice from 2.5 days to 2 weeks. Saline-treated mice entered less than untreated controls at 2.5 days and 1 week. These behaviors in saline-treated mice suggest that injections separate from the type of drug may have affected the number of entries into the periphery and METH-treated mice required more time than saline-treated mice to recover. Furthermore, in contrast to the periphery entries, both saline and METH injected mice entered the center less often compared to untreated controls but it was at later post-treatment times, (2, 4,8, and 12 weeks) after injections. METH and saline-treated mice were also not different from each other except at 2.5 days, when saline-treated mice entered the periphery more than METH treated mice. Since this time point was when METH animals moved around the least, open-field results were likely due to motor deficits, fatigue and injections rather than a METH specific effect on anxiety.

As freezing behavior is a strong measure of anxiety (Crawley, 2007), the data is interesting in that freezing was mostly in the periphery, while most of the fear behaviors were expected in the center. METH animals froze a significant amount of time at 2.5 days in the periphery. Moreover, little to no freezing occurred in the center from any of the mice and no differences between treatment groups were seen in the center at any time point. Not many studies have measured the effects of METH on freezing behavior in the open field. However, freezing under other stressful experimental paradigms is common in

rodents and has been demonstrated in response to a repeated but not single dose of methamphetamine when DA or 5-HT levels are relatively normal (Tsuchiya et al, 1996). This suggests our data is novel in that freezing occurred in the stereotypically less stressful location and that the METH-treated mice might not have been fearful per se, but fatigued.

For time spent in the periphery versus center of the open-field, there were no differences between METH and either of the two control groups except at 12 weeks when compared to saline in the center. All animals spent most of the time in the periphery and the least amount of time in the center. Avoidance of the center and more time spent in the periphery is typical of thigmotatxic behavior in rodents (Simon et al., 1994). However, the data on time spent in the center is unclear because both saline and METH- treated animals statistically spent the same amount of time in the center as the untreated control group when tested at 12 weeks, yet, METH and saline treated mice were different from each other on this measure. This suggested the METH difference from saline may have been due to individual differences or outliers within the METH group. This was confirmed by looking at individual mouse performances. Two METH treated mice did not spend any time at all in the center (data not shown). This skewed the data toward less time in the center while the other four mice on average spent 39 seconds in the center.

It appears from the results for rotarod and open-field movement performance, that anxiety-like behaviors were not METH specific. Motor rather than anxiety behaviors were most affected in METH animals, and is in agreement with multiple studies that revealed altered striatal dopamine, or damage to the striatum, results in motor deficits (De Leonibus et al., 2003, Hollerman and Schultz, Hollerman et al., 2000; 1998; Feathersone

and McDonald, 2004; O'Doherty et al., 2004; Nakamura and Hikosaka, 2006a; Schultz et al., 1989; Wolterink et al., 1993).

Reinforced habit learning on the T-maze

Because METH is known to decrease cognitive performance based on appetitive learning (Achat-Mendez et al., 2005; Izquierdo, et al., 2010; Krasnova et al., 2009a), deficits for the T-maze habit-learning task were expected at the early post-treatment test times (2.5 days-2 weeks). This was predicted because newly generated neurons that survived would hardly begin to express mature histochemical markers or be functional at the early post-treatment time.

The results from measures of cognitive performance on the T-maze task suggest that the reward-based learning component of striatal function recovers. Recovery is observed over the later part of the time course when the new cells mature (four to twelve weeks) and METH-treated mice did not perform differently from controls. The only significant difference from controls observed in METH-treated mice was a slower learning rate when training began at the earliest measured time point at two weeks post-injection. Furthermore, most of the mice generally used the striatal strategy when they reached task criterion except at 8 weeks where only 30% used the strategy. However, the 8-week time-point also had the lowest proportion of saline animals using the striatal strategy at 50%. Although some METH and saline treated mice used the hippocampus strategy at task acquisition, the proportion of animals that used either of the two strategies was not significantly different between treatment groups, as assessed with Fisher's exact test (table 10). However, when all animals performing at criterion levels were assessed

together, animals that used the striatal strategy at two weeks learned faster. Mice that used a striatal strategy at four weeks took a longer time to learn. This was revealed by a significant negative and positive Pearson's correlation between strategy and learning rate at two and four weeks, respectively (table 11). The four-week correlational results on the T-maze appear counterintuitive because METH-treated mice had slower learning progress at two weeks. Furthermore, they responded at controls levels at later post-treatment times. This result might be due to the high accuracy in saline treated mice at two weeks since all the data were included in the correlations rather than split by treatment.

However, given the animals were not separated by treatment group in the correlation analysis, the apparent contradictory result at four weeks suggested that the time it was taking to choose the correct arm at might have influenced making the right choice. Animals that took longer to reach criterion may have entered any arm without spending much time to make the choice. When we went back and looked at the trial-by-trial latencies rather than the average use in the latency correlation, the animals that took the shortest amount of time to make a response when trained at four weeks had more errors. This suggested they quickly entered the arm opposite to the last one entered and this would result in an error score. With greater errors, they would require more time to begin responding at criterion even if the overall latencies to choose between groups were not different. Such behaviors on the T-maze are not uncommon during learning. Rodents with intact short-term memory tend to naturally avoid the last arm entered on a maze task in a behavior called spontaneous alteration (Deacon and Rawlins, 2006). Because they would have to keep the last arm visited in mind for over 90 seconds for the T-maze task,

this suggested that the animals had intact short–term memory but some could not correctly solve the choice conflict between alternating and entering the rewarded arm. METH-induced deficits in choice conflict performance on the T-maze have been demonstrated over a similar time course used in the current work (Friedman et al., 1998). However, to clarify these results would require follow-up studies with better controls specific for choice conflict. In addition more animals in the METH group would allow strategy correlation analysis by drug treatment, since some died before reaching criterion. This resulted in a smaller number of animals for analysis.

In general, there were no differences between METH and saline animals in T-maze learning progress (percent correct arm entries, and days of training to criterion) when training began four or more weeks after treatment. These results are in agreement with studies showing improvement for reward-based maze learning tasks at least four weeks after METH-induced striatal damage (Daberkow et al., 2007 and 2008; Friedman et al., 1998). In the Friedman et al study, up to 80% recovery in striatal DA turnover at the time of behavioral recovery was observed. However, multiple studies have revealed significant DA depletion in the striatum at the same post-METH times measured in our studies, and even as late as six months (Bittner et al., 1981, also see Krasnova and Cadet 2009, review) Therefore, the observed recovery may involve compensatory processes for persistent DA depletion but measures of DA depletion would need to be done in the animals tested in the current study, as this was not a part of the analysis.

Receptors and neurochemicals that are functional in newly generated cells, or the long resident striatal cells that survived the initial damage, might be involved in compensation or contribute to improvement on some behaviors that we observed. It is

interesting that increased dopamine receptor sensitivity is accompanied by behavioral recovery after nigrostriatal depletion with 6-OHDA (Neve et al., 1982). DA receptors have also been observed at late post-treatment times after MPTP damage (Todd et al., 1996), and DA receptor plasticity is suggested to play a role in the habitual behaviors of addiction (see Chen, et al., and 2009 review). DA turnover or its receptor levels were beyond the scope of the current study, however. More studies are needed regarding the role of new cells in relationship to DA and the mechanisms of addiction.

The improved habit learning performance at the same time point new cells express the most mature neurons markers (four to twelve weeks), suggests compensation or recovery of reinforced learning behaviors, to the exclusion of a subtle choice conflict deficit that needs further study. Furthermore, results suggest cytogenesis may play a role in the process and is a METH specific novelty. In conclusion, reinforced habit learning on a maze task recovers at the same time new striatal cells mature but motor coordination worsens; revealing METH-induced cytogenesis in the mouse striatum facilitates only partial recovery from damage.

Chapter 5

Implications for future studies and conclusions

Cytogenesis and neurochemical studies.

Using immunohistochemical assays, psychomotor and habit learning tasks, a study of cytogenesis in the context of neurochemical and behavioral effects following METH-induced cell death in the striatum was presented. The results demonstrated that METH induces robust cytogenesis in the striatum twelve hours after the previously observed loss of approximately 25 percent of striatal cells (Zhu et al., 2006) or 36 hours after METH treatment; a time when we previously reported DA terminals are depleted (Xu et al., 2005). A significant proportion of the new cells die but many also survive as animals show increased striatal volume over three months. A proliferative response leading to neurogenesis in the rodent striatum after neurotoxic METH exposure is a novel finding. Furthermore, maze learning recovery over the same time course as new cells mature is also novel. These data also provide an additional process involved in the observations of Chang et al. (2005, 2007) and Oh et al. (2005) studies, which revealed that humans who previously used METH had enlarged striatal volume that accompany normalized behaviors.

In these previous volume studies, gliogenesis and inflammation were explained as the reason for volume increase. Our studies confirm the gliogenesis hypothesis since new cells included astroglia and microglia. However, the results also provide evidence that neurogenesis is a part of the process. One concern with the data presented is that the

combined percentage of cells displaying necrotic and pyknotic morphology totaled approximately 69.8% of BrdU-positive nuclei over the twelve-week time course, but the percentage of surviving nuclei (non-pyknotic or necrotic morphology) was 38.4% at the twelve-week time point. This is an 8.2% discrepancy which might be due to the some necrotic cells appearing pyknotic that were counted as both types of cell death. Davidson et al. (2001) summarized the evidence that both types of cell death occur in response to METH. Additionally, Kroemer et al. (2009) recently reviewed the evidence that necrotic cells can show moderate shrinking of the nucleus that is usually seen in apoptosis. Although two different individuals blind to the conditions performed the stereological counts, they had the same statistical results within 95% agreement. Furthermore, since this is not a large error in terms of the amount of BrdU-positive nuclei generated at the peak, we deem the results acceptable within an 8.2% error of cell death. Follow up studies using histochemical markers specific for the type of cell death would further clarify this discrepancy.

Another novelty of the data presented is the specificity of the cytogenesis to neurotoxic METH exposure that provides an explanation for the disparity in duration of METH induced cell death. The protracted death of new cells provides an additional phenomenon for studies of METH toxicity. The results also confirm data from other studies, which show injury-induced cytogenesis in the damaged striatum (Collin et al., 2005; and Mao and Wang, 2001). Failure to observe DCX progenitors in the striatum provides additional confirmation for a population of dormant progenitors within this structure, which become activated under injury conditions. An alternative explanation is that the times after treatment measured could have been too late to detect DCX. However,

when we examined a few animals at 2 and 24-hour proliferation time points for DCX staining (data not shown), none were present in the striatum. Since, previous studies also suggest dormant striatal progenitors (Bédard et al., 2002; Mao and Wang, 2001; Parent et al., 2002b), it is not unreasonable to find that the new cells fail to display the DCX marker for migrating progenitors.

The results demonstrate that the striatum also generates specific cell types previously lost to acute METH and suggest cytogenesis and neuron maturation of new cells might be an attempt at neurochemical recovery. However, the levels of recovered neurons were very low. Only two striatal subpopulations were examined because they represented the largest population of neurons previously found to undergo apoptosis during the acute METH response (Zhu et al., 2006). The interneurons we examined immunostained for PV and ChAT but other striatal neurons can be generated in response to damage (Collin et al., 2005; Parent et al., 2002a). For example, DARPP-32 and NPY neurons were found after quinolinic acid lesions (Collin et al., 2005). Additional phenotype studies would determine whether the remaining unidentified population of cells includes other striatal interneurons and projections neurons. The low percentage that we observed for PV and ChAT correspond to the distribution of striatal neurons (Kawaguchi et al 1997) as they normally make up less than 3% of striatal neurons. If the new PV and ChAT cells were also co-localized with NeuN, it would account for 7 and 12 % of NeuN cells respectively. However we did not do triple co-localization and the numbers are not sufficient replacement for the amount of loss these cells undergo.

As METH has been previously shown to induce DA overflow, glutamate and NO upregulation, and consequently DA depletion (Krasnova and Cadet, 2009 review;

also Chapter 1: section II of this document), a question regarding cytogenesis is what is the actual trigger? Numerous studies have implicated DA activity in adult neurogenesis, but as a whole the results from these studies are unclear (Borta and Hoglinger, 2007; Mori et al, 2008 reviews). Our results however, are in agreement with data that show DA agonist induce proliferation, and DA antagonist or depletion, induce survival and maturation of cells that become neurons (Coronas et al., 2004; Hoglinger et al., 2004). Since METH is a DA agonists and cell proliferation peaks at 36 hours; the same time our lab previously reported the beginning of DA depletion (Xu et al., 2005), a case can be made for lack of dopamine promoting the generation of new striatal cells. However, we would have to take measures of DA levels in future studies of METH-induced cytogenesis to clarify these issues. Furthermore, we propose lack of DA is less likely to be driving proliferation of new cells because significant proliferation was already underway at 24 hours.

There is evidence for the DA agonist reducing cytogenesis with the amphetamine analog d-amphetamine. For example, Mao et al. (2001) found decreased cytogenesis, but in the SVZ. The different microenvironment from the striatum may play a role. Furthermore, the striatum has NPY cells that do not suffer cell loss in response to METH. Striatal NPY mRNA is increased within three hours after acute and binge dose of METH, and it is mediated by METH-induced D1 receptor activity (Horner et al., 2006). In addition, NPY promotes the generation of new cells (Agasse et al., 2008; DeCressac et al., 2009; Howell et al., 2007; Thiriet et al., in press). These data suggest that NPY may contribute to the striatal cytogenesis and subsequent neurogenesis, but it needs further testing in a similar context as the current study.

Another interesting hypothesis to test, given the results reported here, is whether the level of cytogenesis observed corresponds to the level of acute cell death of old striatal cells following METH exposure. Alternatively, would animals that do not experience significant METH-induced cell death but still have damage respond in a similar manner? For example, if there are unidentified signals for proliferation that accompany apoptotic cell death after METH, cytogenesis would not be expected after a non-toxic dose of METH or cocaine. If, however, it is D1 receptor stimulation and/or NPY activity that most influences the neurochemical results reported here, cytogenesis may result regardless of the level of cell death. One indication that the levels of new cells may not actually correspond to the level of cells that die is the PV and ChAT results. However, since many new cells remain unidentified, the results of these interneuron types do not provide enough information and further studies with other phenotypes are needed. Another consideration is that NO via SP receptor activity may also influence the generation of new cells. NO has been shown to both promote and inhibit neurogenesis (Cardenas et al., 2005; Luo et al., 2010; Pena-Altimira et al., 2010). It is interesting that D1 and SP receptors are on the NPY/SST/NO cells. Future studies that pharmacologically manipulate this cell type, then measure cytogenesis can further clarify these issues.

Cytogenesis and behavioral studies.

In a different group of animals we looked at behavior over the same time course as the neurochemical studies. METH-treated mice had clear motor deficits on both open-field and rotarod tasks compared to control mice but at very specific post-treatment times. Over the entire time course of the study (2.5 days to 12 weeks), METH-treated mice

performed worse than control mice, but particularly at 12 weeks on the rotarod. They performed worse in the open field on movement measures at 2.5 days. Even though at 12 weeks METH animals performed equally well as controls on other open-field measures, they did not fully recover motor function as assessed by the rotarod performance. Studies have shown that reduced PV interneurons in the striatum are associated with persistent motor deficits (Marrone et al., 2006; Kataoka et al., 2010). This suggests that even though new PV interneurons are generated, they are not sufficient to counter the behavioral function of the striatal cells lost during acute response to METH.

In contrast to the rotarod motor task and open-field psychomotor tasks, METH-treated mice performed more poorly on the appetitive habit learning T-maze task during early post-treatment times (two weeks). However, the improvement to control from four to twelve weeks, suggest some level of recovery. Therefore, another novelty of the results reported here is that the injury-induced cytogenesis and subsequent neuron maturation is accompanied by partial behavioral recovery. This occurs without additional substances to promote neurogenesis. Previous studies that found behavioral recovery along with injury-induced neurogenesis in a basal ganglia nucleus, enhanced the process with 7-OH-DPAT (Van Kampen et al., 2004; Van Kampen and Eckman, 2006; Van Kampen and Robertson, 2005). By the end of the current study, approximately 9% of the new neurons remained. This proportion of new striatal neurons could hypothetically be enhanced by neurogenesis promoting substances like 7-OH-DPAT or BDNF to increase the recovery outcome.

Striatal interneurons in general, and the ACh phenotype in particular, are involved in procedural learning (Kitabatake et al., 2003; Pych, et al., 2005a; 2005b;

Stemmelin et al., 2000). Therefore, the recovered T-maze learning at the same time point new ACh cells are present indicate that they may be functioning. An alternate explanation is that older striatal neurons that survived acute METH damage are capable of compensating for the acute cell loss that affects cognitive, but not motor function. Thus, a consideration of other compensatory processes that influence behavior is important because we could not confirm whether the newly generated ACh and PV cells incorporate into the circuits with the correct connections using the methods of the current work.

Whether the new neurons incorporate into striatal circuits to directly affect behavior is pertinent for future studies because some of the METH-treated animals failed to use a striatal strategy on the habit learning task, even though most used a striatal strategy and they all improved in general. Mice using the striatal strategy acquired the task as quickly as those that used the hippocampus strategy. With the improved habit learning on an appetitive spatial task at later post-METH times, one implication worth exploring is how these data relate to the switch from drug exposure to the behavioral habits seen in addiction. These new cells may contribute to compensatory mechanisms that are involved in the switch from causal to habitual use and would be of clinical significance. However, since our treatment regimen was a single dose, it remains to be seen if similar events occur with an escalating dose over time that is closer to the pattern of use in individuals that abuse METH.

Conclusions

In conclusion, the data from the series of experiments reported here provides evidence for cytogenesis as process for partial neurochemical and partial behavioral recovery after METH- induced cell death. The results also address the gap that existed in the literature regarding METH-induced enlarged striatal volume and the disparity in the time course of cell death. With subsequent studies described suggested above, these events might provide better understanding of the process of cell death and addiction, as well as methods for improving the recovery outcome for those who suffer from the effects of neurotoxic METH exposure. Therefore, the corrected model as depicted below provides an updated timeline of significant events during the first three months after METH exposure, which may be useful for future studies of cell death and repair using neurochemical and behavioral assays.

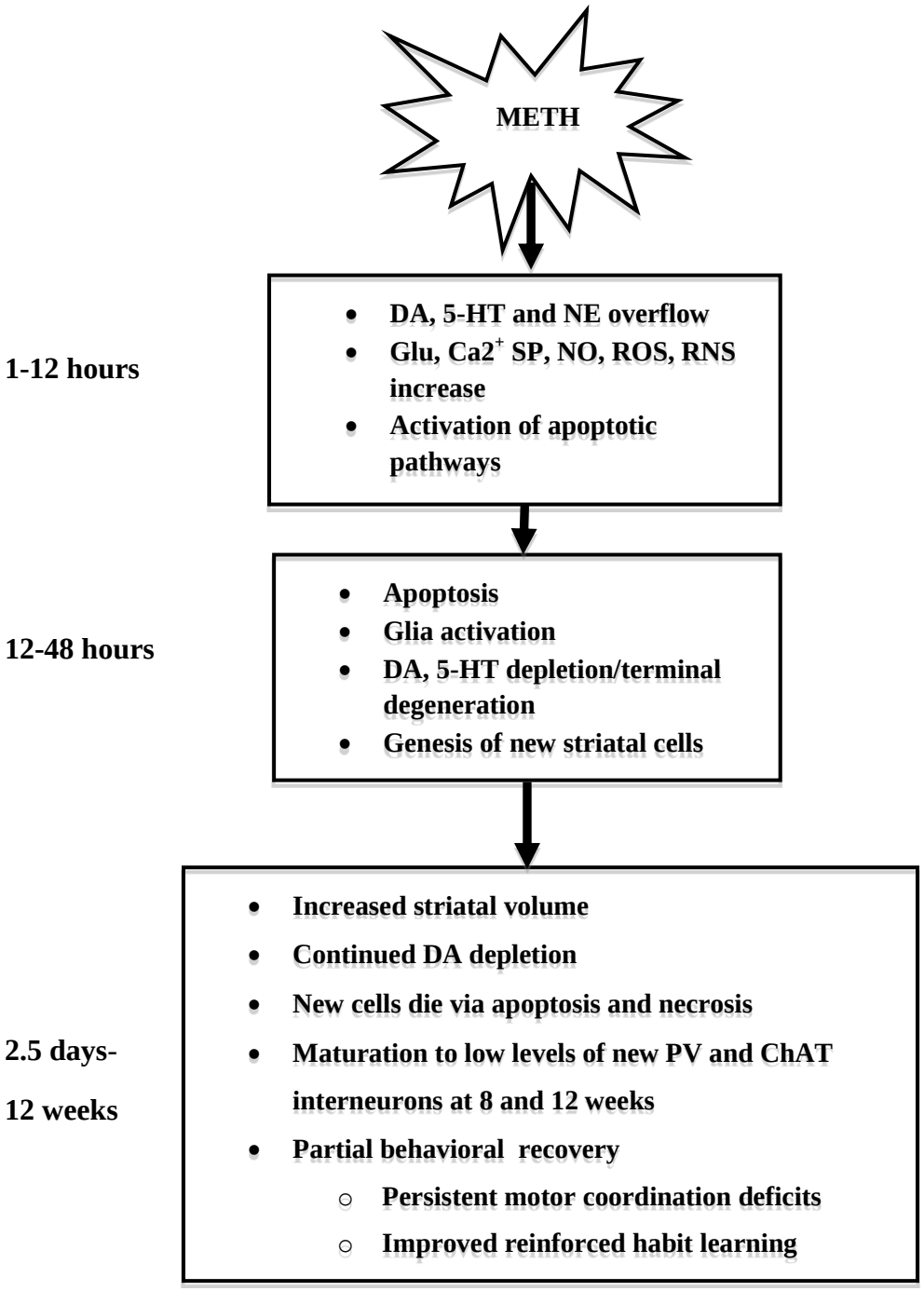

Figure 28. Corrected model of hypothesized events in the striatum following a neurotoxic dose of METH. Note. Significant new additions to the hypothesized model of events after METH are cytogenesis and death of new cells corresponding to volume changes, regeneration of some new neurons, accompanied by persistent motor deficits but improved habit learning.

Appendix A

Tables summarizing open-field statistical analysis

Table 7

Summary of multi-factor ANOVA results of anxiety-like behaviors in the open field

Behaviors and interactions	ANOVA statistic		Contribution to the variance (R^2)
Number of entries			
Location x Treatment x test time	$F(18,120) = 10.6$	***	.37
Treatment x location	$F(2,120) = 20.7$	***	.17
Treatment x test time	$F(2,5) = 14.4$	***	.17
Time spent freezing			
Location x treatment x test time	$F(18,120) = 2.3$	**	.18
Treatment x location	$F(2,120)= 14.4$	***	.18
Treatment x time tested	$F(2,5) =2.5$	*	.08
Total time spent			
Location x treatment x test time	$F(18,120) = 2.2$	**	.02
Treatment x location	$F(2,120) = 583.6$	***	.89
Treatment x time tested	$F(2,5) = .41$	ns	.009

Note. Behaviors analyzed by the multi-factor ANOVA are the number of entries, time spent freezing and total time spent in the open-field on three factors. Factor 1: treatment condition with 3 levels (untreated, saline, METH); Factor 2: post-treatment time tested with 6 levels (2.5days, 1 weeks, 2 weeks, 4 weeks, 8 weeks, 12 weeks), and Factor 3: open-field zone/ location (center, periphery). Effects analyzed were interactions between the location x treatment x time tested; treatment x location and treatment x time tested. ns, not significant; *, $p<.05$, **. $p<.01$, ***, $p<.001$

Table 8

Summary of planned contrasts results of periphery zone activity in the open-field

Drug condition x post-drug time and post-hoc tests		Post-drug time	Drug
Entries	R^2=.12 F (10,75)= 5.3 **	R^2=.16 F(5,75)=13.5 ***	R^2 = .35 F(2,75=14.6 ***
	No treatment vs. Meth	2.5 day 1 week 2 weeks	*MD* = 37 *** *MD* = 30 *** *MD* = 30 ***
	No treatment vs. saline	2.5 day 1 week	*MD* = 27.2 *** *MD* = 36.8 ***
	Saline vs. METH	ns	ns
Freeze	R^2 =.18 F(10,75)= 2.5 * *	R^2 =.09 F(5,75) = 1.8 *	R^2 =.002 F(2,75)=.82 ns
	No treatment vs. METH	2.5 day	*MD*=-49.7 **
	No treatment vs. saline	ns	ns
	Saline vs. METH	2.5 day	*MD*=49.8 **
Time spent	R^2 =.14 F(10,75)= 1.6 ns	R^2 =.039 F(5,75)= .90 ns	R^2 =.025 F(2,75)= 1.3 ns
	No treatment vs. METH No treatment vs. Saline Saline vs. METH	No post-hoc No post-hoc No post-hoc	

Note. Planned analysis included two-way ANOVAs and post-hoc results for 3 types of activity in the peripheral zone of the open-field. Data for entries, freezing and time spent in the periphery were analyzed for significant interactions and differences between effects of the drug condition in an untreated group tested once compared to saline and METH treated animals tested at times ranging from 2.5 days to 12 weeks. ns, not significant *, p<.05, **. p<.01, ***, p<.001.

Table 9

Summary of planned contrast results for center zone activity in the open-field.

	Drug condition x post-drug time	Post-drug time	Drug Condition
Entries	R^2=.20 F (10,75)= 8.3 ***	R^2=.26 F(5,75)=22.0 ***	R^2 = .20 F(2,75)=9.7 **
No treatment vs. METH		2 weeks	*MD*= - 45 .0 ***
		4 week	*MD*= - 26.7 *
		12 weeks	*MD*= - 25.5 *
No treatment vs. saline		2 weeks	*MD* = 31.8 **
		4 weeks	*MD* = 29.3 **
		8 weeks	*MD* = 26.0 *
Saline vs. METH		12 weeks	*MD* = 26.7 *
		2.5 days	*MD* = 33. 0 ***
Freeze	R^2 =.15 F(10, 75) = 1.9 ns	R^2 = .041 F(5,75) = 1.1 ns	R^2 =.065 F(2, 75) = 2.8 ns
No treatment vs. Meth		ns	ns
No treatment vs. saline		ns	ns
Saline vs. METH		ns	ns
Time spent	R^2 =.18 F(10,75)= 2.4 *	R^2 =.077 F(5,75)= 2.1 ns	R^2 =.030 F(5,75)=1.2 ns
No treatment vs. METH		ns	ns
No treatment vs. Saline		ns	ns
Saline vs. METH		12 weeks	*MD* = 46.6 *

Note. Planned analysis included two-way ANOVAs and post-hoc results for activity in the central zone of the open-field. Significant interactions and differences between effects of drug condition and time tested (2.5 days to 12 weeks) were observed. ns, not significant; *, p<.05, **. p<.01, ***, p<.001.

Appendix B

Summary of T-maze statistics

Table 10

Statistical analysis results for the number of mice using striatal versus hippocampus strategy

Strategy	**2 weeks**			**4 weeks**			**8 weeks**			**12 weeks**		
	Sal	METH	Tot	Sal	METH	Tot	Sal	METH	Tot	Sal	METH	Tot
hippocampus	0	2	2	2	4	6	3	4	7	1	2	3
Striatum	6	3	9	4	4	8	3	2	5	3	4	7
Total (n)	6	5	11	6	8	14	6	6	12	4	6	10
Fisher's exact *p*	*p*=.44, ns			*p*=.63, ns			*p*=1.0, ns			*p*=1.0, ns		

(Fisher's exact test).

Note**.** The table summarizes the results of statistical analysis using Fisher's exact test to determine the differences in the number of mice that used striatal or hippocampus strategy to solve the task at criterion. No statistically significant difference in the strategy used at any post-treatment training time was observed. ns, not significant; Sal, saline; tot, total per strategy.

Table 11

Summary of correlational relationship between strategy and T-maze behaviors at task acquisition (Pearson's R)

Test (r and R^2) weeks	**2 weeks**	**4 weeks**	**8 weeks**	**12**
Strategy and number of sessions to criterion				
Pearson's r and effect	r= - 0.70, R^2= .49	r= 0.60, R^2= .37	r= .27, R^2= .07	r= - 0.10, R^2= .01
Significance	p=0.02 *	p=0.02 *	p=0.40	p=0.77
Number of pairs	N=11	N=14	N=12	N=10
	.			
Strategy and latency to correct arm entry				
Pearson's r and effect	r= 0.50, R^2= .25	r= - 0.34, R^2=.12	r= - 0.13, R^2=.02	r= - 0.16, R^2=.03
Significance	p=.14	p=0.229	p= 0.70	p=0.66
Number of pairs	*N*=10	*N*=14	*N*=12	*N*=10

Note. For the relationship between the striatal strategy and performance all correlations are Pearson's R corrected for number of tests. Animals trained 2 weeks after treatment reached criterion faster (negative relationship) if they used striatal strategy. At 4 weeks it was the opposite; they took a longer time to reach criterion if they used striatal strategy. There were no correlations between the strategy used and time it took to choose the correct arm to enter (latency). However, animals that learned the task quickly (sessions to criterion) took longer to choose the correct arm per trial when they were trained at 4 weeks after injections. No statistically significant relationship between strategy and latency to choose was observed. *, $p<0.05$

References

Abekawa, T., Ohmori, T., and Koyama, T. (1994) Effects of repeated administration of high dose of methamphetamine on dopamine and glutamate release in rat striatum and nucleus accumbens. *Brain Research,* 643:276-281

Acikgoz, O., Gonenc, S. and Kayatekin, B.M, Uysal, N., Perekcetin, C., Semin, I., and Gure, A. (1998) Methamphetamine causes lipid peroxidation and increase in superoxide dismutase activity in the rat striatum. *Brain Research,* 813:200-202

Achat-Mendes, C., Ali, S. F. and Itzhak Y. (2005) Differential Effects of Amphetamines-Induced Neurotoxicity on Appetitive and Aversive Pavlovian conditioning in Mice *Neuropsychopharmacology,* 30:1128–1137

Achat-Mendes C, Anderson KL, Itzhak Y. (2007) Impairment in consolidation of learned place preference following dopaminergic neurotoxicity in mice is ameliorated by N-acetylcysteine but not D1 and D2 dopamine receptor agonists. *Neuropsychopharmacology,* 232:531–541

Acheson A., Conover J.C., Fandl. J.P., DeChiara, T.M., Russell, M., Thadani, A., Squinto, S.P., Yancopoulos, G.D. and Lindsay, R.M. (1995). A BDNF autocrine loop in adult sensory neurons prevents cell death. *Nature,* 374 (6521): 450–453

Agasse, F., Bernardino, L., Kristiansen, H., Christiansen, S.H., Ferreira, R., Silva, B., Grade, S., Woldbye, D.P. and Malva, J.O. (2008) Neuropeptide Y promotes neurogenesis in murine subventricular zone. *Stem Cells*, 26(6):1636-1645.

Albers, D.S. and Sonsalla, P.K., (1995). Methamphetamine-induced hyperthermia and dopaminergic neurotoxicity in mice: pharmacological profile of protective and nonprotective agents. *Journal of Pharmacology and Experimental Therapeutics*, 275: 1104–1114

Albertin, S.V., Mulder, A.B., Tabuchi, E., Zugaro, M.B., and Wiener, S.I. (2000). Lesions of the medial shell of the nucleus accumbens impair rats in finding larger rewards, but spare reward-seeking behavior. *Journal of Behavioural Brain Research*, 117: 173-183

Allen, N.J. and Barres, B.A. (2009) Neuroscience: Glia - more than just brain glue. *Nature*, 457(7230):675-7.

American Dental Association (2005) Methamphetamine and oral health. *Journal of American Dental Association,* 136:1491. Retrieved May, 25, 2009 from http//web.archive.org/web/20080226230333/222.ada.org/prog prof/resources/pubs/jada/patient/patient_55.pdf.

Anderson, K.L. and Itzhak, Y. (2006) Methamphetamine-induced selective dopaminergic neurotoxicity is accompanied by an increase in striatal nitrate in the mouse. *Annals of N Y Academy of Science*, 1074:225–233

Ando, K., Johanson, C.E., Seiden, L.S. and Schuster, C.R. (1985). Sensitivity changes to dopaminergic agents in fine motor control of rhesus monkeys after repeated methamphetamine administration. *Pharmacology Biochemistry and Behavior*, 22:737–743.

Angelin, M.D. Burke, C., Perrochet, B., Stamper, E. and Dawud-Noursi, S (2005).History of the methamphetamine problem. *Journal of Psychoactive Drugs,* 32(2):137-141

Angulo, J.A., Angulo, N., Yu, J. (2004) Antagonists of the neurokinin-1 and Dopamine 1 receptors confer protection from methamphetamine on dopamine terminals of the mouse striatum. *Annals of the N.Y. Academy of Science,* 1025:171-180

Arvidsson, A., Collin, T., Kirik, D., Kokaia, Z. and Lindvall, O. (2002) Neuronal replacement from endogenous precursors in the adult brain after stroke. *Nature Medicine,* 8: 963-970.

Axt, K. and Molliver, M.E. (1991) Immunocytochemical evidence for methamphetamine-induced serotonergic axon loss in the rat brain. *Synapse,* 9(4):302–313.

Bacchi, C. E. and Gown, A. M. (1993) Detection of cell proliferation in tissue sections. *Brazilian Journal of Medical and Biological Research*, 26:677-687.

Bakhit, C., Morgan, M.E., Peat, M.A. and Gibb, J.W. (1981) Long-term effects of methamphetamine on the synthesis and metabolism of -hydroxytryptamine in various regions of the rat brain. *Neuropharmacology,* 20: 1135-1140

Balthazar, C.H., Leite, L.H., Ribeiro, R.M., Soares, D.D. and Coimbra, C.C. (2010) Effects of blockade of central dopamine D1 and D2 receptors on thermoregulation, metabolic rate and running performance. *Pharmacological Reports*, 62(1):54-61

Bansar, M., Hery, M., Printemps, R., and Daszuta, A. (2004) Serotonin-induced increases in adult cell proliferation and neurogenesis are mediated through different and common 5-HT receptor subtypes in the dentate gyrus and the subventricular zone. *Neuropsychopharmacology,* 20(3):450-460

Barlow, C., Hirotsune, S., Paylor, R., Liyanage, M., Eckhaus, M., Collins, F., Shiloh, Y., Crawley, J.N., Ried, T., Tagle, D. and Wynshaw-Boris, A. (1996) Atm-deficient mice: a paradigm of ataxia telangiectasia. *Cell*, 86:159–17

Barres, B (2008). The mystery and magic of glia: a perspective of their role in health and disease. *Neuron,* 60(3):430-40.

Barr, A., Panenka, W.J., McEwan, G.W., Thornton, A.E., Lang, D.J., Honer, W.G. and Lecomte, T., (2006), The need for speed: An update on methamphetamine addiction. *Journal of Psychiatry and Neuroscience*, 31:301-313.

Battaglia, G., Fornai, F., Busceti, C.L., Gabriella, A., Cerrito, F., De Blasi, A., Melchiorri, D. and Nicoletti, F. (2002) Selective blockade of mGlu5 metabotropic glutamate receptors is protective against methamphetamine neurotoxicity. *Journal of Neuroscience,* 22(6):2135-2141

Bauer, S. and Patterson, P.H. (2005). The cell cycle-apoptosis connection revisited in the adult brain. *Journal of Cell Biology*, 171(4): 641-650

Bayer, S. A. (1983) 3H-thymidine-radiographic studies of neurogenesis in the rat olfactory bulb. *Experimental Brain Research,* 50: 329-340.

Bédard, A., Cossette, M., Lévesque, M. and Parent, A. (2002) Proliferating cells can differentiate into neurons in the striatum of normal adult monkey. *Neuroscience Letters,* 328:213–216.

Bedard, A., Gavel, C. and Parent, A. (2006) Chemical characterization of newly generated neurons in the striatum of adult primates. *Experimental Brain Research,* 170(4):501-512

Betarbet, R., Turner, R., Chockkan, V., DeLong, M.R., Allers, K.A., Walters, J., Levey, A.I. and Greenamyre, J.T. (1997) Dopaminergic neurons intrinsic to the primate striatum. *Journal of Neuroscience,* 17: 6761-6768

Bittner, S.E., Wagner, G.C., Aigner, T.G. and Seiden, L.S. (1981) Effects of a high-dose treatment of methamphetamine on caudate dopamine and anorexia in rats. *Pharmacology Biochemistry and Behavior,* 14:481– 486

Blin, O. (1999) Comparative review of new antipsychotics. *Canadian Journal of Psychiatry,* 44:235–244

Boda, E. and Buffo, A. (2010) Glial cells in non-germinal territories: insights into their stem/progenitor properties in the intact and injured nervous tissue. *Archives of Italian Biology*, 148(2):119-36.

Boger, H.A., Middaugh, L.D., Patrick, K.S., Ramamoorthy, S., Denehy, E.D., Zhu, H., Pacchioni, G. A., and McGinty, J.F. (2007) Long-Term Consequences of Methamphetamine Exposure in Young Adults are Exacerbated in Glial Cell Line-Derived Neurotrophic Factor Heterozygous Mice. *Journal of Neuroscience,* 27(33): 8816-8825

Boger, H.A., Middaugh, L.D., Granholm, A.C. and McGinty J.F.(2009) Minocycline restores striatal tyrosine hydroxylase in GDNF heterozygous mice but not in methamphetamine-treated mice. *Neurobiology of Disease,* 33(3):459-66.

Bolam, J.P., Wainer, B.H. and Smith A.D. (1984) Characterization of cholinergic neurons in the rat neostriatum. A combination of choline acetyltransferase immunocytochemistry, Golgi-impregnation and electron microscopy. *Neuroscience,* 12(3):711-8.

Borta, A. and Höglinger, G.U. (2007) Dopamine and adult neurogenesis. *Journal of Neurochemistry,* 100(3):587-95.

Botreau, F. and Gisquet-Verrier P. (2010) Re-thinking the role of the dorsal striatum in egocentric/response strategy. *Frontiers in Neuroscience,* 4(7):1-12

Bowyer, J.F., Davies, D.L., Schmued, L., Broening, H.W., Newport, G.D., Slikker, W. and Holson, R.J., (1994). Further studies of the role of hyperthermia in methamphetamine neurotoxicity. *Journal of.Pharmacology,* 268: 1571-1580.

Bowyer, J.K., Jolson, R.R., Miller, D.B. and O'Callaghan, J.P (2001) Phenobarbital and dizocilpine can block methamphetamine-induced neurotoxicity in mice by mechanisms that are independent of thermoregulation. *Brain Research,* 919:179-183

Bowyer, J.F. and Ali, S., (2006) High doses of methamphetamine that cause disruption of the blood–brain barrier in limbic regions produce extensive neuronal degeneration in mouse hippocampus. *Synapse,* 60:521–532.

Bowyer, J.F., Robinson, B., Ali, S. and Schmued, L.C. (2008) Neurotoxic-related changes in tyrosine hydroxylase microglia myelin and the blood-brain barrier in the caudate-putamen from acute methamphetamine exposure. *Synapse,* 62: 193-204

Broening, H.W., Morford, L.L. and Vorhees, C.V. (2005) Interactions of dopamine D1 and D2 receptor antagonists with D-methamphetamine-induced hyperthermia and striatal dopamine and serotonin reductions. S*ynapse,* 56:84–93.

Brown, J.P., Couillard-Després, S., Cooper-Kuhn, C.M., Winkler, J., Aigner L. and Kuhn, H.G. (2003) Transient expression of doublecortin during adult neurogenesis. *Journal of Comparative Neurology,* 467 (1): 1–10.

Bruno, V., Battaglia, G., Ksiazek, I., Van der Putten, H., Catania, M.V., Giuffrida, R., Lukic, S., Leonhardt, T., Inderbitzin, W., Gasparini, F., Kuhn, R., Hampson, D.R., Nicoletti, F. and Flor, P.J. (2000) Selective activation of mGlu4 metabotropic glutamate receptors is protective against excitotoxic neuronal death. *Journal of Neuroscience,* 20(17):6413-20.

Bureau, G., Carrier, M., Lebel, M. and Cyr, M. (2010) Intrastriatal inhibition of extracellular signal-regulated kinases impaired the consolidation phase of motor skill learning. *Neurobiology of Learning and Memory,* 94(1):107-15

Cadet, J.L., Sheng, P., Ali, S., Rothman, R., Carlson, E. and Epstein, C. (1994b) Attenuation of methamphetamine-induced neurotoxicity in copper/zinc superoxide dismutase transgenic mice. *Journal of Neurochemistry,* 62: 380–383.

Cadet, J.L. and Brannock, C. (1998) Free radicals and the pathobiology of brain dopamine systems. *Neurochemistry International,* 32: 117-131

Callaghan, R.C., Cunningham, J.K., Sajeev, G. and Kish, S.J (2010) Incidence of Parkinson's disease among hospital patients with methamphetamine-use disorders. *Movement Disorders,* 25 (14):2333-2339

Calzà, L., Giardino, L., Pozza, M., Bettelli, C., Micera, A. and Aloe, L. (1998) Proliferation and phenotype regulation in the subventricular zone during experimental allergic encephalomyelitis: in vivo evidence of a role for nerve growth factor. *Proceedings of the National Academy of Science U S A.*, 95(6):3209-14

Cappon, G.D., Pu, C. and Vorhees, C.V.(2000) Time-course of methamphetamine-induced neurotoxicity in rat caudate-putamen after single dose treatment. *Brain Research*, 863:106-111

Cardenas, A., Moro, M.A., Hurtado, O., Leza, J.C. and Lizasoain, I. (2005) Dual role of nitric oxide in adult neurogenesis. *Brain Research Review,* 50(1):1-6

Coronas, V., Bantubungi, K., Fombonne, J., Krantic, S., Schiffmann, S.N., and Roger, M. (2004) Dopamine D3 receptor stimulation promotes the proliferation of cells derived from the post-natal subventricular zone, *Journal of Neurochemistry,* 91:1292–1301

Carlsson A. (1970). Amphetamine and brain catecholamines. In: *Amphetamines and Related Compounds*, ed. Garattini, S. & Costa, E. (pp. 289-300). New York: Raven Press.

Chang, L., Smith, L., LoPesti, C., Yonekura, M.L., Kuo, J. and Walot, I., (2004) Smaller subcortical volumes and cognitive deficits in children with prenatal methamphetamine exposure. *Psychiatry Research,* 132: 95-106.

Chang, L., Cloak, C., Patterson, K., Grob, C., Miller, E. and Ernst, T. (2005) Enlarged striatum in abstinent methamphetamine abusers: A possible compensatory response. *Biological Psychiatry,* 57(9): 967-974.

Chang, L. Alicata, D., Ernst, T., Volkow, N.D. (2007) Structural and metabolic changes in the striatum associated with methamphetamine abuse. *Addiction,* 102(1): 16-32

Chaperon,F., Tricklebank, M.D., Unger, L. and Neijt, H.C.(2003) Evidence for regulation of body temperature in rats by dopamine D2 receptor and possible influence of D1 but not D3 and D4 receptors. *Neuropharmacology*, 44(8):1047-1053.

Chen, H.M., Lee, Y.C., Huang, C.L., Liu, H.K., Liao, W,W.C., Lai, W.L., Lin Y.R., and Huang, N.K., (2007) methamphetamine downregulates peroxiredoxins in rat pheochromocytoma cells. *Biochemistry and Biophysics Research,* 354: 96-101

Chen, J.C., Chen, P.C., Chiang, Y.C. and Chang, G. (2009) Molecular mechanisms of psychostimulant addiction *Medical Journal,* 32(2):148-154

Chung Y.A., Peterson, B.S., Yoon, S.J., Cho, S.N., Chai, S., Jeong, J. and Kim, D.J. (2010) Invivo evidence for long-term CNS toxicity, associated with chronic binge use of methamphetamine. *Drug and Alcohol Dependency*, 111(1-2):155-160.

Commins, D.L. and Seiden, L.S. (1986) alpha-Methyltyrosine blocks methylamphetamine-induced degeneration in the rat somatosensory cortex. *Brain Research,* 365:15–120

Colman, E. (2005) Anorectics on trial: A half century of federal regulation of prescription appetite suppressant. *Annals of Internal Medicine,* 143 (5): 380-385

Collin, T., Arvidsson, A., Kokaia, Z.and Lindvall, O. (2005) Quantitative analysis of the generation of different striatal neuronal subtypes in the adult brain following excitotoxic injury. *Experimental Neurology,* 195(1):71-80.

Colton, C.A. and Gilbert, D.L., (1987) Production of superoxide anions by a CNS macrophage, the microglia. *FEBS Lett*ers, 223:284-288

Cooper-Kuhn, C.M. and Kuhn, H.G. (2002) Is it all DNA repair? Methodological considerations for detecting neurogenesis in the adult brain. *Developmental Brain Research,* 134(1-2):13-21.

Crawley J.N. (2007)) Learning and Memory and Emotional Behaviors. In *What's wrong with my mouse? Behavioral phenotyping of transgenic and knockout mice*. 2nd edition (pp 63-69; pp 233). Hoboken NJ: John Wiley and Sons Inc.

Cubells, J.F., Rayport, S., Rajendran, G. and Sulzer, D.(1994) Methamphetamine neurotoxicity involve vacuolation of endocytic organelles and dopamine-dependent intracellular oxidative stress. *Journal of Neuroscience,* 14:2260-2271

Daberkow, D.P., Riedy, M.D., Kesner, R.P., and Keefe, K.A. (2008) Effect of methamphetamine neurotoxicity on learning-induced arc mRNA expression in identified striatal efferent neurons. *Neurotoxicity Research*, 14(4):307-315.

Daberkow, D.P., Riedy, M.D., Kesner, R.P., and Keefe, K.A. (2007) Arc mRNA induction in striatal efferent neurons associated with response learning. *European Journal of Neuroscience*, 26:228-241.

Danaceau, J.P., Deering, C.E., Day, J.E., Smeal, S.J., Johnson-Davis, K.L., Fleckenstein, A.E. and Wilkins, D.G. (2007) Persistence of tolerance to methamphetamine-induced monoamine deficits. *European Journal of Pharmacology*, 559:46–54

Darvas, M., Palmiter R.D. (2010) Restricting dopaminergic signaling to either the dorsolateral or medial striatum facilitates cognition. *Journal of Neuroscience*, 30 (3):1158-65.

Davidson, C., Gow, A.J., Lee, T.H. Ellinwood, E.H. (2001) Methamphetamine neurotoxicity: necrotic and apoptotic mechanisms and relevance to human abuse and treatment. *Brain Research Reviews*, 36(1):1-22.

Deacon, R.M. and Rawlins, J.N. (2006). T-maze alternation in the rodent. *Nature Protocols, 1(1):7-12*

Dean, A. (2004) Pharmacology of psychostimulants. In Baker A., Lee N., Jenner. L (Eds). *Models of intervention and care for psychostimulant users 2nd ed.* (pp 35-39) National Drug Strategy Monograph series No. 51. Canberra: Australian Government Department of health and ageing

Decressac, M., Prestoz, L., Veran, J., Cantereau, A., Jaber, M. and Gaillard A. (2009) Neuropeptide Y stimulates proliferation, migration and differentiation of neural precursors from the subventricular zone in adult mice. *Neurobiology of Disease*, 34(3):441-9.

De Leonibus, E., Lafenetre, P., Oliverio, A. and Mele, A. (2003b). Pharmacological evidence of the role of the dorsal striatum in spatial learning in mice. *Behavioral Neuroscience*, 117:685–694

De Leonibus, E., Oliverio, A., and Mele, A., (2005) A study on the role of the dorsal striatum and the nucleus accumbens in allocentric and egocentric spatial memory consolidation *Learning and Memory*, 12: 491-503

De Leonibus, E., Pascucci, T., Lopez, S., Oliverio, A., Amalric, M. and Mele A.(2007). Spatial deficits in a mouse model of Parkinson disease. *Psychopharmacology*, 194(4):517-25.

Delis, F., Grant, S., Wang, G., Volkow, N. and Thanos, P. (2010) Three months of daily methamphetamine exposure increase the volume of the rat striatum. *Society for Neuroscience Annual Meeting Abstracts,* 69.15.

Denenberg, V.H. (1969) Open-field behavior in the rat: what does it mean? *Annals of NY Academy of Science*, 159: 852–859.

Deng, X., Ladenheim, B., Tsao, L.I. and Cadet, J.L. (1999) Null mutation of c-fos causes exacerbation of methamphetamine-induced neurotoxicity. *Journal of Neuroscience*, 19:10107–10115

Deng, X., Wang, Y., Chou, J., and Cadet, J.L. (2001) Methamphetamine causes widespread apoptosis in the mouse brain: evidence from using an improved TUNEL histochemical method. *Molecular Brain Research,* 93:64-69.

Diaz, J., Ridray, S., Mignon, V., Griffon, N., Schwartz, J.C. and Sokoloff, P. (1997). Selective expression of dopamine D3 receptor mRNA in proliferative zones during embryonic development of the rat brain. *Journal of Neuroscience*, 17(11):4282-92.

Dihné, M., Block, F., Korr, H. and Töpper, R. (2001) Time course of glial proliferation and glial apoptosis following excitotoxic CNS injury. *Brain Research,* 902(2):178-89.

Di Monte, D.A., Royland, J.E., Jakowec, M.W. and Langston, J.W (1996) Role of nitric oxide in methamphetamine neurotoxicity: protection by 7-nitroindazole, an inhibitor of neuronal nitric oxide synthase. *Journal of Neurochemistry,* 67(6):2443-50.

Dunham, N. W. and Miya, T.S. (1957) A note on a simple apparatus for detecting neurological deficit in rats and mice, *Journal of American Pharmacological Association,* 46: 208–209.

Eisch A.J., Gaffney, M, Weilmuller, F.B., O'Dell, S.J. and Marshall, J.F (1992). Striatal subregions are differentially vulnerable to the neurotoxic effects of methamphetamine. *Brain Research*, 598: 321-326

Eisch, A. J. and Marshall, J. F. (1998) Methamphetamine neurotoxicity: dissociation of striatal dopamine terminal damage from parietal cortical cell body injury. *Synapse*, 30:433-445.

Emerich, D.F, Vasconcellos, A.V; Elliott, R.B; Skinner S.J.M; Borlongan, CV. (2004) The choroid plexus: function, pathology and therapeutic potential of its transplantation. *Expert Opinion on Biological Therapy*, 4: 8, 1191-1201

Ernst, T., Chang, L., Leonido-Yee, M. and Speck, O. (2000) Evidence for long-term neurotoxicity associated with methamphetamine abuse: a 1H MRS study. *Neurology,* 54:1344-1349.

Escalante, D. and Ellinwood Jr., E. H. (1970) Central nervous system cytopathological changes in cats with chronic methdrine intoxication, *Brain Research.,* 21:151-155.

Eyerman D.J., Yamamoto, B.K. (2005) Lobeline attenuates methamphetamine-induced changes in vesicular monoamine transporter 2 immunoreactivity and monoamine depletions in the striatum. *Pharmacology and Experimental Therapeutics,* 312(1):160-169.

Eyerman, D.J., and Yamamoto, B.K. (2007) A rapid oxidation and persistent decrease in the vesicular monoamine transporter 2 after methamphetamine. *Journal of Neurochemistry,* 103:1219–1227.

Fantegrossi, W.E., Ciullo, J.R., Wakabayashi, K.T., De La Garza, R. 2nd, Traynor, J.R.. and Woods JH. (2008) A comparison of the physiological, behavioral, neurochemical and microglial effects of methamphetamine and 3,4-methylenedioxymethamphetamine in the mouse. *Journal of Neuroscience*, 151(2):533-43

Featherstone, R.E. and McDonald R. J. (2004) Dorsal striatum and stimulus-response learning: lesions of the dorsolateral, but not dorsomedial, striatum impair acquisition of a stimulus-response-based instrumental discrimination task, while sparing conditioned place preference learning. *Journal of Neuroscience*, 124(1):23-31.

Fibiger, H. C. and McGeer, E. G. (1971) Effect of acute and chronic methamphetamine treatment on tyrosine hydroxylase activity in brain and adrenal medulla. *European Journal of Pharmacology,* 16:176-180. 175

Figueredo-Cardenas, G., Medina, L. and Reiner, A. (1996) Calretinin is largely localized to a unique population of striatal interneurons in rats. *Brain Research*, 709(1) 145:150

Finnegan, K.T., Ricaurte, G., Seiden, L.S. and Schuster, C.R. (1982) Altered sensitivity to d-methylamphetamine, apomorphine, and haloperidol in rhesus monkeys depleted of caudate dopamine by repeated administration of d-methylamphetamine. *Psychopharmacology,* 77:43–52.

Friedman, S.D., Castañeda, E., and Hodge, G.K. (1998) Long-Term Monoamine Depletion, Differential Recovery, and Subtle Behavioral Impairment Following Methamphetamine-Induced Neurotoxicity. *Pharmacology Biochemistry and Behavior,* 61(1):35-44

Fukui, K., Nakajima, T., Kariyama, H., Kashiba, A., Kato, N., Tohyama, I. and Kimura, H. (1989) Selective reduction of serotonin immunoreactivity in some forebrain regions of rats induced by acute methamphetamine treatment; quantitative morphometric analysis by serotonin immunocytochemistry. *Brain Research*, 482:198–203.

Fuller, R.W., Hemrick-Luecke, S.K. and Ornstein, P.L. (1992) Protection against amphetamine-induced neurotoxicity toward striatal dopamine neurons in rodents by LY274614, an excitatory amino acid antagonist. *Neuropharmacology*, 31:1027–1032.

Fumagalli, F., Gainetdinov, R.R., Valenzano, K.J, and Caron, M.G. (1998). Role of dopamine transporter in methamphetamine-induced neurotoxicity: evidence from mice lacking the transporter. *Journal of Neuroscience,* 18:4861–4869.

Fumagalli, F., Gainetdinov, R.R., Wang, Y.M., Valenzano, K.J., Miller, G.W. and Caron, M.G. (1999). Increased methamphetamine neurotoxicity in heterozygous vesicular monoamine transporter 2 knock-out mice. *Journal of Neuroscience,* 19:2424–2431

Garofalo, R., Mustanski, B.S., McKirnan, D.J., Herrick, A. and Donenberg, G.R. (2007) Methamphetamine and young men who have sex with men: understanding patterns and correlates of use and the association with HIV-related sexual risk. *Archives of Pediatric Adolescent Medicine*, 161(6):591-6.

Garwood, E.R., Bekele, W., McCulloch, C.E. and Christine, C.W. (2006) Amphetamine exposure is elevated in Parkinson's disease. *Neurotoxicology*, 27(6):1000-1006

Gelowitz, D.L., Richardson, J.S., Wishart, T.B., Yu, P.H. and Lai, C.T. (1994) Chronic L-deprenyl or L amphetamine: equal cognitive enhancement, unequal MAO inhibition. *Pharmacology Biochemistry and Behavior,* 47(1):41-5

Gerald, M. C. and Gupta, T. K. (1977) The effects of amphetamine isomers on rotarod performance. *Psychopharmacology,* 55: 83–86.

Gerfen, C. R. (1992) The Neostriatal Mosaic: multiple levels of compartmental organization in the basal ganglia, *Annual Review of Neuroscience,* 15:285-320.

Gerfen, C.R., Engber, T.M., Mahan, L.C., Susel, Z., Chase, T.N., Monsma, F.J. Jr. and Sibley, D.R.(1990) D1 and D2 dopamine receptor-regulated gene expression of striatonigral and striatopallidal neurons. *Science*, 250 (4986):1429-32.

Giovanni, A., Liang, L.P., Hastings, T.G. and Zigmond, M.M. (1995) Estimating hydroxyl radical content in rat brain using systemic and intraventricular salicylate: impact of methamphetamine. *Journal of Neurochemistry,* 64: 1819-1825

Glowinski, J. (1970). Effects of amphetamine on various aspect of catecholamine metabolism in the central nervous system of the rat. In: Costa, E. & Garattini, S. (Eds.) *Amphetamines and Related Compounds,* (pp. 3301-316) New York: Raven Press

Gonzales, C.F, Barrington, E. and Walton, M. (2000) cocaine and methamphetamine: differential addiction rates. *Psychology of Addictive Behaviors,* 14: 200-396

Gould, E. and Tanapat, P. (1997) Lesion-induced proliferation of neuronal progenitors in the dentate gyrus of the adult rat. *Journal of Neuroscience,* 80(2):427-436.

Graham, D.L., Noailles, P.A. and Cadet, J.L. (2008) Differential neurochemical consequences of an escalating dose- binge regimen followed by single-day multiple-dose methamphetamine challenges. *Journal of Neurochemistry,* 105:1873–1885

Graybeil, A.M., Aosaki, T., Flaherty, A.W. and Kimura, M (1994) The Basal Ganglia and adaptive motor control. *Science,* 265(5180) 1831-1871

Gratzner, H.G., (1982) Monoclonal antibody to 5-bromo- and 5-iododeoxyuridine: a new for detection of DNA replication. *Science,* 218: 474–475.

Green, A.R., De Souza, R.J., Williams, J.L., Murray, T.K. and Cross, A.J. (1992) The neurotoxic effects of methamphetamine on 5-hydroxytryptamine and dopamine in brain: evidence for the protective effect of chlormethiazole. *Neuropharmacology,* 31(4):315-321

Greenberg, D.A. and Jin, K. (2007) Regenerating the brain. *International Review of Neurobiology*, 77:1-29

Grinspoon, L. and Hedblom, P. (1975). The contemporary Amphetamine Scene. In *Speed Culture: Amphetamine use and abuse in America*: (pp 11-28). Cambridge: MA, Harvard University Press.

Grollman, A. (1954) *Pharmacology and Therapeutics: a textbook for students and practitioners of medicine*: (pp 209) Philadelphia: PA, Lea and Febiger.

Guilarte, T.R., Nihei, M.K., McGlothan, J.L. and Howard, A.S. (2003) Methamphetamine-induced deficits of brain monoaminergic neuronal markers: distal axotomy or neuronal plasticity. *Journal of Neuroscience,* 122:499–513.

Guillot, T.S., Shepherd, K.R., Richardson, J.R., Wang, M.Z., Li, Y., Emson, P.C. and Miller, G.W. (2008) Reduced vesicular storage of dopamine exacerbates methamphetamine-induced neurodegeneration and astrogliosis. *Journal of Neurochemistry,* 106(5):2205-2217

Gunasekar, P.G., Kanthasamy, A.G., Borowitz, J.L. and Isom, G.E. (1995) NMDA receptor activation produces concurrent generation of nitric oxide and reactive oxygen species: Implications for cell death. *Journal of Neurochemistry,* 64:2016-2021

Gygi, M.P., Gygi, S.P., Johnson, M., Wilkins, D.G., Gibb, J.W. and Hanson, G.R. (2006) Mechanisms for tolerance to methamphetamine effects. *Neuropharmacology,* 35(6):751-757.

Haelewyn, B., Freret, T., Pacary, E., Schumann-Bard, P., Boulouard, M., Bernaudin, M. and Bouët, V. (2007) Long-term evaluation of sensorimotor and mnesic behaviour following striatal NMDA-induced unilateral excitotoxic lesion in the mouse. *Behavioral Brain Research,* 178(2):235-43.

Hall, D.A., Stanis, J.J., Marquez, A. H. and Gulley, J.M. (2008) A comparison of amphetamine- and methamphetamine-induced locomotor activity in rats: evidence for qualitative differences in behavior. *Psychopharmacology,* 195(4):469-78.

Hallbergson, A.F., Gnatenco, C. and Peterson, D.A. (2003) Neurogenesis and brain injury: managing a renewable resource for repair. *Journal of Clinical Investigation,* 112(8):1128-1133.

.

Hamann, M., Sander, S.E. and Richter, A. (2005) Age-dependent alterations of striatal calretinin interneuron density in a genetic animal model of primary paroxysmal dystonia. *Neuropathology and Experimental Neurology*, 64(9):776-781

Hartfuss, E., Förster, E., Bock, H.H., Hack, M.A., Leprince, P., Luque, J.M., Herz, J., Frotscher, M. and Götz, M. (2003) Reelin signaling directly affects radial glia morphology and biochemical maturation. *Development,* 130(19):4597-4609.

Hart, C.L., Ward, A.S., Haney, M., Flotin R.W., Fischman, M.W. (2001) Methamphetamine self-administration in humans. *Psychopharmacology,* 157(1) 75-81

Hasenöhrl, R.U., De Souza-Silva, M.A., Nikolaus, S., Tomaz, C., Brandao M.l., Schwarting, R.K.W., Huston, J.P.W. (2000) Substance P and its role in neural Mechanisms governing learning, anxiety and functional recovery. *Neuropeptides,* 34(5): 272–280

Hashimoto, K., Tsukada, H, Nishiyama, S., Fukumoto, D. Kakiuchi, T., Shimizu, E., and Iyo, M. (2004) protective effects of N-acetyl-L-cysteine on the reduction of dopamine transporters in the striatum of monkeys treated with methamphetamine. *Neuropsychopharmacology*, 29:2018-2023

Hof, P., Young, W., Bloom, F., Belichenko, P. and Celio, M.R (2000). *Comparative cytoarchitectonic atlas of the C57BL/6 and 129/Sv mouse brains*. New York: Elsevier.

Höglinger, G.U., Rizk, P., Muriel, M.P., Duyckaerts, C., Oertel, W.H., Caille, I. and Hirsch, E.C. (2004) Dopamine depletion impairs precursor cell proliferation in Parkinson disease. *Nature Neuroscience*, 27(7):726-35.

Hollerman, J.R. and Schultz, W.(1998) Dopamine neurons report an error in the temporal prediction of reward during learning. *Nature Neurosc*ience, 1(4): 204-309

Hollerman, J.R., Tremblay, L. and Schultz W. (2000) Involvement of basal ganglia and orbitofrontal cortex in goal-directed behavior *Progress in Brain Research*, 126:193-215.

Holt, D.J., Herman, M.M., Hyde, T.M., Kleinman, J.E., Sinton, C.M., German, D.C., Hersh, L.B., Graybiel, A.M. and Saper, C.B. (1999) Evidence for a deficit in cholinergic interneurons in the striatum in schizophrenia. *Journal of Neuroscience*, 94(1):21-31.

Homer, B.D., Solomon, T.M., Moeller, R.W., Mascia, A., DeRaleau. L., Halkitis, P.N (2008) Methamphetamine abuse and impairment of social functioning: a review of the underlying neurophysiological causes and behavioral implications. *Psychological Bulletin*, 134:301-310

Horner, K.A., Westwood, S.C., Hanson, G.R. and Keefe, K.A. (2006) Multiple high doses of methamphetamine increase the number of preproneuropeptide Y mRNA-expressing neurons in the striatum of rat via a dopamine D1 receptor-dependent mechanism. *Journal of Pharmacology and Experimental Therapeutics, 319* (1): 414-421

Hotchkiss, A. J. and Gibb, J. W. (1980) Long-term effects of multiple doses of methamphetamine on tryptophan hydroxylase and tyrosine hydroxylase activity in rat brain. *Journal of Pharmacology and Experimental Therapeutics*, 214:257-262

Howell, O.W., Silva, S., Scharfman, H.E., Sosunov, A.A., Zaben, M., Shatya, A., McKhann, G. 2nd, Herzog, H., Laskowski, A. and Gray, W.P.(2007) Neuropeptide Y is important for basal and seizure-induced precursor cell proliferation in the hippocampus. *Neurobiology of Disease,* 26(1):174-188

Huang, E.J., Reichardt and L.F. (2001). Neurotrophins: roles in neuronal development and function. *Annual Review of Neuroscience,* 24: 677–736.

Imam, S.Z., Newport, G.D., Itzhak, Y., Cadet, J.L., Islam, F., Slikker Jr.,W. and Ali, S.F., (2001.a.) Peroxynitrite plays a role in methamphetamine-induced dopaminergic neurotoxicity: evidence from mice lacking neuronal nitric oxide synthase gene or

overexpressing copper–zinc superoxide dismutase. *Journal of Neurochemistry,* 76, 745–749.

Imam, S.Z., Itzhak, Y., Cadet, J.L., Islam, F., Slikker Jr., W. and Ali, S.F. (2001b). Methamphetamine-induced alteration in striatal p53 and bcl-2 expressions in mice. *Molecular Brain Research,* 91: 174–178.

Imam, S.Z., Jankovic, J., Ali, S.F., Skinner, J.T., Xie, W., Conneely, O.M. and Le, W.D. (2005). Nitric oxide mediates increased susceptibility to dopaminergic damage in Nurr1 heterozygous mice. *FASEB Journal*, 19:1441–1450.

Imperato, A., Honore, T. and Jensen, L.H. *(*1990a*)* Dopamine release in the nucleus caudatus and in the nucleus accumbens is under glutamatergic control through non-NMDA receptors: A study in freely-moving rats. *Brain Research,* 530*:*223–228

Itzhak, Y. and Ali, S.F. (1996) The neuronal nitric oxide synthase inhibitor, 7-nitroindazole, protects against methamphetamine-induced neurotoxicity in vivo. *Journal of Neurochemistry,* 67:1770-1773

Itzhak, Y., Gandia, C., Huang, P.L. and Ali, S.F., (1998). Resistance of neuronal nitric oxide synthase-deficient mice to methamphetamine-induced dopaminergic neurotoxicity *J. Pharmacology and Experimental Therapeutics*, 284:1040–1047.

Itzhak, Y. and Ali, S.F (2002) Behavioral consequences of methamphetamine-induced neurotoxicity in mice: relevance to the psychopathology of methamphetamine addiction. *Annals of NY Academy of Science*, 965:127-35

Izquierdo, A., Belcher, A.M., Scott, L., Cazares., V.A., Chen, J., O'Dell, S.J., Malvaez, M., Wu, T. and Marshall, J.F. (2010) Reversal-specific learning impairments after a binge regimen of methamphetamine in rats: possible involvement of striatal dopamine. *Neuropsychopharmacology*, 35: 505-514

Iversen, L. (2006) Neurotransmitter transporters and their impact on the development of psychopharmacology. *British Journal of Pharmacology,* 147(S1): S82-S88

Jayanthi, S., Ladenheim, B., and Cadet, J.L (1998) Methamphetamine-induced changes in antioxidant enzymes and lipid peroxidation in copper/zinc superoxide dismutase transgenic mice. *Annals of NY Academy of Science*, 844:92-102

Jayanthi, S., Deng, X., Noailles, P.A., Landenheim, B., Cadet, J.L (2004). Methamphetamine induces neuronal apoptosis via cross-talk between endoplasmic reticulum and mitochondria-dependent death cascades. *FASEB Journal,* 18:238-251

Jayanthi, S., Deng, X., Landenheim, B., McCoy, M.T., Cluster, A., Cai, N.S and Cadet, J.L (2005) Calcinerurin/NFAT-induced up-regulation of the Fas ligand/Fas death pathway is involved in methamphetamine-induced apoptosis. *Proceedings of the National Academy of Science USA*, 102: 868-873.

Jenner, L and McKetin, R. (2004) Prevalence and patterns of psychostimulant use. In Baker, A., Lee N, Jenner. L. (Eds.) *Models of intervention and care for psychostimulant users 2nd ed*. (pp 15-20). National Drug Strategy Monograph series No. 51 "Canberra: Australian Government Department of health and Ageing.

Jernigan, T.L., Gamst, A.C., Archibald, S.L., Fennema-Notestine, C., Mindt, M.R., Marcotte, T.L., Heaton, R.K., Ellis, R.J. and Grant, I. (2005) Effects of methamphetamine dependence and HIV infection on cerebral morphology. *American Journal of Psychiatry*, 162:1461-1472.

Jin, K., Minami, M., Lan, J.Q., Mao, X.O., Batteur, S., Simon, R.P. and Greenberg, D.A. (2001) Neurogenesis in dentate subgranular zone and rostral subventricular zone after focal cerebral ischemia in the rat. *Proceedings of the National Academy of Science*, 98(8): 410-415

Jin, K., Sun, Y., Xie, L., Peel, A., Mao, X.O., Batteur, S. and Greenberg D.A. (2003). Directed migration of neuronal precursors into the ischemic cerebral cortex and striatum. *Molecular and Cellular Neuroscience*, 24(1):171-89.

Johanson, C.E., Frey, K.A., Lundhal, L.H., Keenan, P., Lockhart N., Roll J., Galloway, G., Koeppe, R.A., Kilbourn, M.R., Robbins, T., and Schuster, C.R. (2006) Cognitive function and nigrostriatal markers in abstinent Methamphetamine abusers. *Psychopharmacology*, 185: 327-228.

Jones, B.J. and Roberts, D.J. (1968a) A rotarod suitable for quantitative measurements of motor incoordination in naive mice. *Naunyn Schmiedebergs Archives of Experimental Pathology and Pharmacology*, 259(2):211.

Jones, B.J. and Roberts, D.J. (1968b) The quantitative measurement of motor inco-ordination in naive mice using an accelerating rotarod. *Journal of Pharmacy and Pharmacology*, 20:302–304.

Jones, S.R, Gainetdinow, R.R., Wightman, R.M., and Caron, M.G. (1998) Mechanisms of amphetamine action revealed in mice lacking the dopamine transporter. *Journal of Neuroscience*, 18:1979-1986. 181

Johnson-Davis, K.L., Fleckenstein, A.E., Wilkins, D.G. (2003) The role of hyperthermia and metabolism as mechanisms of tolerance to methamphetamine neurotoxicity. *European Journal of Pharmacology*, 482:151–154.

Kadota, T. and Kadota, K. (2004) Neurotoxic morphological changes induced in the medial prefrontal cortex of rats behaviorally sensitized to methamphetamine. *Archives of Histology and Cytology,* 67:241–251.

Kalant, H. (1973) Relationship between psychological and physiological dependence and drug addiction. *La Vie medicale au Canada francais,* 2(8):766-74. (Personal Translation, May 25, 2010)

Kalonia, H., Kumar, P., Nehru, B. and Kumar, A. (2009) Neuroprotective effect of MK-801 against intra-striatal quinolinic acid induced behavioral, oxidative stress and cellular alterations in rats. *Indian Journal of Experimental Biology,* 47(11):880-92

Kataoka, Y., Kalanithi, P.S., Grantz, H., Schwartz, M.L., Saper, C., Leckman, J.F. and Vaccarino, F.M. (2010) Decreased number of parvalbumin and cholinergic interneurons in the striatum of individuals with Tourette syndrome. *Journal of Comparative Neurology,* 518(3):277-91.

Kay, J.N. and Blum, M. (2000) differential response of ventral midbrain and striatal progenitor cells to lesions of the nigrostriatal dopaminergic projection. *Developmental Neuroscience,* 22(1-2): 56-67

Kawaguchi, Y. (1997) Neostriatal cell subtypes and their functional roles. *Journal of Neuroscience Research,* 27: 1-8

Kawaguchi, Y., Wilson, C. J., Augood, S. J. and Emson, P. C. (1995) Striatal interneurones: chemical, physiological and morphological characterization. *Trends in Neuroscience,* 18(12): 527-535

Kerr, J.F., Wyllie, A.H. and Currie A.R. (1972) Apoptosis: a basic biological phenomenon with wide-ranging implications in tissue kinetics. *British Journal of Cancer*, 26:239–25

Kew, J.N.C. and Kemp, J.A. (2005) Ionotropic and metabotropic glutamate receptor structure and pharmacology. *Pharmacology,* 179:4-29.

Kippin, T.E., Kapur, S. and Van der Kooy, D. (2005) Dopamine specifically inhibits forebrain neural stem cell proliferation, suggesting a novel effect of antipsychotic drugs. *Journal of Neuroscience,* 25(24): 5815-5823

Kirkpatrick, M.G., Metcalfe, J., Greene, M.J. and Hart, C.L (2008) Effects of intranasal methamphetamine on metacognition of agency. *Psychopharmacology*, 197(1): 137-144

Kita, T., Wagner, G.C., Philbert, M.A., King, L.A. and Lowndes, H.E. (1995) Effects of pargyline and pyrogallol on the methamphetamine-induced dopamine depletion.

Molecular Chemical Neuropathology, 24(1):31-41

Kita, T., Miyazaki, I., Asanuma, M., Takeshima, M.and Wagner, G.C. (2009) Dopamine-induced behavioral changes and oxidative stress in methamphetamine-induced neurotoxicity. *International Review of Neurobiology*, 88:43-64.

Kitabatake, Y., Hikida, T., Watanabe, D., Pastan, I., and Nakanishi, S. (2003) Impairment of reward-related learning by cholinergic cell ablation in the striatum *Proceedings from the National Academy of Science U S A*, 100(13): 7965–7970.

Kiyatkin, E.A., Brown, P.L. and Sharma, H.S. (2007) Brain edema and breakdown of the blood-brain barrier during methamphetamine intoxication: critical role of brain hyperthermia. *European Journal of Neuroscience*, 26:1242–1253.

Knight, H (1997, June 25) Methamphetamine abuse rising in the US, Report Says. *Los Angeles Times online edition*. Retrieved May, 30 2010 http://articles.latimes.com/1997-06-25/news/mn-667_1_drug-abuse.

Kobayashi, T., Ahlenius, H., Thored, P., Kobayashi, R., Kokaia, Z. and Lindvall, O. (2006) Intracerebral infusion of glial cell line-derived neurotrophic factor promotes striatal neurogenesis after stroke in adult rats. *Stroke,* 37(9):2361-2367

Knowlton, B., Mangels, J.A. and Squire, L (1996) A neostriatal habit learning system in humans. *Science,* 273:1339-1402

Knowlton, B, (2002) The role of the basal ganglia in learning and memory. In Squire, L R., Schacter, D. L. (Eds.) *in Neuropsychology of memo*ry *3rd Ed* (pp. 143-153). New York, NY, US: Guilford Press.

Koos, T. and Tepper, J.M., 1999. Inhibitory control of neostriatal projection neurons by GABAergic interneurons. *Nature Neuroscience*, 2: 467–472

Krasnova, I. and Cadet, J. L., (2009) Methamphetamine toxicity and messengers of death. *Brain Research Review*, 60:327-407

Krasnova, I., Hodges, A.B., Ladenheim, B., Rhoades, R., Phillip, C.G., Cesena, A., Ivanova, E., Hohmann, C.F. and Cadet, J.L. (2009) Methamphetamine treatment causes delayed decrease in novelty-induced locomotor activity in mice. *Neuroscience Research*, 65:160-165

Krasnova, I.N., Landenheim, B., Jayanthi, S., Oyler, J., Moran, T.H. Huestis, M.A. and Cadet, J.L. (2001) Amphetamine-induced toxicity in dopamine terminals on CD-1 and C57BL/6J 183 mice: complex roles for oxygen based species and temperature regulation. *Journal of Neuroscience,* 107(2):265-274

Kraus-Ruppert, R., Laissue, J., Burki, H. and Odartchenko, N. (1973) Proliferation and turnover of glial cells in the forebrain of young adult mice as studied by repeated injections of ^{3}H-thymidine over a prolonged period of time. *Comparative Neurology* 148 (2): 211-216

Kreitzer, A.C. (2009) Physiology and pharmacology of striatal neurons. *Annual Reviews in Neuroscience*, 32:127-147

Kroemer, G. G., Galluzzi, L. L., Vandenabeele, P. P., Abrams, J. J., Alnemri, E. S., Baehrecke, E. H. and Piacentini, M. M. (2009). Classification of cell death: recommendations of the Nomenclature Committee on Cell Death. *Cell Death and Differentiation*, 16(1), 3-11

Kuczenski, R. and Segal, D.S. (1997) Effects of methylphenidate on extracellular dopamine, serotonin, and norepinephrine: comparison with amphetamine. *Journal of Neurochemistry,* 68 (5): 2032–2037.

Kuczenski, R., Everall, I.P., Crews, L., Adame, A., Grant, I. and Masliah, E. (2007) Escalating dose-multiple binge methamphetamine exposure results in degeneration of the neocortex and limbic system in the rat. *Experimental Neurology*, 207:42–51

Kuhn, D.M., Arthur Jr., R.E., Thomas, D.M., Elferink, L.A., 1999. Tyrosine hydroxylase is inactivated by catechol-quinones and converted to a redox-cycling quinoprotein: possible relevance to Parkinson's disease. *Journal of Neurochemistry*, 73, 1309–1317.

Kuhn, H.G., Palmer, T.D. and Fuchs, E. (2001) Adult neurogenesis: a compensatory mechanism for neuronal damage. *European Archives of Psychiatry and Clinical Neuroscience*, 251(4):152-8.

Lafon-Cazal, M., Pietri, S., Culcasi, M. and Bockaert, J. (1993). NMDA-dependent superoxide production and neurotoxicity. *Nature*, 364:535–537.

Ladenheim, B., Krasnova, I.N., Deng, X., Oyler, J.M., Polettini, A., Moran, T.H., Huestis, M.A. and Cadet, J.L. (2000) Methamphetamine-induced neurotoxicity is attenuated in transgenic mice with a null mutation for Interleukin-6. *Molecular Pharmacology*, 58:1247–1256.

Larsen, K.E., Fon, E.A., Hastings, T.G., Edwards, R.H. and Sulzer, D. (2002) Methamphetamine-induced neurotoxicity degeneration of dopaminergic neurons involves autophagy and upregulation of dopamine synthesis. *Journal of Neuroscience*, 22:8952-8960

Laskowski, A., Howell, O.W., Sosunov, A.A., McKhann, G. and Gray, W.P. (2007) NPY mediates basal and seizure-induced proliferation in the subcallosal zone. *Neuroreport,* 18(10):1005-1008

Lau, J.W.S., Senok, S., Stadlin, A. (2000) Methamphetamine-induced oxidative stress in cultured mouse astrocytes. *Annals of NY Academy of Science*, 914 146-156

LaVoie, M.J. and Hastings, T.G. (1999b). Dopamine quinine formation and protein modification associated with striatal neurotoxicity of methamphetamine: evidence against the role for extracellular dopamine. *Journal of Neuroscience,* 19:1484-1491.

LaVoie, M.J., Card, J.P., Hastings, T.G. (2004) Microglia activation precedes dopamine terminal pathology in methamphetamine-induced neurotoxicity. *Experimental Neurology,* 187:47-57.

Lee, N.E., Taylor, M.M., Bancroft, E., Ruane, P.J. and McCoy, L. (2005) Risk factors for community-acquired methicilin-resistant staphylococcus aureus skin infections among HIV-positive men who have sex with men. *Clinical Infectious Disease,* 40: 1529-1534

Le Moine, C., Normand, E. and Bloch. B. (1991) Phenotypical characterization of the rat striatal neurons expressing the D1 dopamine receptor gene. *Proceedings of the National Academy of Science,* 88(10):4205-4209

Le Moine, C., Kieffer, B., Gaveriaux-Ruff, C., Befort, K. and Bloch, B. (1994) Delta-opioid receptor gene expression in the mouse forebrain: localization in cholinergic neurons of the striatum. *Journal of Neuroscience*, (3):635-640.

Li, J.L., Kaneko, T. and Mizuno, N. (2001) Colocalization of neuronal nitric oxide synthase and neurokinin-1 receptor in striatal interneurons in the rat. *Neuroscience Letters,* 310(2-3):109-112.

Lie, D.C., Song, H., Colamarino, S.A., Ming, G.L. and Gage, F.H. (2004) Neurogenesis in the adult brain: new strategies for central nervous system diseases. *Annual Review of Pharmacology and Toxicology*, 44:399-42

Lineberry, T. W. and Bostwick, J.M, (2006) methamphetamine abuse: a perfect storm of complications. *Mayo Clinic proceedings,* 81(1):77-84

Lichtenwalner, R.J and Parent, J.M. (2006) Adult neurogenesis and the ischemic forebrain. *Cerebral Blood Flow and Metabolism*, 26:1-20.

Lorez, H. (1981) Fluorescence histochemistry indicates damage of striatal dopamine nerve terminals in rats after multiple doses of methamphetamine. *Life Science,* 28:911–916.

Lundbeck Inc. (2009) Desoxyn methamphetamine hydrochloride tablets USP-product sheet. Accessed May 30, 2010 *www.lundbeckinc.com/USA/products/CNS/desocyn/usa_des_mg__may_09.pdf*.

Luo, C.X., Jin, X., Cao, C.C., Zhu, M.M., Wang, B., Chang, L., Zhou, Q.G., Wu, H.Y. and Zhu DY. (2010) Bidirectional regulation of neurogenesis by neuronal nitric oxide synthase derived from neurons and neural stem cells. *Stem Cells,* 28(11):2041-52

Machiyama, Y. (1992) Chronic methamphetamine intoxication model of schizophrenia in animals *Schizophrenia Bulletin*, 18(1):107-113.

Magavi, S.S., Leavitt, B.R. and Macklis, J.D. (2000) Induction of neurogenesis in the neocortex of adult mice. *Nature,* 405: 951-955

Magavi, S.S. and Macklis, J.D. (2002) Induction of neuronal type-specific neurogenesis in the cerebral cortex of adult mice: manipulation of neural precursors in situ. *Developmental Brain Research,* 134(1-2):57-76.

Mansergh, G., Purcell, D.W., Stall, R., McFarlane, M., Semaan, S., Valentine, J. and Valdiserri, R. (2006) CDC consultation on methamphetamine use and sexual risk behavior for HIV/STD infection: summary and suggestions. *Public Health Reports,* 121:127–132

Mao, L. and Wang, J. Q. (2001) Gliogenesis in the striatum of the adult rat: alteration in neural progenitor population after psychostimulant exposure, *Developmental Brain Research,* 130: 41-51.

Mao, L., Lau, Y., Petroske, E., & Wang, J. (2001). Profound astrogenesis in the striatum of adult mice following nigrostriatal dopaminergic lesion by repeated MPTP administration. *Developmental Brain Research, 131*(1-2): 57-65

Mao, L. and Wang, J. Q. (2001) Gliogenesis in the striatum of the adult rat: alteration in neural progenitor population after psychostimulant exposure. *Developmental Brain Research,* 130: 41-51.

Marek, G.J., Vosmer, G. and Seiden, L.S. (1990) Dopamine uptake inhibitors block long-term neurotoxic effects of methamphetamine upon dopaminergic neurons. *Brain Research,* 513:274–279

Mark, K.A., Sogjomonian, J.J. and Yamamoto, B.K., (2004) High-dose methamphetamine acutely activates the striatonigral pathway to increase striatal glutamate and mediate long-term dopamine toxicity. *Journal of Neuroscience,* 24:11449-11456

Mark, K.A., Quinton, M.S., Russek, S.J. and Yamamoto, B.K. (2007) Dynamic changes in vesicular glutamate transporter 1 function and expression related to methamphetamine-induced glutamate release. *Journal of Neuroscience,* 27:6823–6831

Marrone, M.C., Marinelli, S., Biamonte, F., Keller, F., Sgobio, C.A., Ammassari-Teule, M, Bernardi, G. and Mercuri, N.B., (2006) Altered cortico-striatal synaptic plasticity and related behavioural impairments in reeler mice. *European Journal of Neuroscience,* 24(7):2061-2070

Marshall, J.F., Belcher, A.M., Feinstein E.M., and O'Dell, S.J (2007) Methamphetamine-induced neural and cognitive changes in rodents. *Addiction,* 102 (S1):61 - 69

McCann, U.D., Wong, D.F., Yokoi, F., Villemagne, V., Dannals, R.F. and Ricaurte G.A. (1998) Reduced striatal dopamine transporter density in abstinent methamphetamine and methcathinone users: evidence from positron emission tomography studies with [11C] WIN-35,428. *Journal of Neuroscience*, 18:8417-8422

McKinney, M., Kent C. (1994) Differential expression of GAP-43 mRNA in adult central cholinergic neuronal populations. *Molecular Brain Research,* 23(3):213-20.

Melega, W.P., Jorgensen, M.J., Lacan, G., Way, B.M., Pham, J., Morton, G., Cho, A.K and Fairbanks, L.A. (2008). Long-term methamphetamine administration in the vervet monkey models aspects of a human exposure: brain neurotoxicity and behavioral profiles. *Neuropsychopharmacology*, 33:1441–1452

Melega, W.P., Lacan, G., Harvey, D.C., and Way, B.M. (2007) Methamphetamine increases basal ganglia iron to levels observed in aging. *Neuroreport*, 18:1741-1745

Melega, W.P., Lacan, G., Desalles, A.A. and Phelps, M.E. (2000) Long-term methamphetamine-induced decreases of [(11) C] WIN 35,428 binding in striatum are reduced by GDNF: PET studies in the vervet monkey. *Synapse*, 35:243–249.

Melega, W.P., Raleigh, M.J., Stout, D.B., Lacan, G., Huang, S.C. and Phelps, M.E. (1997) Recovery of striatal dopamine function after acute amphetamine- and methamphetamine-induced neurotoxicity in the vervet monkey. *Brain Research,* 766:113–120.

Meredith, C.W., Jaffe, C., Ang-Lee, K. and Saxon, A.J., (2005) Implications of chromic methamphetamine use: A literature review. *Harvard Review of Psychiatry,* 13: 141-154

Miller, D.B. and O'Callaghan (1994) Environment-drug and - stress-induced alteration in body temperature affect the neurotoxicity of substituted amphetamines in the C57BL/6J mouse. *Pharmacology and Experimental Therapeutics,* 270:752-760.

Milosevic, J., Schwarz, S.C., Maisel, M., Poppe-Wagner, M., Dieterlen, M.T., Storch, A. and Schwarz, J.(2007) Dopamine D2/D3 receptor stimulation fails to promote dopaminergic neurogenesis of murine and human midbrain-derived neural precursor cells in vitro. *Stem Cells Development,* 16(4):625-35.

Montine, T.J., Picklo, M.J., Amarnath, V., Whetsell Jr., W.O. and Graham, D.G., (1997)Neurotoxicity of endogenous cysteinylcatechols. *Experimental Neurology,* 148:26–33.

Morino, T., Ogata, T., Horiuchi, H., Takeba, J., Okumura, H., Miyazaki, T., and Yamamoto, H. (2003) Delayed neuronal damage related to microglia proliferation after mild spinal cord compression injury. *Neuroscience Research,* 46(3): 309-318

Mouton, P. R. (2002) *Principles and Practices of Unbiased Stereology*. Baltimore, MD: Johns Hopkins University Press.

National Drug Intelligence Center (NDIC) (2007) Methamphetamine threat assessment December 2008 report document-Q0317-006. Retrieved November 27, 2010 from *http://www.justice.gov/ndic/pubs26/26594/index.htm*

National institutes of Health, National institute on drug abuse (NIDA) (2006) Research Report Series: Methamphetamine Abuse andAddiction. Revision. Retrieved May 15, 2009. *http://www.drugabuse.gov /ResearchReports/methamph/methamph2.html#what*

Nakamura, K. and Hikosaka, O. (2006a) Role of dopamine in primate caudate-nucleus in reward modulation of saccades. *Journal of Neuroscience,* 26(20):2360-5369

National institutes of health, national institute on drug abuse (NIDA) info facts series: Methamphetamine (2010) https: Retrieved May 15, 2010 from *NIDA.nih.gov/pfd/infofacts/methamphetamaine10.pdf*

Neve, K.A., Kozlowski, M.R. and Marshall, J.F. (1982) Plasticity of neostriatal dopamine receptors after nigrostriatal injury: relationship to recovery of sensorimotor functions and behavioral supersensitivity. *Brain Research,* 244(1):33-44.

Newton, T.F., Kalechstein, A.D., Duran, S., Vansluis, N. and Ling, W. (2004) Methamphetamine abstinence syndrome: Preliminary findings. *American Journal on Addictions,* 13(3):248-255

Nicosa, N., Pacula, R.L., Kilmer, B., Lundberg, R. and Chiesa, J. (2009) Economic cost of methamphetamine use in the US, 2005, Santa Monica, CA: Drug Policy Res. Cent., RAND corp. Retrieved May 15, 2010 from *http://www.rand.org/pubs/monographs/MG829*

Nordhal, T.E., Salo, R., Natsuki, Y., Galloway, G.P., Waters C., Moore, C, D., Kile and S., Cuonocore, M.H (2005) Methamphetamine users in sustained abstinence: a proton magnetic resonance spectroscopy study. *Archives of General Psychiatry,* 62(4): 444-452.

Nordhal, T.E., Salo, R., Spssin, K., Gibson, D.R., Flynn, D., Learmon, M., Galloway, G.P., Pfefferbaum, A., Speilman D.M., Adalsteinsson, E., Sullivan, E.V., (2002) Low, N-acetyl-aspartate and high choline in the anterior cingulum of recently abstinent methamphetamine-dependent subjects: a preliminary proton MRS study. Magnetic resonance spectroscopy. *Psychiatry Research*, 116(1-2)43-53 188

Numachi, Y., Ohara, A., Yamashita, M., Fukushima, S., Kobayashi, H., Hata, H., Watanabe, H., Hall, F.S., Lesch, K.P., Murphy, D.L., Uhl, G.R. and Sora, I. (2007). Methamphetamine-induced hyperthermia and lethal toxicity: role of the dopamine and serotonin transporters. *European Journal of Pharmacology*, 572: 120–128.

O'Callaghan, J.P., Sriram, K. and Miller, D.B. (2008) Defining "neuroinflammation." *Annals of New York Academy of Science,* 1139:318-30.

O'Dell, S.J., Weihmuller, F.B. and Marshall, J.F. (1993).Methamphetamine-induced dopamine overflow and injury to striatal dopamine terminals: attenuation by dopamine D1 or D2 antagonists. *Journal of Neurochemistry*, 60:1792–1799

O'Donnell, P. and Grace, A.A. (1998) Dysfunctions in multiple interrelated systems as the neurobiological bases of schizophrenic symptom clusters. *Schizophrenia Bulletin*, 24(2):267-83.

O'Doherty, J., Dayan, P., Schultz, J., Deichmann, R., Friston, K. and Dolan RJ.(2004) Dissociable roles of the ventral and dorsal striatum in instrumental conditioning. *Science,* 304(5669):452-454.

Oh. J.S., Lyoo, I.K., Sung, Y.H., Hwang, J., Kim, J., Chung, A., Park, K.S., Kim S.J., Renshaw P.F., and Song, I.C. (2005) Shape changes of the corpus callosum in abstinent methamphetamine users. *Neuroscience Letters*, 384(1-2):76-81

Pacher, P., Beckman, J.S and Liaudet, L. (2007) Nitric oxide and peroxynitrite in health and disease. *Physiological Reviews,* 87:315–424

Packard, M. G., Hirsh, R. and White, N. M. (1989) Differential effects of fornix and caudate nucleus lesions on two radial maze tasks: evidence for multiple memory systems. *Journal of Neuroscience,* 9:1465–1472

Packard, M.G. and McGaugh, J.L. (1996) Inactivation of hippocampus or caudate nucleus with lidocaine differentially affects expression of place and response learning. *Neurobiology of Learning and Memory*, 65:65-72.

Packard, M.G. (1999) Glutamate infused posttraining into the hippocampus or caudate-putamen differentially strengthens place and response learning. *Proceedings of the National Academy of Science,* 96:12881-12886.

Packard, M. G. (2009). Exhumed from thought: basal ganglia and response learning in the plus-maze. *Behavioral Brain Research,* 199, 24–31.

Packard, M.G., Knowlton, B.J., (2002) learning and memory functions of the basal ganglia. *Annual Reviews of Neuroscience,* 25:563-593 189

Parent, J.M., Valentine, V.V. and Lowenstein, D.H. (2002a) Prolonged seizures increase proliferating neuroblasts in the adult rat subventricular zone olfactory bulb pathway. *Journal of Neuroscience,* 22(8)-3174-3188.

Parent, J.M., Vexler, Z.S., Gong, C., Derugin, N. and Ferriero, D.M. (2002b) Rat forebrain neurogenesis and striatal neuron replacement after focal stroke. *Annals of Neurology*, 52:802-813.

Peck, J.A., Shoptaw, S., Rotheram-Fller, E., Reback, C.J and Bierman, B. (2005) HIV-associated medical, behavioral and psychiatric characteristics of treatment seeking, methamphetamine-dependent men who have sex with men. *Journal of Addictive Diseases,* 24:115-132

Pena-Altimira, E., Petazzi, P. and Contestabile, A. (2010) Nitric oxide control of proliferation in nerve cells and in tumor cells of nervous origin. *Current Pharmaceutical Design,* 16(4):440-450

Perry, V.H., Cunningham, C. and Holmes, C. (2007) Systemic infections and inflammation affect chronic neurodegeneration. *Nature Reviews Immunology,* 7:161–167.

Peterson, D. A. (1999) Quantitative Histology using confocal microscopy: implementation of unbiased stereology procedures. *Methods: A Companion to Methods in Enzymology,* 18:493-507

Pietrzak, R.H., Snyder, P.J. and Maruff, P. (2010) Use of an acute challenge with d-amphetamine to model cognitive improvement in chronic schizophrenia. *Human psychopharmacology,* 25(4):353-8

Pisani, A., Calabresi, P., Centonze, D. and Bernardi, G. (1997) Enhancement of NMDA responses by group I metabotropic glutamate receptors. *British Journal of Pharmacology*, 120: 1007-1014

Potashkin, J.A. and Meredith, G.E. (2006) The role of oxidative stress in the dysregulation of gene expression and protein metabolism in neurogedenerative disease. *Antioxidants and redox signaling*, 8:144-151

Preston, K.L., Schuster, C.R. and Seiden LS. (1985a)Methamphetamine, physostigmine, atropine and mecamylamine: effects on force lever performance. *Pharmacology Biochemistry and Behavavior,* 23:781–788

Preston, K.L., Wagner, G.C., Schuster, C.R. and Seiden, L.S. (1985b) Long-term effects of repeated methylamphetamine administration on monoamine neurons in the rhesus monkey brain. *Brain Res*. 338:243–248.

Pych, J.C., Chang, Q., Colon-Rivera, C., Haag, R. and Gold, P.E. (2005b) Acetylcholine release in the hippocampus and striatum during place and response training. *Learning and Memmory,* 12(6):564-572.

Pych, J.C., Chang, Q., Colon-Rivera C., Gold, P.E.(2005a) Acetylcholine release in the hippocampus and striatum during testing on a rewarded spontaneous alternation task. *Neurobiology o*f *Learning and Memory,* 84(2):93-101

Pu, C., Broening, H. W. and Vorhees, C. V. (1996) Effect of methamphetamine on glutamate-positive neurons in the adult and developing rat somatosensory cortex, *Synapse*, 23:328-334.

Rakic P. (1971a) Neuron-glia relationship during granule cell migration in developing cerebellar cortex. A Golgi and electronmicroscopic study in Macacus Rhesus. *Journal of Comparative Neurology,* 141(3):283-312

Ragozzino, K. E., Leutgeb, S. and Mizumori, S.J.Y. (2001) Dorsal striatal head direction and hippocampal place representations during spatial navigation. *Experimental Brain Research*, 139:372-376.

Rasmussen, N. (2008). Speed and total war in *On Speed: The many lives of Amphetamines*. (pp 63-86) New York University Press

Reiter, L.W., MacPhail and R.C (1982). Factors influencing motor activity measurements in neurotoxicology: In (Mitchell CL, Ed). *Nervous System Toxicology,* (pp 45-65) New York:Raven Press.

Rendell, P.G., Mazur, M. and Henry, J. J. (2009) Prospective memory impairment in former users of methamphetamine. *Pharmacology,* 203: 509-616

Restle, F. (1957) discrimination cues in mazes: a resolution of the place-vs-response question. *Psychological Review,* 64:217-228

Reynolds, B.A. and Weiss, S. (1992) Generation of neurons and astrocytes from isolated cells of the adult mammalian central nervous system. *Science,* 255(5052):1707-1710.

Ricaurte, G.A., Guillery, R.W., Seiden, L.S., Schuster, C.R. and Moore, R.Y. (1982) Dopamine nerve terminal degeneration produced by high doses of methylamphetamine in the rat brain. *Brain Research,* 235:93-103. 191

Ricuarte, G.A., Schuster, C.R., Seiden, L.S (1980) Long-term effects of repeated methylamphetamine administration on dopamine and serotonin neurons in the rat brain: A regional study. *Brain Research,* 193:153-163

Ricuarte, G.A., Seiden, L.S., Schuster, C.R. (1984) Further evidence that amphetamines produce long lasting dopamine neurochemical deficits by destroying dopamine nerve fibers. *Brain Research,* 303:359-364

Richards J.B., Baggott M.J., Sabol K.E. and Seiden L.S. (1993) A high-dose methamphetamine regimen results in long-lasting deficits on performance of a reaction-time task. *Brain Research,* 627 (2): 254-260.

Riddle, E.L., Kokoshka, J.M., Wilkins, D.G., Hanson, G.R. and Fleckenstein, A., E. (2002a) Tolerance to the neurotoxic effects of methamphetamine in young rats. *European Journal of Pharmacology,* 435: 181-185

Riddle, E.L., Topham, J.W., Haycock, G.R., and Fleckenstein, A.E. (2002b) differential trafficking of the vesicular monoamine transporter-2 caused by methamphetamine and cocaine. *European Journal of Pharmacology,* 449:71-74

Rothermundt, M., Peters, M., Prehn, J.H. and Arolt, V. (2003) S100B in brain damage and neurodegeneration. *Microscopy research and technique,* 60(6):614-32.

Ryan L.J., Martone, M.E., Linder, J.C., Groves, P.M (1988) cocaine in contrast to D-amphetamine, does not cause axonal terminal degeneration in the neostriatum and agranular frontal cortex of long-evans rats. *Life Sciences*, 43(17):1403-1409

Saka, E., Iadarola, M., Fitzgerald, D.J. and Graybiel, A.M. (2002) Local circuit neurons in the striatum regulate neural and behavioral responses to dopaminergic stimulation. *Proceedings of the National Academy of Science U S A,* 99(13):9004-9

Saliasuta, N., Abulseoud, O., Hernandez, M., Haghani, P and Ross, B.D., (2010) Metabolic abnormalities in abstinent methamphetamine dependent subjects. *Substance Abuse*, 4:9-20

Sandoval, V., Hanson, G.R., Fleckenstein, A.E. (2000) Methamphetamine decreases mouse striatal dopamine transporter activity: roles of hyperthermia and dopamine. *European Journal of Pharmacology,* 409: 265-271

Sandoval, V., Riddle, E.L., Hanson, G.R., Fleckenstein, A.E (2003) Methylphenidate alters vesicular monoamine transport and prevents methamphetamine-induced dopaminergic deficits *Journal of Pharmacology and Experimental Therapeutics,* 304 (3):1181-1187

Santos, A.P., Wilson, A. K., Hornung, C.A., Polk, H.C., Rodriguez, J.L., and Franklin, G.A., (2005) Methamphetamine laboratory explosions: A new and emerging burn injury, *Journal of Burn Care and Rehabilitation, 26:228-232*

Schmidt, C. J. and Gibb, J. W. (1985) Role of the dopamine uptake carrier in the neurochemical response to methamphetamine: Effects of amfonelic acid, *European. Journal of Pharmacology*, 109:73-80.

Schmidt, C.J., Sonsalla, P.K., Hanson, G.R., Peat, M.A., Gibb, J.W (1985b). Methamphetamine-induced depression of monoamine synthesis in the rat: development of tolerance. *Journal of Neurochemistry,* 44(3):852-855.

Schultz, W., Romo, R., Scarnati, E., Sundström, E., Jonsson, G. and Studer, A. (1989) Saccadic reaction times, eye-arm coordination and spontaneous eye movements in normal and MPTP-treated monkeys. *Experimental Brain Research,* 78(2):253-267.

Scott, J.C, Woods, S.P., Matt, G, E., Meyer, R.A., Heaton, R.K. (2007) Neurocognitive effects of methamphetamine: A critical review and meta-analysis. *Neuropsychology Review,* 17: 275-297

Segal, D.S and Kuczenski, R. (1997) Repeated binge exposures to amphetamine and methamphetamine: behavioral and neurochemical characterization. *Journal of Pharmacology and Experimental Therapeutics*, 282:561-573

Segal, D.S., Kuczenski R., O'Neil, M.L., Melega. W.P. and Cho, A.K. (2003). Escalating dose methamphetamine pretreatment alters the behavioral and neurochemical profiles associated with exposure to a high- dose methamphetamine binge. *Neuropsychopharmacology,* 28:1730–1740.

Segal, D.S., Kuczenski, R., O'Neil, M.L., Melega, W.P. and Cho, A.K. (2005) Prolonged exposure of rats to intravenous methamphetamine: behavioral and neurochemical characterization. *Psychopharmacology,* 180:501–512

Seiden, L. S., Fischman, M. W., and Schuster, C.R., (1976) Long-term methamphetamine induced changes in brain catecholamines in tolerant rhesus monkeys. *Drug Alcohol Dependence*.1:215-209

Seiden, l. S., and Vosmer, G. (1984). Formation of 6-hydroxydopamine in caudate nucleus of the rat brain after a single large dose of methylamphetamine. *Pharmacology Biochemistry and Behavior*. 21:29-31

Seiden, L.S., MacPhail, R.C. and Oglesby, M.W. (1975) Catecholamines and drug-behavior interactions. *Federation of American Societies for Experimental Biology; National Library of Medicine (U.SA),* 34(9):1823-1831

Sekine, Y., Iyo, M., Ouchi, Y., Matsunaga, T., Tsukada, H., Okada, H., Yoshikawa, E., Futatsubashi, M., Takei, N., Mori, N. (2001) Methamphetamine-related psychiatric symptoms and reduced brain dopamine transporters studied with PET. *American Journal of Psychiatry*, 158: 1206-1214

Sekine, Y., Ouchi, Y., Sugihara, G., Takei, N., Yoshikawa, E., Nakamura, K., Iwata, Y., Tsuchiya, K.J., Suda, S., Suzuki, K., Kawai, M., Takebayashi, K., Yamamoto, S., Matsuzaki, H., Ueki, T., Mori, N., Gold, M.S. and Cadet, J.L. (2008) Methamphetamine causes microglial activation in the brains of human abusers. *Journal of Neuroscience*, 28(22):5756-5761

Shaner, J.W (2002) Caries associated with methamphetamine abuse. *Journal of Michigan Dental Association*, 84(9):42-27

Sharma, H.S. and Kiyatkin, E.A., (2009). Rapid morphological brain abnormalities during acute methamphetamine intoxication in the rat: an experimental study using light and electron microscopy. *Chemical Neuroanatomy,* 37: 18–32.

Sharma, H.S., Sjoquist, P.O. and Ali, S.F., (2007). Drugs of abuse-induced hyperthermia, blood–brain barrier dysfunction and neurotoxicity: neuroprotective effects of a new antioxidant compound H-290/51. *Current Pharmaceutical Design,* 13: 1903–1923.

Sheng, P., Cerruti, C., Ali, S., Cadet, J.L. (1996) Nitric oxide is a mediator of methamphetamine (METH)-induced neurotoxicity. In vitro evidence from primary cultures of mesencephalic cells. *Annals of the N Y Academy of Science,* 801:174–186.

Simon, S.L., Domier, C., Carnell, J., Brethen, P., Rawson, R., and Ling, W. (2000) cognitive impairments in individuals currently using methamphetamine. *American Journal on Addictions*, 9 (3):222-231

Simon, P, Dupuis, R and Costentin, J. (1994) Thigmotaxis as an index of anxiety in mice: Influence of dopaminergic transmission. *Behavioral Brain Research*, 61(1):59-64

Simon, S.L., Dean, A.C., Cordova, X., Monterosso, J.R. and London, E.D. (2010) Methamphetamine dependence and neuropsychological functioning: evaluating change during early abstinence. *Journal of the Study of Alcohol and Drugs*, 71(3):335-44.

Shoblock, J. R., Sullivan, E. B., Maisonneuve, I. M. and Glick, S. D. (2003). Neurochemical and behavioral differences between d-methamphetamine and d-amphetamine in rats. *Psychopharmacology*, 165(4), 359.

Smith, L.M., Chang, L., Yonekura, M.L., Grob, C., Osborn D. and Ernst, T. (2001) Brain proton magnetic resonance spectroscopy in children exposed to methamphetamine in utero. *Neurology*, 57:255-260

Soetens, E., Casaer, S., D‟Hooge, R. and Hueting, J.E. (1995). Effect of amphetamine on long-term retention of verbal material. *Psychopharmacology*, 119(2):155-162

Sohur, U.S., Emsley, J.G., Mitchell, B.D., Macklis, J.D. (2006) Adult neurogenesis and cellular brain repair with neural progenitors, precursors and stem cells. *Philosophical transactions of the Royal Society of London. Series B, Biological sciences*, 361(1473):1477-1497

Sonsalla, P.K., Gibb, J.W. and Hanson, G.R. (1986) Roles of D1 and D2 dopamine receptor subtypes in mediating the methamphetamine-induced changes in monoamine systems. *J Pharmacology and Experimental Therapeutics,* 238 (3):932-937

Sonsalla, P.K., Nicklas, W.J. and Heikkila, R.E. (1989). Role for excitatory amino acids in methamphetamine-induced nigrostriatal dopaminergic toxicity. *Science*, 243:398–400.

Sonsalla, P.K., Jochnowitz, N.D., Zeevalk, G.D., Oostveen, J.A. and Hall, E.D. (1996) Treatment of mice with methamphetamine produces cell loss in the substantia nigra. *Brain Research,* 28; 738(1):172-175.

Sonsalla, P.K., Albers, D.S. and Zeevalk, G.D. (1998) Role of glutamate in neurodegeneration of dopamine neurons in several animal models of Parkinsonism. *Amino Acids,* 14:69–74.

Soriano, E., Del Rio, J.A and Auladell, C. (1993) Characterization of the Phenotype and Birthdates of Pyknotic Dead Cells in the Nervous System by a Combination of DNA Staining and Immunohistochemistry for 5‟-Bromodeoxyuridine and Neural Antigens. *The Journal of Histochemistry and Cytochemistry*, 41(6):819-827

Spencer, J.P., Whiteman, M., Jenner, P. and Halliwell, B. (2002) 5-s-Cysteinyl-conjugates of catecholamines induce cell damage, extensive DNA base modification and increases in caspase-3 activity in neurons. *Journal of Neurochemistry,* 81:122-129

Squire, L. (2004) Memory systems of the brain: A brief history and current perspective. *Neurobiology of learning and Memory*, 82: 171-177

Starke, K., Gothert, M. and Kilbinger, H. (1989) Modulation of neurotransmitter release by presynaptic autoreceptors. *Physiological Review,* 69:864-889

Steiner, H., Gerfen, C.R. (1998) Role of dynorphin and enkephalin in the regulation of striatal output pathways and behavior. *Experimental Brain Research,* 123(1-2):60-76

Stemmelin, J., Lazarus, C., Cassel, S., Kelche, C. and Cassel, J.C. (2000) Immunohistochemical and neurochemical correlates of learning deficits in aged rats. *Journal of Neuroscience*, 96(2):275-289

Stephans, S.E. and Yamamoto, B.K., (1994). Methamphetamine-induced neurotoxicity: roles for glutamate and dopamine efflux. S*ynapse,* 17:203-209

Stephans, S. and Yamamoto, B. (1996). Methamphetamines pretreatment and the vulnerability of the striatum to methamphetamine neurotoxicity. *Journal of Neuroscience,* 72:593–600.

Stichel, C.C. and Muller, H.W. (1998). The CNS lesion scar: new vistas on an old regeneration barrier. *Cell and Tissue Research*, 294:1-9

Streit, W.J. (2002) Microglia as immunoprotective immunocompetent cells of the CNS *Gila,* 40:133-139

Stocco, A., Lebiere, C. and Anderson, J.R. (2010). Conditional routing of information to the cortex: A model of the basal ganglia's role in cognitive coordination. *Psychological Review,* 117(2): 541-574

Substance Abuse and Mental Health Service Administration Office of Applied Studies (2009a) *Results from the 2008 National Survey on Drug use and Health: National Survey.* OAS, NSDUH Series H-36, HHS Publication No. SMA 09-4434, Rockville, MD. http://www.oas.samhsa.gov/NSDUHlatest.htm (Accessed May 15, 2010)

Substance Abuse and Mental Health Services Administration. (2010). *Results from the 2009 National Survey on Drug Use and Health: Volume I. Summary of National Findings* (Office of Applied Studies, NSDUH Series H-38A, HHS Publication

No. SMA 10-4856 Findings). Rockville, MD. http://www.oas.samhsa.gov/NSDUHlatest.htm (Accessed December 7, 2010)

Substance Abuse and Mental Health Service Administration Office of applied studies (2009b). Treatment episode data set (TEDS) highlights-2007, national admissions to substance abuse treatment services. OAS series # S-45 HHS Publication No. (SMA) 09-4360, Rockville Maryland. https://www.dasis.samhsa.gov/ted07/tedshigh2k7.pdf (Accessed May 15, 2010)

Sulzer, D., Chen, T.-K., Lau, Y. Y., Kristensen, H., Rayport, S. and Ewing, A. (1995) Amphetamine redistributes dopamine from synaptic vesicles to the cytosol and promotes reverse transport. *Journal of Neuroscience*, 15:4102-4108.

Sulzer, D., Sonders, M.S., Poulsen, N.W., Galli, A. (2005) Mechanisms of neurotransmitter release by amphetamines: *A Review of Progress in Neurobiology*, 75: 406-433.

Szele, F.G. and Chesselet, M.F. (1996) Cortical lesions induce an increase in cell number and PSA-NCAM expression in the subventricular zone of adult rats. *Journal of Comparative Neurology*, 368(3):439-54.

Takano, H., Fukushi, H., Morishima, Y. and Shirasaki, Y (2003) Calmodulin and calmodulin-dependent kinase II mediate neuronal cell death induced by depolarization. *Brain Research*, 962(1) 41-47

Takasawa, K., Kitagawa, K., Yagita, Y., Sasaki, T., Tanaka, S., Matsushita, K., Ohstuki, T., Miyata, T., Okano, H., Hori, M. and Matsumoto M. (2002) Increased proliferation of neural progenitor cells but reduced survival of newborn cells in the contralateral hippocampus after focal cerebral ischemia in rats. *Journal Cerebral Blood Flow and Metabolism,* 22(3):299-307.

Tandé, D., Höglinger, G., Debeir, T., Freundlieb, N., Hirsch, E.C. and François, C. (2006).New striatal dopamine neurons in MPTP-treated macaques result from a phenotypic shift and not neurogenesis. *Journal of Neurology, Brain*, 129 5):1194-1200

Tata, D.A., Raudensky, J. and Yamamoto, B.K. (2007). Augmentation of methamphetamine- induced toxicity in the rat striatum by unpredictable stress: contribution of enhanced hyperthermia. *European Journal of Neuroscience*, 26, 739–748

Taupin, P. (2007) Protocols for studying adult neurogenesis: insights and recent developments. *Regenerative Medicine,* 2(1):51-62

Tepper, J.M. and Bolam, J.P. (2004) Functional diversity and specificity of neostriatal interneurons. *Current Neurobiology,* 12:685-92

Tepper, J.M., Wilson, C.J. and Koós, T. (2008) Feedforward and feedback inhibition in neostriatal GABAergic spiny neurons. *Brain Research Reviews,* 58(2):272-81.

Thiede, H., Valleroy, L.A., MacKellar, D.A., Celentano, D.D., Ford, W.L., Hagan, H., Koblin, B.A., LaLota, M., McFarland, W., Shehan, D.A. and Torian, L.V. (2003) Regional patterns and correlates of substance use among young men who have sex with men in 7 US urban areas. *American Journal of Public Health*, 93:1915–1921.

Thiriet, N., Agasse, F., Nicoleau, C., Guégan, C., Vallette, F., Cadet, J.L., Jaber, M., Malva, J.O. and Coronas, V. (in press) NPY promotes chemokinesis and neurogenesis in the rat subventricular zone. *Journal of Neurochemistry,* 116 *(*early online view): Accessed http://onlinelibrary.wiley.com/journal/10.1111/%28ISSN%291471-4159/earlyview

Thomas D.M., Kuhn, D.M. (2005a) Attenuated microglial activation mediates tolerance to the neurotoxic effects of methamphetamine. *Journal of Neurochemistry,* 92(4): 790-797

Thomas, D.M., Walker, P.D., Benjamins, J.A., Geddes, T.J. and Kuhn, D.M. (2004c) Methamphetamine neurotoxicity in dopamine nerve endings of the striatum is associated with microglial activation. *Journal of Pharmacology and Experimental Therapeutics,* 311:1–7.

Thompson, P., Hayashi, K., Simon, S., Geaga, J., Jong, M., Sui, Y., Tiga, A., W., Ling, W. and London, E.D. (2004). Structural abnormalities in the brains of human subjects who use methamphetamine. *Journal of Neuroscience*, 24(26): 6028-6036.

Todd, R.D., Carl, J., Harmon, S., O'Malley, K.L. and Perlmutter, J.S. (1996) Dynamic changes in striatal dopamine D2 and D3 receptor protein and mRNA in response to 1-methyl-4-phenyl-1,2,3,6-tetrahydropyridine (MPTP) denervation in baboons. *Journal of Neuroscience,* 16(23):7776-7782.

Tokunaga, M., Seneca, N., Shin, R.M., Maeda, J., Obayashi, S., Okauchi, T., Nagai, Y., Zhang, M.R., Nakao, R., Ito, H., Innis, R.B., Halldin, C., Suzuki, K., Higuchi, M. and Suharam T. (2009) Neuroimaging and physiological evidence for involvement of glutamatergic transmission in regulation of striatal dopaminergic system. *Neurobiology of Disease,* 29(6):1887-1896

Tolman, E.C., Ritchie, B.F. and Kalish, D. (1946) Studies in spatial learning II: Place learning versus response learning. *Journal of Experimental Psychology*, 37:385-392

Tremblay, L., Hollerman, J.R. and Schultz, W. (1998) Modifications of reward expectation-related neuronal activity during learning in primate striatum. *Neurophysiology,* 80:964–977

Truong, J.G., Newman, A.H., Hanson, C.R. and Fleckenstein, A.E. (2004) Dopamine D2 receptor activation increases vesicular dopamine uptake and redistributes vesicular monoamine transporter-2 protein. *European Journal of Pharmacology*, 504:27-32

Tsuchiya, K., Inoue, T. and Koyama, T. (1996) Effect of repeated methamphetamine pre-treatment on behavior induced by conditioned fear stress. *Pharmacology Biochemistry and Behavior*, 54(4) 687-691

Uberti, D., Ferrari, T. G. and Memo, M. (2003). Involvement of DNA damage and repair systems in neurodegenerative process. *Toxicology Letters,* 139(2-3), 99-105.

Ugarte, Y., Rau, K.S., Riddle, E.L., Hanson, G.R and Fleckenstein, A.E. (2003) Methamphetamine rapidly decreases mouse vesicular dopamine update: role of hyperthermia and Dopamine D2 receptors. *European Journal of Pharmacology, 472*(3):165-171

United Nations Office on Drugs and Crime (UNODC). World Drug Report, 2007. Vienna, Austria: UNODC Research and Analysis Section, (2007), http://www.unodc.org/pdf/research/wdr07/WDR_2007.pdf (accessed 27 September 2008).

United Nations Office on Drugs and Crime (UNODC). World Drug Report Annual overview 2008: UNDC Research and Analysis 2008. http://www.unodc.org/documents/wdr/WDR_2008/WDR2008_Overview Section. (Accessed 4 April 2009)

United Nations Office on Drugs and Crime (UNODC). (2009) World Drug Report Highlights.http://www.unodc.org/unodc/en/press/releases/2009/june/world-drug-report-2009-highlights-links-between-drugs-and-crime.html (accessed Sept 30, 2009)

US Department of Justice, Drug Enforcement Administration. Office of Diversion Control (DEA-ODC, 2007) Combat Methamphetamine Act of 2005: Procedures for establishment of individual import, manufacturing and procurement quotas Assessment of Annual Needs questions and Answers as of 7/10/2007.

Van de Berg, W.D., Kwaijtaal, M., De Louw. A.J., Lissone, N.P., Schmitz, C., Faull, R.L., Blokland, A., Blanco, C.E. and Steinbusch, .H.W. (2003) Impact of perinatal asphyxia on the GABAergic and locomotor system. *Journal of Neuroscience*, 117(1):83-96.

Van Kampen, J.M., Hagg, T. and Toertson, H.A. (2004) Induction of neurogenesis in the adult rat subventricular zone and neostriatum following dopamine D3 receptor stimulation, *European Journal of Neuroscience*, 19: 2377-2387

Van Kampen, J. M. and Eckman, C. B. (2006) Dopamine D3 receptor agonist delivery to a model of Parkinson's disease restores the nigrostriatal pathway and improves locomotor behavior. *Journal of Neuroscience*, 26:7272-7280. 198

Van Kampen, J. M. and Robertson, H. A. (2005) A possible role for dopamine D3 receptor stimulation in the induction of neurogenesis in the adult rat substantia nigra. *Journal of Neuroscience,* 136: 381-386.

Van Kampen, J.M. and Stoessl, A.J (2003) Effects of oligonucleotide antisense to dopamine D3 receptor mRNA in a rodent model of behavioral sensitization to levodopa. *Journal of Neuroscience*, 111(1):207-314

Villemagne, V., Yuan, J., Wong, D.F., Dannals, R.F., Hatzidimitriou, G., Mathews, W.B., Ravert, H.T., Musachio, J, McCann, U.D., and Ricaurte, G.A. (1998) Brain dopamine neurotoxicity in baboons treated with doses of methamphetamine comparable to those recreationally abused by humans: evidence from [11C]WIN-35,428 positron emission tomography studies and direct in vitro determinations. *Journal of Neuroscience*, 18:419-427.

Volkow, N. D., Chang, L., Wang, G. J., Fowler, J. S., Franceschi, D., Sedler, M. J., Gatley, S. J., Hitzemann, R., Ding, Y. S., Wong, C. and Logan, J. (2001a) Higher cortical and lower subcortical metabolism in detoxified methamphetamine abusers, *American Journal of Psychiatry*, 158:383-389.

Volkow, N. D., Chang, L., Wang, G. J., Fowler, J. S., Leonido-Yee, M., Franceschi, D., Sedler, M. J., Gatley, S. J., Hitzemann, R., Ding, Y. S., Logan, J., Wong, C., and Miller, E. N. (2001b) Association of dopamine transporter reduction with psychomotor impairment in methamphetamine abusers. *American Journal of Psychiatry,* 158: 377-382.

Volkow, N. D., Chang, L., Wang, G.-J., Fowler, J. S., Franceschi, D., Sedler, M., Gatley, S. J., Miller, E., Hitzemann, R., Ding, Y. S. and Logan, J. (2001c) Loss of dopamine transporters in methamphetamine abusers recovers with protracted abstinence. *Journal of Neuroscience,* 21:9414-9418.

Volkow, N. D., Chang, L., Wang, G.J., Fowler, J.S., Ding, Y.S., Sedler, M., Logan, J., Franceschi, D., Gatley, J., Hitzemann, R., Gifford, A., Wong, C., Pappas, N., (2001d). Low level of Brain dopamine D2 receptors in methamphetamine abusers: Association with metabolism in the orbitofrontal cortex. *American Journal of Psychiatry*, 158(12): 2015-2021

Wagner, G. C., Ricaurte, G. A., Seiden, L. S., Schuster, C. R., Miller, R. J. and Westley, J. (1980) Long-lasting depletions of striatal dopamine and loss of dopamine uptake sites following repeated administration of methamphetamine. *Brain Research*, 181:151-160.

Wagner, G.C., Lucot, J.B., Schuster, C.R., Seiden, L.S., 1983. Alpha-methyltyrosine attenuates and reserpine increases methamphetamine-induced neuronal changes. *Brain Research*, 270:285–288.

Wakade, C.G., Mahadik, S.P., Waller, J.L. and Chiu, F.C. (2002) Atypical neuroleptics stimulate neurogenesis in adult rat brain. *Neuroscience Research,* 69(1):72-79

Walaas, I. (1981) Biochemical evidence for the overlapping neocortical and allocortical glutamate projections to the nucleus accumbens and rostral caudatoputamen in the rat brain. *Journal of Neuroscience,* 6(3): 399-405

Walter L., Neumann, H. (2009) Role of microglia in neuronal degeneration and regeneration. *Seminars in Immunopathology*, 31(4)513-525

Wang, J., Xu, W., Ali, S.F. and Angulo, J.A. (2008) Connection between the striatal neurokinin-1 receptor and nitric oxide formation during methamphetamine exposure. *Annals of the N Y Academy of Science,* 1139:164-171.

Weeber, E.J., Beffert, U., Jones, C., Christian, J.M., Forster, E., Sweatt, J.D. and Herz, J. (2002) Reelin and ApoE receptors cooperate to enhance hippocampal synaptic plasticity and learning. *Journal Biological Chemistry*, 277 (42):39944–39952.

Weiner D.M., Levey, A. I., Sunahara, R. K., Niznik, H.B., O'Dowd, B. F., Seeman, P., and Brann M. R. (1991) D1 and D2 dopamine receptor mRNA in rat brain. *Proceedings of the National Academy of Science USA*, 88:1859-1863.

West, M.J., Slomianka, L. and Gundersen, H.J.G. (1991) Unbiased stereological estimation of the total number of neurons in the subdivisions of the rat hippocampus using the optical fractionator. *The Anatomical Record*, 231:482-497

Whimbey, A.E., Denenberg, V.H. (1967) Two independent behavioral dimensions in open-field performance. *Comparative Physiological Psychology*, 63(3):500-504.

Whishaw, I. Q., Mittleman, G., Bunch, S. T. and Dunnett, S. B. (1987) Impairments in the acquisition, retention and selection of spatial navigation strategies after medial caudate-putamen lesions in rats. *Behavioral Brain Research,* 24:125–138

Wiegmann, D.A., Stanny, R.R., McKay, D.L., Meri, D.F., and McCardie, A.H. (1996) Methamphetamine effects on cognitive processing during extended wakefulness. *International journal of aviation psychology*, 6(4): 379-397

Wilson, J. M., Kalasinsky, K. S., Levey, A. I., Bergeron, C., Reiber, G., Anthony, R. M., Schmunk, G. A., Shannak, K., Haycock, J. W. and Kish, S. J. (1996) Striatal dopamine nerve terminal markers in human, chronic methamphetamine users, *Nature Medicine*, 2(6): 699-703.

Wilhelm, C.J., Johnson, R.A., Lysko, P.G., Eshleman, A.J. and Janowsky, A. (2004) Effects of methamphetamine and lobeline on vesicular monoamine and dopamine transporter-mediated dopamine release in a cotransfected model system. *Journal of Pharmacology and Experimental Therapeutics*, 310(3):1142-1145

Winner, B., Desplats, P., Hagl, C., Klucken, J., Aigner, R., Ploetz, S., Laemke, J., Karl, A., Aigner, L., Masliah, E., Buerger, E., Winkler, J., (2009) Dopamine receptor activation promotes adult neurogenesis in an acute Parkinson model. *Experimental Neurology*, 9(2):543-52

Winner, B., Geyer, M., Couillard-Despres, S., Aigner, R., Bogdahn, U., Aigner, L., Kuhn, G. and Winkler, J. (2006). Striatal differentiation increases dopaminergic neurogenesis in the olfactory bulb. *Experimental Neurology*, 197(6): 112-121

Whimbey, A.E. and Denenberg, V.H. (1967) Two independent behavioral dimensions in open-field performance. *Comparative Physiological Psychology*, 63:500-504

White, I.M., Whitaker, C. and White, W. (2006) Amphetamine-induced hyperlocomotion in rats: hippocampal modulation of the nucleus accumbens. *Hippocampus*, 16:596–603

Willis, P., Berry, M., and Riches, A.C (1976) Effects of trauma on cell proliferation in the subenpendymal layer of the rat neocortex. *Neuropathology and Applied Neurobiology*, 2:377-388

Wilson, J. M., Kalasinsky, K. S., Levey, A. I., Bergeron, C., Reiber, G., Anthony, R. M., Schmunk, G. A., Shannak, K., Haycock, J. W. and Kish, S. J. (1996) Striatal dopamine nerve terminal markers in human, chronic methamphetamine users, *Nature Medicine*, 2: 699-703.

Wolterink, G., Phillips, G., Cador, M., Donselaar-Wolterink, I., Robbins, T.W. and Everitt, B.J. (1993). Relative roles of ventral striatal D1 and D2 dopamine receptors in responding with conditioned reinforcement. *Psychopharmacology*, 110(3):355-64

Woolverton, W.L., Ricuarte, G.A., Forno, L.S. and Seiden, L.S. (1989) Long-term effects of chronic methamphetamine administration in rhesus monkeys. *Brain Research*, 486(1): 73-78

Xie, T., McCann, U.D., Kim, S., Yuan, J. and Ricaurte, G.A. (2000). Effect of temperature on dopamine transporter function and intracellular accumulation of

methamphetamine: implications for methamphetamine-induced dopaminergic neurotoxicity. *Journal of Neuroscience,* 20:7838–7845.

Xu, W., Zhu, J.P.Q., and Angulo, J.A. (2005) Induction of Striatal Pre- and Postsynaptic Damage by Methamphetamine Requires the Dopamine Receptors. *Synapse*, 58(2):110-121

Yamaguchi, T., Kuraishi, Y., Minami, M., Nakai, S., Hirai, Y. and Satoh, M. (1991) Methamphetamine-induced expression of interleukin-1 beta mRNA in the rat hypothalamus. *Neuroscience Letters,* 128:90–92

Yamamoto, B. K., and Bankson, M. G. (2005) Amphetamine neurotoxicity: cause and consequence of oxidative stress. *Critical Reviews in Neurobiology*, 17:87-117

Yang, P., Arnold, S.A., Habas, A., Hetman, M. and Hagg, T. (2008) Ciliary neurotrophic factor mediates dopamine D2 receptor-induced CNS neurogenesis in adult mice. *Journal of Neuroscience,* 28(9):2231-2241.

Yin, H.H. and Knowlton, B.J. (2004) Contributions of striatal subregions to place and response learning. *Learning and Memory,* 11(4):459-63.

Yu, K., Wang, J., Cadet, J.L., Angulo, J.A. (2004). Histological evidence supporting a role for the striatal neurokinin-1 receptor in methamphetamine-induced neurotoxicity in the mouse brain. *Brain Research,* 1007(1-2):124-131

Yu, J., Cadet, J.L. and Angulo, J.A. (2002) Neurokinin-1 (NK-1) receptor antagonists abrogate methamphetamine-induced striatal dopaminergic neurotoxicity in the murine brain. *Journal of Neurochemistry*, 83(3):613-22.

Záborszky, L., Alheid, G.F., Beinfeld, M.C., Eiden, L.E., Heimer, L., Palkovits, M. (1985) Cholecystokinin innervation of the ventral striatum: a morphological and radioimmunological study. *Journal of Neuroscience*, 14(2):427-453.

Zafar, K.S., Siegel, D. and Ross, D. (2006) A potential role for cyclized quinones derived from dopamine, DOPA, and 3, 4-dihydroxyphenylacetic acid in proteasomal inhibition. *Molecular Pharmacology*, 70:1079–1086.

Zarrindast, M.R., Tabatabai, S.A., (1992) Involvement of dopamine receptor subtypes in mouse thermoregulation. *Psychopharmacology*, 107: 341–346.

Ziegler, U. and Groscurth, P. (2004) Morphological features of cell death. *News in Physiological Science,* 19:124-128.

Zhang, R.L., Zhang, Z.G., Zhang, L. and Chopp, M. (2001) Proliferation and differentiation of progenitor cells in the cortex and the subventricular zone in the adult rat after focal cerebral ischemia. *Journal of Neuroscience,* 105:33−41.

Zhao, M., Momma, S., Delfani, K., Carlen, M., Cassidy, R., Johansson, C. and Janson, A. (2003). Evidence for neurogenesis in the adult mammalian substantia nigra. *Proceedings of the National Academy of Science USA*, 100(13):7925-7930.

Zhu, J. P. Q., Xu, W. and Angulo, J. A. (2005) Disparity in the temporal appearance of methamphetamine-induced apoptosis and depletion of dopamine terminal markers in the striatum of mice. *Brain Research*, 1049: 171-181.

Zhu, J. P. Q., Xu, W., and Angulo, J. A. (2006) Methamphetamine-induced cell death: selective vulnerability in neuronal subpopulations of the striatum in mice. *Journal of Neuroscience*, 140:607-622.

Zhu, J., Xu, W., Wang, J., Ali, S.F. and Angulo, J.A. (2009) The neurokinin-1 receptor modulates the methamphetamine-induced striatal apoptosis and nitric oxide formation in mice. *Journal of neurochemistry*, 111(3):656 -668